ANA VERA ALVES MACHADO

CHEMISTRY, MORPHOLOGY AND RHEOLOGY EVOLUTION ALONG THE EXTRUDER

Tese submetida à Universidade do Minho para a obtenção do grau de Doutor em Ciência e Engenharia de Polímeros.

UNIVERSIDADE DO MINHO

2000

This work would not have been possible without the help and the support of a large number of people and institutions.

I am very grateful to Prof. José A. Covas for taking me through the complexity of extruders and rheometers. For the discussions and the contribution to this manuscript.

I would like to express my gratitude to Dr. Martin van Duin for providing me the opportunity to work in a multidisciplinary subject. He provided support and advice while preserving my initiative.

I would like to thank the Departamento de Engenharia de Polímeros (DEP) and all the members for the facilities and support to this research program.

Many thanks to Guilherme Caldeira, who helped me setting the screw configurations.

This project involved the collaboration of many experts in different departments of DSM Research. To all of them goes my appreciation.

Special thanks are addressed to Monique Walet, who performed the TEM work and Marcel Aussems who gave me assistance in the analytical work.

I am grateful to the students (Lúcia Chaves, Mónica Rodrigues and Flor Liberta) that helped in this work.

I am also thankful to INVOTAN, who provided financial support for traveling and accommodation during my stages in Holland.

At last, a very special thanks to my parents and friends who gave me support during this work.

In this work an investigation of the evolution of physico-chemical phenomena along a co-rotating twin-screw extruder was carried out in order to enhance the understanding of reactive extrusion.

A new sampling device, which allows the collection in a few seconds of small amounts of material from the melt during processing, was tested using a reactive system and an immiscible blend. PA-6/EPM blending and SMA imidation experiments are reported in terms of morphology development and evolution of the chemical conversion along the extruder, respectively. Comparison of the results obtained using the new sampling technique with those of classical screw pulling experiments evidenced the potential erroneous conclusions than can be drawn from the latter.

Subsequently, a number of these sampling devices was used at various locations of the extruder to study in more detail polyolefin modification and compatibilization of blends of polyamide-6 and MA-containing polymers.

Polyolefin modification (degradation, crosslinking and grafting of MA) along the extruder axis was investigated. The main conclusions are that the degree of branching/crosslinking and/or degradation depends on the ethene/propene ratio, on the original polymer molecular weight and on the amount of peroxide added. A similar evolution of the MA grafting content for PE, EPM and PP was observed, but the final MA contents were different. A good correlation between MA grafting and peroxide decomposition was established. The MA graft content is low for polyolefins with high propene content, increases as the propene content decreases and reaches a plateau at propene levels below 50 wt.%. Branching/crosslinking occurs for polyolefins with low propene content, while degradation is the main side reaction for polyolefins with high propene content. A detailed chemical mechanism is proposed in order to explain these results.

Since one of the main applications of maleated polyolefins is their use as compatibilizers for polymers blends, the development of chemistry, morphology and rheology of blends of PA-6 and MA containing polymers was studied. The chemical conversion and morphological evolution of PA-6/EPM/EPM-g-MA blends were monitored along the extruder. The results show that the MA content of the MA-

containing polymer in all blends decreases drastically in the first zone of the extruder, i.e., upon melting of the blend components. Dramatic changes in morphology are also observed in this stage. The processing conditions, particularly temperature profile and screw speed, affect both the chemical conversion and the morphological evolution. Using low temperatures and low screw speeds it became possible to observe in real time the evolution of morphology development of a reactive blend.

RESUMO

Este trabalho tem como objectivo estudar a evolução de fenómenos fìsico-químicos ao longo de uma extrusora duplo-fuso, de modo a melhorar os conhecimentos existentes sobre extrusão reactiva.

Uma nova vávula de colheita, que permite recolher pequenas quantidades de material fundido em poucos segundos durante o processamento, foi testada um sistema reactivo e uma mistura de polímeros imiscíveis. Os resultados das experiências da mistura de PA-6/EPM e imidização de SMA são expressos em termos de desenvolvimento de morfologia e evolução da conversão química a longo da extrusora. A comparação dos resultados obtidos com a nova técnica de amostragem e com o método clássico de remover os parafusos evidenciaram que conclusões erradas podem ser inferidas a partir do último.

Em seguida, algumas destas válvulas foram colocadas em várias localizações específicas da extrusora de modo a estudar com maior detalhe a modificação de poliolefinas e a compatibilização de misturas de poliamida-6 e polímeros que contêm anidrido maleico.

O estudo sobre modificação de poliolefinas (degradação, reticulação e enxerto de MA) ao longo da extrusora foi abordado em duas partes. As conclusões princípais foram que o grau de ramificação/reticulação e/ou degradação depende da razão de eteno/propeno, da massa molecular inicial e da quantidade de peróxido adicionado. Relativamente à quantidade de MA enxertado em PE, EPM e PP, similar evolução foi observada, contudo as quantidades finais de MA enxertado foram diferentes. Foi possível estabelecer uma boa correlação entre o enxerto de MA e a decomposição do peróxido. A quantidade de MA enxertado é baixa para poliolefinas com elevado teor de propeno, aumenta à mediada que o teor de propeno diminui atigindo um patamar para teores de propeno abaixo de 50 wt.%. Ramificação/reticulação occurre para poliolefinas com baixo teor de propeno, enquanto a degradação é a reacção secundária principal para poliolefinas com elevado teor de propeno. Foi proposto um mecanismo químico detalhado para explicar estes resultados.

Como uma das aplicações principais das poliolefinas modificadas com MA é o seu uso como compatibilizadores em misturas de polímeros, foi realizado um estudo sobre desenvolvimento químico, morfológico e reológico de misturas de PA-6 e polímeros que contêm MA. A conversão química e a evolução morfológica de misturas de PA-6/EPM/EPM-g-MA foram monitorizadas ao longo da extrusora. Os resultados mostraram que em todas as misturas a quantidade de MA dos polímeros que contêm MA diminui drasticamente na primeira zona da extrusora, i.e., durante a fusão dos componentes da mistura. Durante esta fase observam-se alterações drásticas de morfologia. As condições de processamento, particularmente perfil de temperatura e velocidade de rotação dos fusos, afecta a conversão química e a evolução da morfologia. A observação da evolução do desenvolvimento da morfologia para uma mistura reactiva foi possível utilizando baixas temperaturas e baixas velocidades de rotação dos fusos.

Contents

Contents

LIST OF FIGURES

LIST OF TABLES

Part I

Introduction

1. 1 - INTRODUCTION

1.1.1 - Reactive Extrusion

Over the past three decades the growing demands for specialty grades of plastic materials has led to increasing scientific and industrial interest in melt blending and chemical modification of polymers. These routes allow the development and production of new polymers without the use of new monomers. Classically, polymer modification has been achieved in solution. The use of solvents facilitates the control and adjustment of the reactivity between the polymers and the other chemicals. Another approach is to perform these reactions in the melt in mixing equipment. The use of extruders as chemical reactors is nowadays commonly called reactive extrusion (REX) and has proven to be a key technology in the polymer industry [1-6]. The polarity and the viscosity of the medium, i.e., the molten polymer, are determined by the chemical composition and the molecular weight. They are different from those of solvents, thus affecting reaction and processing parameters. Due to its complexity, REX became highly challenging from a scientific point of view.

At the present time, REX is viewed as an efficient means of continuously polymerizing monomers, and chemically modifying existing polymers. It combines two operations traditionally separated, i.e., the chemical reactions for the synthesis or the modification of macromolecules and the processing of the polymer.

Single and twin screw extruders have been adapted to be used for REX, using secondary solid feed and liquid injection ports, special screw designs and various kinds of pressure and temperature sensors. The use of an extruder as a chemical reactor has several advantages, such as:

(i) polymerization and chemical modification of polymers in the absence of solvents (the extruder can handle the high viscosity of polymers) which is beneficial for health, environmental and economic reasons;

(ii) sequential reaction initiation by multiple injection ports, which is relevant for highly reactive species like free radical initiators;

(iii) controlled residence time distribution;

(iv) geometrical flexibility, especially in modular equipment, which allows different residence times and degrees of mixing;

(v) broad range of processing conditions, i.e., a large range of pressure (0 - 500 atm) and temperature (70 - 500 ºC);

(vi) polymers materials are produced in a ready-to-use form.

However, the extruder as a reactor has also disadvantages, namely:

(i) the polymer velocity field is rather complex and difficult to be quantitatively correlated with the main processing parameters;

(ii) the average residence time is rather small (< 5 min), limiting the chemical conversion;

(iii) it is difficult to control heat transfer.

1.1.2 - Extruders

REX involves different steps, such as feeding, melting, mixing, reaction and devolatilization in a single process. Extruders must also deal with a melt with continuously changing nature. Consequently, the design of screws for reactive extrusion applications (a extruder layout is depicted in Figure 1.1) involves the manipulation of information and knowledge from several scientific areas.

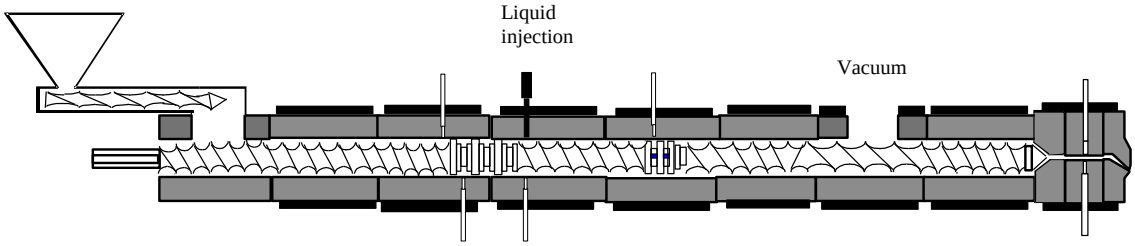

Figure 1.1 – Typical extruder layout for REX.

Although both single and twin-screw extruders have been used successfully for REX [1-8], twin-screw extruders are increasingly being favoured. The main reasons include the extended control of the residence time distribution, the mixing intensity and the superior heat transfer capabilities. Also, while in single-screw extruders, material conveying depends on frictional forces in the solid conveying zone and on viscous

forces in the melting and pumping zones, twin-screw machines are almost positive pumping devices.

According to their specific characteristics, twin-screw extruders can handle complex tasks such as homogenisation, additives dispersion, reactive compounding, devolatilization and polymerisation [8,9]. Nowadays, most manufacturers propose modular solutions, offering a choice of feeding devices (gravity, volumetric and gravimetric feeding systems), barrel sections (conventional, for lateral feeding, for venting) and screw elements (conveying sections, left handed elements, kneading blocks, mixing elements) that are mounted sequentially on a shaft, defining the most appropriate geometry for a given reactive system.

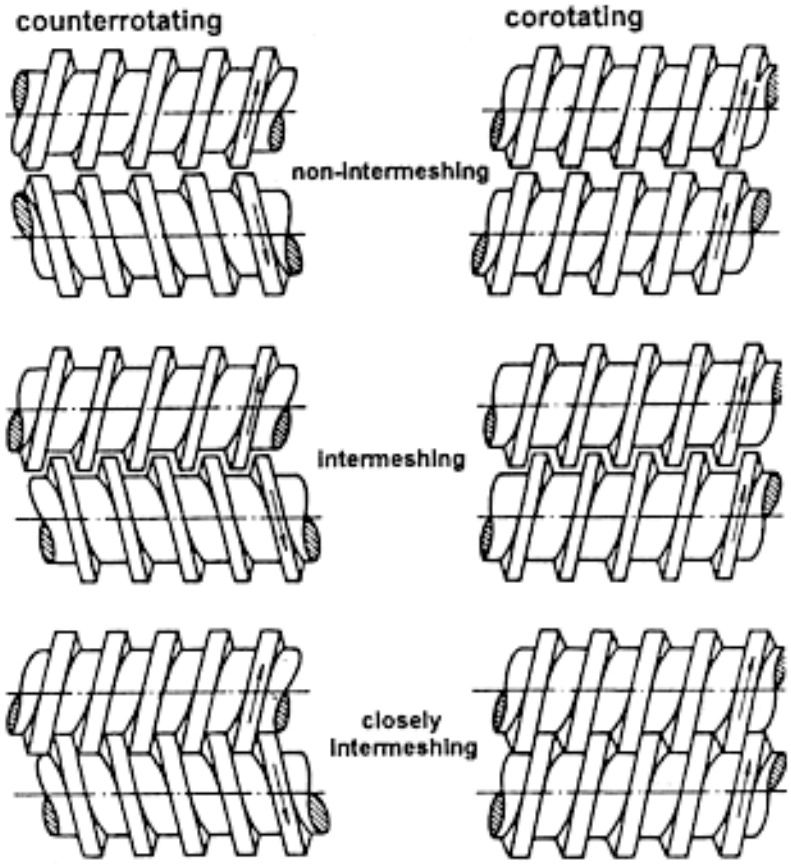

Figure 1.2 – Classification of twin-screw extruders.

Twin-screw extruders can be classified as co-rotating or counter-rotating. As shown in Figure 1.2, the degree of intermeshing can also vary. In the case of closely intermeshing

screws, the material is conveyed from one screw to the other, in a figure of 8 path. Because of the high screw speed, high shear rates are achieved. By contrast, screws in the counter-rotating mode convey the material forward axially, the kneading action in the calendar gap (i.e., the gap between the root of one screw and the flight tip of the adjacent one) pushes the screws apart and against the barrel, which prevents operation at high screw speeds [10-13].

Although each type of twin-screw extruder has a certain uniqueness regarding ingredients, type of reaction and polymer produced, co-rotating intermeshing twin-screw extruders have been found to be suitable for many REX processes [9].

The sequence of screw elements affects the degree of filling along the screw, the melting location, the residence time distribution and the mixing intensity. Two types of elements are widely used in co-rotating twin-screw extruders: conveying screw elements and kneading discs [10-13]. Conveying elements move the material along the extruder. Kneading discs are the most commonly used mixing elements. A set of consecutive discs between conveying elements is usually referred as a kneading block. Kneading blocks are primarily used for melting and dispersion of partially molten polymer particles and reactive agents into the melt. Kneading discs can be staggered in forward, reverse conveying or neutral directions, as it is illustrated in Figure 1.6 [12].

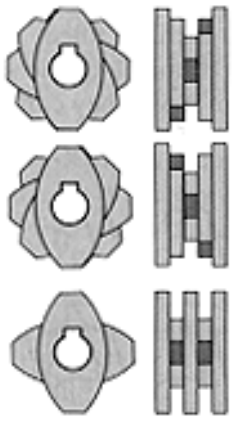

Figure 1.3 – Kneading blocks: forward, reverse conveying and neutral directions (from top to bottom).

Left hand screw elements should be considered as kneading blocks, since the barrier exhibited to the incoming material induces the same type of effect of those elements.

In self-wiping co-rotating twin-screw extruders the flight of each screw scraps the material contained in the channel of the adjacent screw, preventing its helical progression under conditions similar to those of the single screw extruder. Since, as shown in Figure 1.4, there is a considerable aperture between corresponding channels of the two screws, the material contained in one screw channel flows into the channel of the adjacent screw, developing a figure 8 pattern, as mentioned above. Therefore, the conveying capacity is greatly determined by geometrical features, such as screw diameter, centreline distance, helix angle and number of flights in parallel (Figure 1.5 shows screw profiles with 1 to 4 parallel flights).

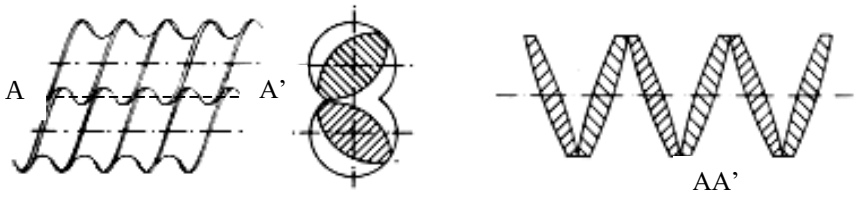

Figure 1.4 – Self wiping co-rotating screws a) general view; b) cross-section c) longitudinal section.

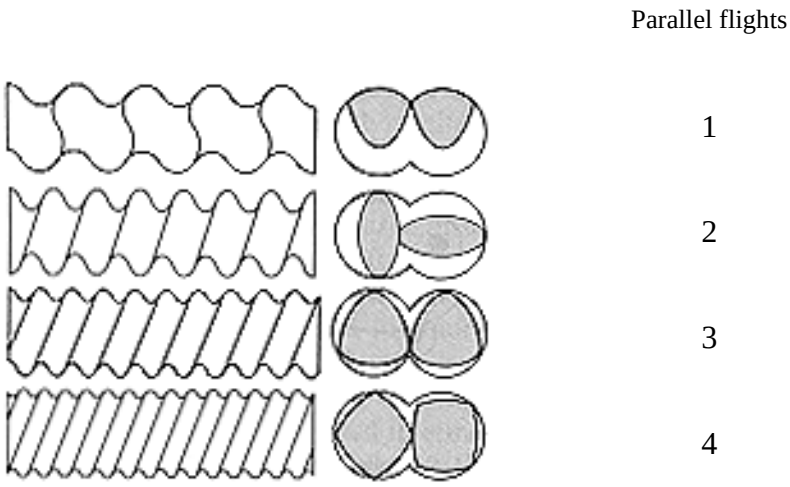

Figure 1.5 – Self-wiping screws.

Initially, screws with three flights were used. However, two-flight designs are more common in modern machines, because they offer greater free volume, and provide better mixing, but lower shearing forces and worst heat transfer. Thus, two-flighted

screws are adequate for reactive extrusion, since they offer the largest reactive volume combined with the minimum shear work input [13].

1.1.3 - Chemistry

The work carried out by various research groups [14-24] has shown that the following types of reactions can be performed in extruders:

(i) bulk polymerisation – preparation of high molecular weight polymers from monomers or pre-polymers with low molecular weight;

(ii) grafting – formation of graft copolymers via reaction of a polymer and a monomer;

(iii) interchain copolymer formation – reaction of two or more polymers to form graft or block copolymers;

(iv) coupling or branching – reaction of polymers with polyfunctional coupling or branching agents to build up molecular weight by chain extension or branching;

(v) controlled degradation – degradation of polymers of high molecular weight;

(vi) functionalization/modification – introduction of functional groups onto the polymer backbone or modification of the existing functional groups.

1.2 - REVIEW OF FUNDAMENTAL STUDIES

1.2.1 - Free radical processing and functionalization of polymers

Although the first study on free radical reactions of polymers was based on modification induced by mechanochemistry [1-4]. However, the process was shown not to be powerful and controllable enough for efficient free radical initiation of grafting reactions. Therefore, most of the free radical reactions are initiated by free radical generators, such as peroxides [1-4].

1.2.2 - Degradation

Degradation by free radical reactions in the melt is restricted to polyolefins, especially polypropylene (PP). This type of reaction can be induced by mechanochemistry as a result of elevated temperature, high shear stress and the presence of oxygen. However, for higher reactivity peroxides are used. In the case of PP, the free radicals generated by peroxide decomposition abstract hydrogen atoms from the tertiary carbon sites, leading to β-scission. As a result, a reduction of molecular weight is obtained, which corresponds to lower melt viscosity and improved processability. PP is produced commercially with heterogeneous Ziegler-Natta catalysts. The synthesized polymers have a very broad molecular weight distribution with a high molecular weight tail, which accounts for high melt elasticity levels. The use of controlled chain degradation became an important industrial application for the production of PP with controlled rheology [19-30]. It is generally accepted that degradation of PP follows a series of free radical reactions, i.e., peroxide decomposition, hydrogen abstraction, chain scission and termination [22-30] (Figure 1.6). Some kinetic models for PP degradation have been developed and combined with a simplified model of the melting mechanism in the extruder, in order to predict the molecular weight average [20-24].

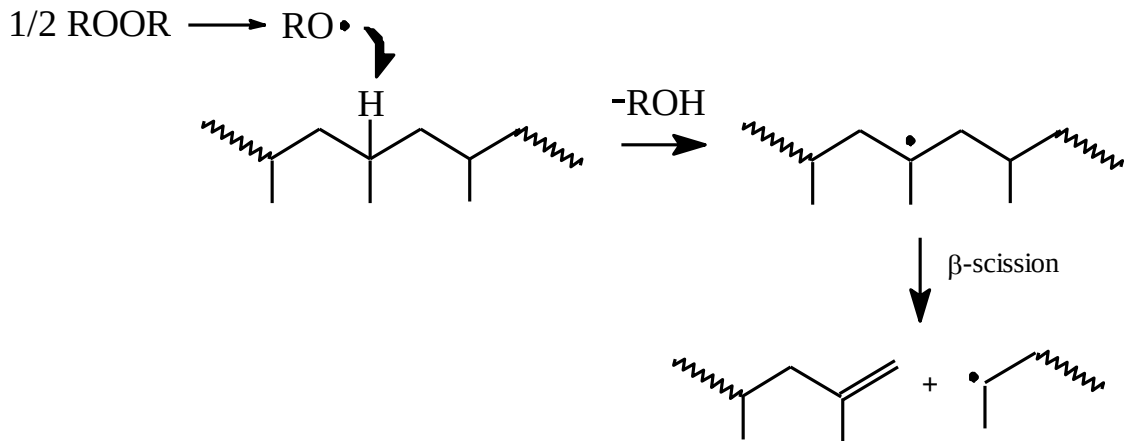

Figure 1.6 – Mechanism of peroxide induced degradation of PP.

1.2.3 - Branching/crosslinking

Long side chains are formed when the macroradicals, formed by hydrogen abstraction experience bimolecular termination by combination (Figure 1.7). If this long chain branching continues, a three-dimensional network will form with high levels of insoluble gel (crosslinking). The formation of high molecular weight chains due to branching increases the melt strength and the die swell and improves the strain hardening properties [31-44].

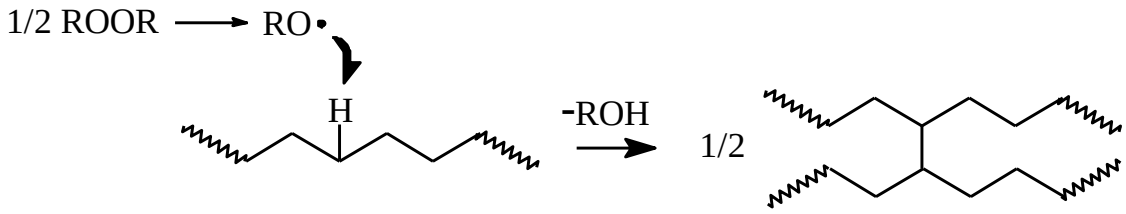

Figure 1.7 – Mechanism of branching/crosslinking reaction of polyolefins.

Often, crosslinking is considered undesirable because of reduced processability. However, it may also brings some property enhancement to the polymer, such as increased service temperature, solvent resistance, flexural modulus and dimensional stability.

1.2.4 - Grafting of maleic anhydride

Grafting reactions performed in the presence of one (or more) monomers lead to chemical and physical modifications of the original polymeric backbone. When long branches are grafted onto the polymer skeleton a new material is obtained with physical properties different from those of the original polymer. In the case of short length grafts the modified polymer evidences similar mechanical properties. An example, which has been widely used, is the functionalization of polyolefins in order to improve the polarity and/or the reactivity of the molecular backbone [1-4, 44-47]. Grafting of MA onto polyolefins and rubbers by REX provides polymers mainly with short grafts.

Nowadays, grafting of polyolefins with maleic anhydride (MA) is widely applied, since it improves the adhesive polymers properties and their compatibilizing abilities [1-4].

For example, the production of EPM-g-MA has a great economical value. The modified polymer has the same mechanical and physical properties of the original EPM. EPM-g-MA is increasingly used as a reactive product leading to the "in-situ" formation of a compatibilizer for immiscible polymer blends of EPM and PA. The anhydride groups of the modified EPM react with the amine end groups of PA in order to form a graft copolymer at the interface. As it will be pointed out later in section 2.2, the copolymer formed at the interface will reduce the interfacial tension and will improve the dispersion and stabilization of the dispersed phase. In this way tough PA is obtained.

A free-radical grafting system usually involves three types of reactants: polymer, vinyl monomer and peroxide. First of all, free radicals are generated by the decomposition of the peroxide. The free radical can react with the monomer, which can lead to the undesired formation of free homopolymer. However, when the free radical abstracts a hydrogen from the polymer backbone a macroradical is formed. Depending on the structure, this macroradical can follow three different reactions: grafting, crosslinking and chain scission. If the macroradical reacts with the monomer, this molecule is grafted into the polymer backbone forming a branched macroradical. The latter can react with more monomer molecules to form longer grafts, or it may undergo transfer with a hydrogen atom, from the same or another polymer backbone, forming a new macroradical. Chain transfer is important as a way of forming new macroradicals, repeating the grafting cycle and, thus, increasing the grafting efficiency.

Due to the low reactivity of MA, MA grafting has to compete with side reactions such as crosslinking or chain degradation in the case of PE and PP, respectively (Figure 1.8).

Many studies have been published concerning the mechanism of free radical grafting of polyolefins [48-59]. However, little quantitative information or experimental data for the various steps are available. Polyolefins contain different types of hydrogen atoms having different reactivities and, as a consequence, the corresponding macroradicals are not equally reactive to the monomer to be grafted. In PE there are almost exclusively methylene carbons, whereas in PP each repetitive unit has three different carbons: methyl, methylene and methine.

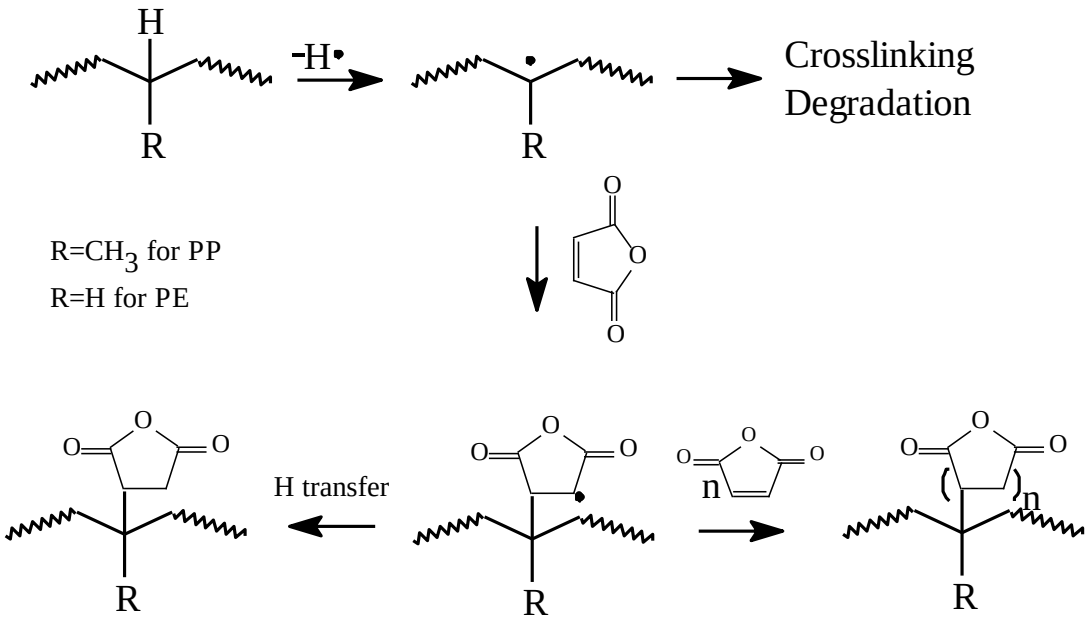

Figure 1.8 – Mechanism of free radical grafting of MA onto polyolefins.

Avela *et al* [60] showed that the yield of MA grafting on PP was lower than for PE. Hogt *et al* [61] investigated the effect of MA and peroxide concentration on the grafting of MA. The efficiency of MA grafting onto polyolefins was determined by the peroxide/MA ratio. Rosales *et al.* [62] modified different commercial PE grades. Grafting efficiency increased with increasing peroxide content and the functionalization reaction did not change the molecular weight distribution. The authors suggested that grafting occurs preferentially on the longer, or less substituted, methylene sequences. Bray *et al.* [63] performed MA grafting onto PE by reactive extrusion, achieving grafting efficiencies of up to 85%. Higher reaction temperatures, higher initiator levels and lower throughput were reported to increase grafting efficiency. However, in all these studies single units and oligomeric MA grafts could not be distinguished. Russel *et al.* [58] used low molecular weight model compounds to study MA grafting onto polyolefins. It was suggested that grafts occur as single units, especially at temperatures at which melt grafting is performed. Heinen *et al*. [64] investigated the reaction products from the radically initiated grafting of ^{13}C-enriched maleic anhydride ([2,3-$^{13}C_2$]MA) onto PP, HDPE, LDPE and EPM. They found that MA was grafted attached in the form of single succinic anhydride moieties both in the melt and in solution. Short MA oligomers have only been demonstrated for melt grafting of HDPE. Using model

compounds Ranganathan *et al.* [65] also observed that the grafts occur predominantly as single units and not as oligomeric grafts. Grafting occurs almost exclusively at the tertiary sites in the case of squalene and pristine. However, they are more randomly distributed in the case of linear hydrocarbons.

The performance of grafting process is not only affected by the chemistry involved, but also by the processing conditions. In order to maximize the grafting yield and minimise the side reactions, different processing parameters have to be optimised, such as:

(i) Mixing efficiency- in order to produce high grafting yields, an efficient mixing of the monomer, initiator and polymer is crucial;

(ii) Temperature – it influences the peroxide decomposition, the solubility of the peroxide and monomer and the rheological parameters;

(iii) Pressure – higher pressure can provide enhanced solubility of the peroxide and/or monomer in the polymer melt;

(iv) Devolatilization – removal of the unreacted monomer.

Much effort has been spent in understanding the effects of processing parameters on free radical grafting in extruders. However, the knowledge of REX is still limited, probably because in all these studies only extrudates were characterized (grafting content and crosslinking/degradation), very little information being available on the evolution of the reaction along the extruder. It is very important to have a greater insight into free radical grafting in extruders, in order to maximise the grafting efficiency and optimise the product properties.

1.3 - COMPATIBILIZATION OF POLYMER BLENDS

Blending polymers has become a useful technique to produce new polymeric materials with a useful combination of properties, for a relatively low development and production cost [66-71]. As prepared by the physical combination of at least two polymers, most polymer blends are immiscible and have poor physical properties. Compatibility and interfacial adhesion can be improved by the addition of suitable block or graft copolymers that act as interfacial agents. The potential of twin-screw extruders as high-speed continuous reactive blenders has become the driving force behind the present interest in reactive mixing techniques. REX, with the possibility of

"in-situ" synthesis of bock or graft copolymers, sharply increased new developments in polymer blends. For technical and economical reasons, reactive extrusion may provide viable mechanisms for the production of blends with controlled structure and morphology [1,67-71].

1.3.1 - Miscibility

As for other mixtures, polymer/polymer miscibility is governed by thermodynamic laws [68,70]. In order to have thermodynamically miscibility, the free energy of mixing ΔG_m should be negative, as expressed by,

$$\Delta G_m = \Delta H_m - T\Delta S_m < 0 \qquad [1]$$

where ΔG_m, ΔH_m and ΔS_m are the changes in Gibbs free energy, the enthalpy and the entropy upon mixing, respectively. Since the monomer units are covalently bonded to each other in the polymer chains, the number of ways that they can be arranged in a mixture is limited. Thus, ΔS_m is very small for polymer mixtures and approaches zero in very high molecular weight polymers. Consequently, equation 1 predicts that polymer/polymer miscibility has to result from the exothermic heat of mixing ($\Delta H_m < 0$).

A negative heat of mixing results when the interactions between neighbouring segments of structurally different polymers are energetically more favourable than the intermolecular interactions between segment pairs. Examples of interactions giving exothermic heats of mixing include hydrogen bonds, dipole-dipole and anionic interactions.

1.3.2 - Compatibilization

The main challenge of polymer compatibilization is to produce materials with a stable optimum morphology that maximises the mechanical performance [68-77]. Poor chemical or physical interaction between two polymers usually implies high interfacial

energy and low interfacial thickness. The properties of the interface such as thickness, strength and interfacial tension strongly determine the bulk properties. Therefore, the key to overcome problems related with the coarse morphology of polymer blends is to reduce the interfacial tension in order to improve the interaction between the immiscible phases. This can be achieved by adding compounds known as “interfacial agents”, “emulsifiers”, “adhesion promoters” or, most frequently, “compatibilizers”, to the heterogeneous blends. As a result of compatibilization a fine and stabilized morphology can be accomplished; the interfacial thickness increases and the interface is strengthened due to interpenetration of the two types of chains across the interface. Several ways can be followed in order to promote blend compatibilization [67-80], such as addition of a compatibilizer during blending, crosslinking of one of the two phases, chemical interactions and formation "in-situ" of a copolymer during blending.

1.3.3 - Compatibilizers

Compatibilizers can be classified as follows:

(i) Pre-synthesized block or graft copolymers;
(ii) reactive low molecular weight coupling agents;
(iii) reactive copolymers.

The last case involves the synthesis of a copolymer "in-situ" during blending, which has some advantages over the others. The copolymer is formed at the interface, where it is needed for reducing the interfacial tension between the two phases. The block or graft copolymers formed at the interface are represented schematically in Figure 1.9.

As stated above, polymers have been chemically modified in order to improve polymer compatibilization. Due to its reactivity, MA is frequently used for compatibilization. Some examples of polymers modified with MA used in polymer blends are presented in Table 1.1.

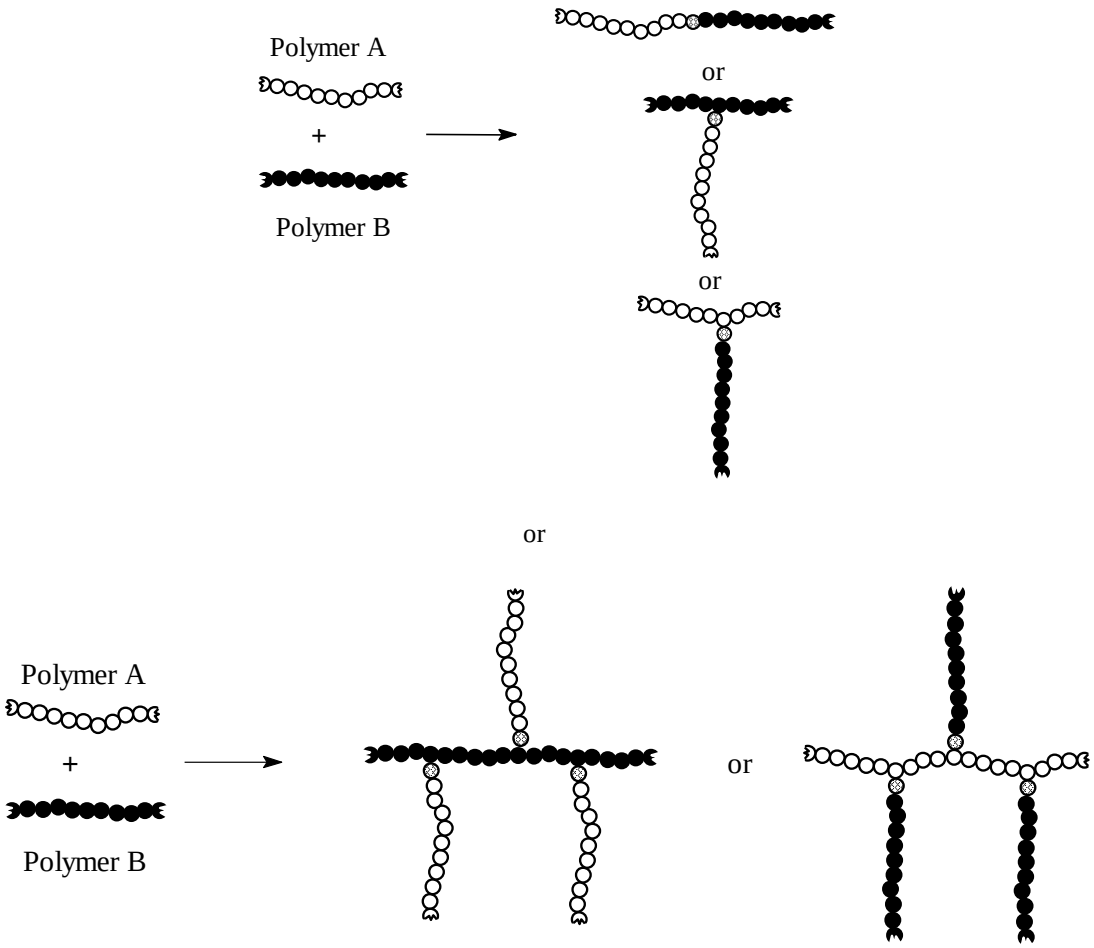

Figure 1.9 - "In-situ" formation of block or graft copolymers.

1.4 - MORPHOLOGY DEVELOPMENT

Morphology control is a key parameter for producing polymer blends with superior properties [1,2]. However, the morphology depends on the thermodynamic and the rheological properties of the blend components, as well as on the processing conditions and equipment used. The multiphase nature of polymer blends and the variation of the structure upon processing imply that flow responses may be complex. Thus, during blend preparation not only the parameters controlling homogeneous polymer systems, but also the morphology and its evolution should be considered. Know how on the development of the blend morphology, i.e., the evolution of the blend morphology from

mm size particles to submicrometre droplets, in the final blend in (industrial) processing equipment, such as extruders, is essential [3-6].

Table 1.1 – Maleic anhydride containing polymer, blend, type of reaction and most improved property [73-75].

Polymer	Reactive group	Blend	Reaction type	Property
EPM	grafted MA	PA-6/EPM	Imidation	Impact
		PA-6,6/EPM	Imidation	Impact
		PBT/EPM	Ester interchange	Impact
EPDM	grafted MA	PA-6/EPDM	Imidation	Impact
PE	grafted MA	PA-6/PE	Imidation	Impact
		PE/EPDM	Ionic	Tensile
PP	grafted MA	PA-6/PP	Imidation	Impact
		PP/NBR	Imidation	Tensile
		PP/EPM	Esterification	Impact
ABS	grafted MA	PA-6/ABS	Imidation	Tensile
SEBS	grafted MA	PA/SEBS	Imidation	Impact
SMA	Copolymerized MA	PA-6/SAN	Imidation	Impact
		PA-6/ABS	Imidation	Impact
		PA-6/PS	Imidation	Tensile
SAN	Terpolymerized MA	PA/ABS	Imidation	Impact

The two main mechanisms determining the morphology of a polymer blend are breakup and coalescence. The stability of the droplet is characterized by a dimensionless number, usually called the capillary number, k, which is the ratio of the viscous stress $\eta_m \dot{\gamma}$, (which tends to deform the drop) and the interfacial stress ν_{12}/R, (which tends to restore the initial shape):

$$k = \frac{R\eta_m \dot{\gamma}}{\nu_{12}} \qquad [2]$$

where η_m is the matrix viscosity, $\dot{\gamma}$ is the shear rate, R is the droplet radius, and ν_{12} is the interfacial tension. From experimental studies on droplet deformation and breakup in simple flow situations, a critical capillary number k* has been defined, whose comparison with local capillary numbers will define the general tendency for deformation or breakup. Most of the studies [81-89] have indicated that when:

k<k*, drops may deform, but they do not break;

k*<k<2k*, drops are unstable and may break into two sister drops;

k>2k*, drops are deformed into fibers, following the affine deformation of the matrix.

A number of authors [90-92] have published experimental results defining the critical capillary number k* as a function of the viscosity ratio, $\lambda=\eta_d/\eta_m$, i.e., the viscosity ratio of the dispersed and the matrix and depends on the type of the flow. Within the range of capillary number, 1< k*<4, drop-splitting leads to two identical smaller droplets. The kinetics of the breakup process depends on the viscosity ratio. The dimensionless time for breakup t_b^* under constant stress has been reported by Grace [90] and it is defined as

$t_b^* = \frac{t_b \dot{\gamma}}{2k}$, t_b is the real time for breakup. Grace reports that t_b^* depends on the viscosity ratio and capillary number. For simple shear breakup is impossible when the viscosity ratio becomes higher than 4, whereas breakup remains possible in elongational flow whatever the viscosity ratio.

The droplets collision in the flow field may result in increased particle size due to coalescence. The coalescence process is divided in two steps: the formation of the colliding nodules and drainage of the fluid situated in-between. Experimental studies [93,94] have shown that coalescence may occur as soon as the volume fraction of the dispersed phase exceeds 0.5%. Theoretical approaches on coalescence concluded that it is possible to calculate an equilibrium droplet size, resulting from continuous mechanisms of breakup and coalescence. For concentrated systems coalescence becomes important; the particle size of the dispersed phase is affected not only by the viscosity ratio and the capillary number, but also by the presence of an emulsifier. The latter decreases the interfacial tension and acts in the interface to prevent coalescence.

Several factors influence the morphology development during blending: composition, viscosity and viscosity ratio and processing conditions (screw configuration, time of mixing, screw rotation speed, temperature, throughput, etc.) [83]. However, the number of studies on how morphology actually develops is rather small. There are many important questions concerning this process. There has been much speculation about the mechanisms of particle size reduction and the effect of interfacial reaction on morphology development. Some results have been reported on how the morphology develops as a function of time during blending. Karger-Kocsis *et al.* [95] reported no significant changes in morphology from 5 to 40 minutes of mixing blends of rubbers dispersed in PP. Favis *et al.* [96] prepared blends of PP and PC in a batch mixer and concluded that the most significant changes in morphology occurred during the first 2 min of mixing, when melting and softening of the materials also occur. Scott and Macosko [97,98] reported model experiments, showing that at short mixing times the phases are sheared into ribbon or sheet structures, followed by a shear and interfacial tension driven breakup of these sheets or ribbons. Sunduraraj *et al.* [99-101] showed that the most significant morphology development of a polystyrene and polypropylene (PS/PP) blend in a twin-screw extruder occurred in the first two kneaders of the first kneading section. They also observed sheet structures and demonstrated that after the initial breakup the particle size is not reduced significantly. Moreover, they observed a phase inversion mechanism when the minor component melted or softened at a lower temperature than the major component. Cartier *et al.* [102] studied blends in a co-rotating twin-screw extruder and showed that the morphology of polypropylene and polyamide-6 (PP/PA-6) develops very rapidly and that in the case of in situ compatibilized blends with maleic anhydride modified PP (PP-g-MA) it develops even faster. In the latter case, the size of the dispersed phase undergoes an abrupt reduction from a few millimeters to sub-micrometer levels during phase transition from solid pellets to a viscoelastic fluid. The final morphology is reached as soon as the phase transition is completed.

1.5 - AIM OF THE INVESTIGATION

Although REX has been studied and used for commercial purposes for many years, the mechanisms occurring inside the extruder are still far from bring fully understood. Extruders are still used as a black box. The aim of this study is to investigate the evolution of physico-chemical phenomena along a co-rotating twin-screw extruder, in order to enhance the understanding of REX. This knowledge build up can be used for the optimisation of REX processes and to improve the properties of REX products.

1.6 - METHODOLOGY AND SCOPE OF THE THESIS

Most of the data available on the mechanism of chemical reactions using REX are based on the characterisation of extrudates. Data on morphology development in an extruder was obtained from screw pulling experiments, experiments with a split barrel, by removing molten samples at entry ports with tweezers or by diverging a small amount of material from inside the extruder through a hole in the barrel [103-106]. Usually these techniques require between 1 and 5 minutes to collect the sample. Unfortunately, during this period the final morphology can change as a result of coalescence, i.e., if these techniques are used to study the evolution of a chemical reaction, the results will provide an erroneous value of the chemical conversion or morphology evolution.

To reach the aim of this work, a device to collect samples of molten polymer in less than five seconds was developed [107]. The apparatus can be inserted between barrel segments or, alternatively, barrel segments can be replaced by a set of these devices. This provides the possibility of obtaining polymer samples at relatively small increments along the length of the screw. Thus, in this work these sampling devices will be used to collect samples at specific locations along the extruder where the most significant changes in chemistry, morphology and rheology are anticipated.

Given the purpose of this investigation and the methodology adopted, this thesis is divided in four parts.

Part I includes an overview of REX, and its application to polymer modification and reactive blending (Chapter 1). Moreover, the data obtained using the sampling devices is presented (Chapter 2).

Part II is dedicated to the study of polyolefin modification along the screw axis. Chapter 3 deals with the effect of polyolefin structure on grafting of maleic anhydride, while Chapter 4 is devoted to polyolefin modification due to the effect of peroxide. The grafting of maleic anhydride onto polyolefins along the extruder is discussed in Chapter 5.

The investigation of the evolution of chemistry, morphology and rheology of blends of PA-6/EPM/EPM-g-MA along the extruder is dealt with in Part III. The effect of maleic anhydride content, blend composition and processing conditions on chemistry and morphology development is discussed in Chapters 6 and 7, respectively. The evolution of the rheological behaviour of the blends is reported in Chapter 8.

Finally, in Part IV (Chapter 9) the main conclusions produced by this work and recommendations for future work are presented.

1.7 - REFERENCES

[1] – Reactive Extrusion, M. Xanthos (Ed.), Hanser Publishers, New York, 1992.

[2] – M. Lambla, Reactive Processing of Thermoplastic Polymers, In Comprehensive Polymer Science, S. Russo, S, Aggarwal, (Eds.), Pergamon Press, New York, 1993.

[3] - M. Lambla, Reactive Extrusion: A new toll for the diversification of polymeric materials, In Rheological Fundamentals of Polymer Processing, J. A. Covas, *et al*. (Eds.) Kluwer, London, 1994.

[4] – Reactive Modifiers for Polymers, S. Al-Malaika (Ed.), Blackie Academic & Professional, London, 1997.

[5] – S. B. Brown and C. M. Orlando, Encyclopedia of Polymer Science Engineering, **14**, 169 (1988)

[6] – C. Tzoganakis, Adv. Polym. Techn., **9**, 321 (1989).

[7] - C. Maier, Etude des Reactions de Condensation Interpolymere sur Extrudeuse Double-vis, PhD Thesis, University Louis Pasteur, France (1994).

[8] – W. Michaeli and A. Grefenstein, *Polym. Eng. Sci.*, 3**5**, 1485 (1995).

[9] – J. L. White, W. Szydlowski, K. Min and M. Kim, *Adv. Polym. Technol*., **7**, 295 (1987).

[10] – Plastics Compounding, D. B. Todd (Ed.), Hanser Publishers, New York, 1998.

[11] – C. Rauwendal, Polymer Mixing, Hanser Publishers, New York, 1998.

[12] – C. Rauwendal, Polymer Extrusion, Hanser Publishers, Munich, 1990.

[13] – R. H. Wildi and C. Maier, Compounding, Hanser Publishers, Munich, 1998.

[14] – D. C. Wahrmund, D. R. Paul and J. W. Barlow, *J. Appl. Polym. Sci*., **22**, 2155 (1978).

[15] – A. M. Kotliar, *J. Polym. Sci.-Macromol. Rev*., **16**, 367 (1981).

[16] – J. Devaux, P. Godard and J. P. Mercier, *Polym. Eng. Sci*., **22**, 229 (1982).

[17] – R. S. Porter, *Thermochimica*, **134**, 251 (1988).

[18] – M. Lambla, J. Druz and F. Mazeres, *Plast. Rubber.Proces. Appl*., **13**, 75 (1990).

[19] – M. Dorn, *Adv. Polym. Technol*., **5**, 87 (1985).

[20] - D. Suwanda, R. Lew and T. Balke, *J. Appl. Polym. Sci.*, **35**, 1019 (1988).

[21] – D. Suwanda, R. Lew and T. Balke, *J. Appl. Polym. Sci.*, **35**, 1033 (1988).

[22] – C. Tzoganakis, J. Vlachopoulos and A. E. Hamielec, *Polym. Eng. Sci*., **28**, 170 (1988).

[23] – C. Tzoganakis, Y. Tang and J. Vlachopoulos, *Polym. Plast. Technol. Eng.*, **28**, 319 (1989).

[24] – A. Pabedinskas, W.Cluett and S.Balke, *Polym. Eng. Sci.*, **34**, 993 (1994).

[25] – K. Ebner and J. L. White, *Intern. Polym. Processing IX*, 233 (1994).

[26] – M. G. Lachtermacher and A. Rudin, *J. Appl. Polym. Sci.*, **58**, 2077 (1995).

[27] – M. G. Lachtermacher and A. Rudin, *J. Appl. Polym. Sci*., **58**, 2433 (1995).

[28] – A. C. Kolbert, J: G. Didier and L. Xu, *Macromolecules*, 8598 (1996).

[29] – M. G. Lachtermacher and A. Rudin, *J. Appl. Polym. Sci*., **59**, 1775 (1996).

[30] – M. G. Lachtermacher and A. Rudin, *J. Appl. Polym. Sci*., **59**, 1213 (1996).

[31] – A. Holmstrom and E. M. Sorvik, *J. Polym. Sci*., **57**, 33 (1976).

[32] – G. R. Rideal and J. C. Padget, *J. Polymer Sci.: Symp*., **57**, 1 (1976).

[33] – G. E. Hulse, R. James and D. R: Warfel, *J. Polym. Sci.:Part A: Polym. Chem.*, **19**, 655 (1981).

[34] – J. Boer and A. J. Pennings, *Makromol. Chem.*, **2**, 749 (1981).

[35] – A. K. Khitrin, *J. Polym. Sci.:Part A: Polym. Chem*., **33**, 2413 (1991).

[36] – K. J. Kim, Y. S. Ok and B. K. Kim, *Eur. Polym. J*., **28**, 1487 (1992).

[37] – J. Sohma, *Colloid Polym. Sci*., **27**, 1060 (1992).

[38] – D. Suwanda and S. T. Balke, *Polym. Eng. Sci*., **33**, 1585 (1993).

[39] – S. Suyama, H. Ishigaki, Y. Watanabe and T. Nakamura, *Polym. J*., **27**, 371 (1995).

[40] – S. Suyama, H. Ishigaki, Y. Watanabe and T. Nakamura, *Polym. J*., **27**, 503 (1995).

[41] – A. Harlin and E. Heino, *J. Polym. Sci.: Part B: Polym. Physics*, **33**, 479 (1995).

[42] – P. Ghosh, D. Dev and A. Chakrabarti, *Polymer*, **38**, 6175 (1997).

[43] – A. Smedberg, T. Hjertberg and B. Gustafsson, *Polymer*, **38**, 4127 (1997).

[44] – N. G. Gaylord and R. Metha, *J. Polym. Sci.: Polym. Letters Ed.*, **21**, 23 (1983).

[45] – N. G. Gaylord and R. Metha, *J. Polym. Sci.: Part A: Polym. Chem.*, **26**, 1188 (1988).

[46] – K. E. Russel and E. C. Kelusky, *J. Polym. Sci.: Part A: Polym. Chem.*, **26**, 2273 (1988).

[47] – N. G. Gaylord, R. Metha, V. Kumar and M.Tazi, , *J. Appl. Polym. Sci.*, **38**, 359 (1989).

[48] – A. Sipos, J. McCarthy and K. E. Russel, *J. Polym. Sci.: Part A: Polym. Chem.*, **27**, 3353 (1989).

[49] – R. Rengarajan, V. R. Parameswaram and S. Lee, *Polymer*, **31**, 1703 (1990)

[59] – M. Aglietto, R. Bertani, G. Ruggeri and A. L. Segre, *Macromolecules*, **23**, 1928 (1990)

[51] – C. H. Wu and A. C. Su, *Polym. Eng. Sci.*, **31**, 1629 (1991).

[52] – R. Greco and P. Musto, *J. Appl. Polym. Sci*., **44**, 781 (1992).

[53] – A. J. Oostenbrink and R. J. Gaymans, *Polymer*, **33**, 3086 (1992).

[54] – C. H. Wu and A. C. Su, *Polymer*, **33**, 1989 (1992).

[55] – K. J. Ganzeveld and L. P. Janssen, *Polym. Eng. Sci.*, **32**, 467 (1992).

[56] – C. Wu, C. Chen, E.Woo and J. Kuo, *J. Polym. Sci.: Part A: Polym. Chem.*, **31**, 3405 (1993).

[57] – B. De Roover, M. Aclavons, V. Carlier, J. Devaux, R. Legras and A. Momtaz, *J. Polym. Sci.: Part A: Polrm. Chem.*, **33**, 829 (1995).

[58] – K. E. Russel, *J. Polym. Sci.: Part A: Polym. Chem.*, **33**, 555 (1995).

[59] – J. B. Wong Sing, W. E. Baker and K. E. Russel , *J. Polym. Sci.: Part A: Polym. Chem.*, **33**, 633 (1995).

[60] – M. Avela, N. Lanzetta and G.Maglio, In Polymer Blends (M. Kryszewski, A. Galeski and E. Martuscelli, Eds.) vol.2, Plenum, New York, 1984.

[61] – A. H. Hogt, Proc. Compalloy'90, New Orleans, USA, 1990.

[62] – C. Rosales, R. Perera, M. Ichazo, J. Gonzalez, H. Rojas, A. Sánchez and A. Barrios, *J. Appl. Polym. Sci*., **70**, 161 (1998).

[63] – B. Bray, S. Damiris, A. Grace, G. Moad, M. O'Shea, E. Rizzardo and G. Diepen, *Macromol. Symp.*, **129**, 109 (1998).

[64] – W. Heinen, C. H. Rosenmöller, C. B. Wenzel, H. J. M. de Groot, J. Lugtenburg and M. van Duin, *Macromolecules*, **29**, 1151 (1996).

[65] – S. Ranganathan, W. E Baker, K. E. Russel and R. A. Whitney, *J. Polym. Sci.: Part A: Polym. Chem.*, **37**, 3817 (1999).

[66] – L.A. Utracki, *Polymer Alloys and Blends*, Hanser Publishers, New York, 1989.

[67] – D. R. Paul, J. W. Barlow and H. Keskkula, Encycl. Polym. Sci. Eng., 2nd Ed., **12**, 399 (1988).

[68] – D. R. Paul and S. Newman, *Polymer Blends*, Academic Press, New York, 1979.

[69] – L.A. Utracki, Encyclopaedic Dictionary of Commercial Polymer Blends, ChemTec Publishing, Toronto, 1994.

[70] – S. Datta and D. Lohse, Polymeric Compatibilizers, Hanser Publishers, New York, 1996.

[71] - C. Koning, M. van Duin, C. Pagnoulle and R. Jerome, *Prog. Polym. Sci*., **23**, 707 (1998).

[72] – N. Gaylord, *J. Macromol. Sci.*, **26**, 1211 (1989).

[73] – M. Xanthos and S. Dagli, *Polym. Eng. Sci.*, **31**, 929 (1991).

[74] – V. J. Triacca, S. Ziaee, J. W. Barlow, H. Keskkula and D. R. Paul, *Polymer*, **32**, 1401 (1991).

[75] – N. Liu and W.E. Baker, *Adv. Polym. Tech.*, **11**, 249 (1992).

[76] – F. P. Mantia, *Adv. Polym. Tech*., **12**, 47 (1993).

[77] – S. S. Dali, M. Xanthos and J. A. Biesenberger, *Polym. Eng. Sci.*, **43**, 1720 (1994).

[78] – J. D. Lee and S. M. Yang, *Polym. Eng. Sci.*, **35**, 1821 (1995).

[79] – N. Choudhury and A. Bhowmick, *J. Appl. Polym. Sci.*, **38**, 1091 (1989).

[80] – A. Fumio, *J. Appl. Polym. Sci.*, **18**, 963 (1974).

[81] – J. J. Elmendorp and A. K. van der Vegt, *Polym. Eng. Sci.*, **26**, 1332 (1986).

[82] – S. Wu, *Polym. Eng. Sci.*, **27**, 335 (1987).

[83] – P. H. M. Elemans and H. E. M. Meijer, *Polym. Eng. Sci.*, **28**, 2751 (1988).

[84] – J. M. Willis, V. Caldas and B. D. Favis, *J. Mater. Sci*., **26**, 4742 (1991)

[85] – L. A. Utracki, *Polym. Networks Blends*, **1**, 61 (1991).

[86] – L. A. Utracki and Z. H. Shi, *Polym. Eng. Sci.*, **32**, 1824 (1992).

[87] – L. A. Utracki and Z. H. Shi, *Polym. Eng. Sci.*, **32**, 1834 (1992).

[88] – V. Bordereau, Z. H. Shi, L. A. Utracki, P. Sammut and M. Carrega, *Polym. Eng. Sci.*, **32**, 1846 (1992).

[89] – M. A. Huneault, Z. H. Shi and L. A. Utracki, *Polym. Eng. Sci.*, **35**, 115 (1995).

[90] – H. P. Grace, *Chem. Eng. Comm.*, **14**, 225 (1982).

[91] – D. Rumscheidt and S. G. Mason, *J. Coll. Sci.*, **16**, 238 (1961).

[92] – S. Torza, R. G. Cox and S. G. Mason, *J. Coll. Interf. Sci.*, **38**, 395 (1972).

[93] – L. Delamare and B. Vergnes, L. A. *Polym. Eng. Sci.*, **36**, 1685 (1996).

[94] – D. Young Moon and O. Park, *Adv. Polym. Tech.*, **17**, 203 (1998).

[95] – J. Karger-Kocsis and B. Vergnes, *Polym. Eng. Sci.*, **36**, 1685 (1996).

[96] – B. D. Favis and J. P. Chalifoux, *Polymer*, **29**, 1761 (1988)

[97] – C. E. Scott and C. W. Macosko, *Polym. Bulletin*, **26**, 341 (1991).

[98] – C. E. Scott and C. W. Macosko, *Polymer*, **35**, 5422 (1994).

[99] – U. Sundararaj, Y. Dori and C. W. Macosko, *Polymer*, **36**, 1995 (1995).

[100] – U. Sundararaj and C. W. Macosko, *Macromolecules*, **28**, 2647 (1995).

[101] – U. Sundararaj and C. W. Macosko, *Polym. Eng. Sci.*, **36**, 1769 (1996).

[102] – H. Cartier and G.H. Hu, *J. Polym. Eng. Sci.*, **39**, 996 (1999).

[103] – M. A. Huneault, M. F. Champagne, and A. Luciani, *Polym. Eng. Sci*., **36**, 1694 (1996).

[104] – O. Chung and A. Y. Coran, American Chemical Society Rubber Division, Kentucky, 1996.

[105] – T. Sakai, *Adv. Polym. Tech.*, **14**, 277 (1995).

[106] – O. Franzheim, M. Stephan, T. Rische, P. Heidemeyer, U. Burkhardt and A. Kiani, *Adv. Polym. Tech.*, **16**, 1 (1997).

[107] – J.A. Covas, Portuguese Patent n.101941 (1996).

2.1 - INTRODUCTION

Compounding with fillers and/or additives, blending and chemically modifying existing polymers are attractive methods of developing new materials for specific applications with an improved properties/cost balance. Polymer blends and compounds are commonly prepared by mechanical mixing of their components in the molten state. The performance of the materials produced is determined, amongst others, by the final morphology and dispersion, respectively. For blends the morphology depends on composition, rheological and physical characteristics of the components, relative compatibility and nature and intensity of the mixing. In fact, it is well known that using different mixers, and/or varying the mixing parameters, it becomes possible to control phase morphology [1-4] and, in this way, to improve the blend performance. Therefore, it is important to monitor the evolution of the morphology of polymer blends during their preparation and relate it to the mixing conditions used in industrial processes.

A variety of reactions has been used for the chemical modification of polymers [5,6], the most important being grafting, crosslinking, halogenation, condensation and exchange. In the case of reactive extrusion, it is important to know the effect of the operating conditions on the evolution of chemical conversion. This knowledge is necessary to identify side reactions and to guarantee high conversion.

Intermeshing co-rotating twin-screw extruders are often used for preparing polymer blends and/or modifying polymers on a commercial scale. However, there is relatively little information available on the morphology development or on the evolution of chemical conversion occurring along the screw in this type of equipment. Actually, an extruder can still be viewed as a black box. Most of the available data has been gathered using screw-pulling experiments, similar to those used in the late fifties for the understanding of the mechanisms involved in plastication in single-screw extruders [7]. These experiments are not only complicated, but also time consuming, several minutes elapse before actually taking the sample. Since freezing the polymer inside the extruder

to prevent any subsequent morphological changes is difficult, it is not surprising that coalescence of the minor phase has been reported [8,9].

The problem of collecting samples from the extruder has been revisited recently by a number of workers. The aim is to produce real time information that can be used to improve the efficiency of the physical and/or chemical processes, the design of the equipment and the capacity for on-line control. The approaches proposed encompass using a split barrel, stopping the extruder and pouring liquid nitrogen into entry ports [10], removing molten samples at entry ports with tweezers and quenching the material [8,11] and diverging a small amount of material from inside the extruder through a hole in the barrel and quenching it [9,12]. The use of these techniques decreases the required sampling time from several minutes in the screw pulling experiment to a few seconds. However, most of the above routines i) can either work only in pressurised, or conversely, partially filled zones of the screw, ii) require stopping the extruder prior to collecting samples, iii) may affect the melt flow conditions in the extruder, and/or iv) are laborious to manage. An on-line FT-IR technique has also been developed for studying reactive extrusion, but absolute chemical conversions could not be obtained as a result of polymer melt sticking to the IR probe [13].

A new device for collecting samples in less than five seconds, using the melt detour concept, was recently developed [14]. The apparatus can be inserted between any two extruder barrel segments or, alternatively, barrel segments can be replaced by several adjacent collecting units. This provides the possibility of obtaining polymer samples at relatively small increments along the length of the screw. This is particularly relevant when the aim of the work is to study the evolution of the chemical conversion of a reactive system along the extruder. The device can be operated quite simply while running the extruder, both with filled or partially filled screws, although in the later case collecting the same amount of material takes more time. This principle has already been used to measure residence time distributions at different locations of the extruder [15].

This work aims at ascertaining the practical interest offered by this new sampling device in terms of the information on physical and chemical processes occurring inside

the extruder. This will be accomplished by studying two different systems. Firstly, the morphology development of a non-compatibilized PA-6/EPM (polyamide-6/ethylene propylene rubber) blend was studied as a function of screw rate. Secondly, the evolution of chemical conversion of imidation of SMA (styrene/maleic anhydride copolymer) with 1-aminonaphtalene along the extruder was determined. In both cases, characteristics of the samples collected using the sampling device were compared with those obtained using the conventional screw pulling technique.

2.2 - EXPERIMENTAL PROCEDURE

2.2.1 – Materials

Commercial PA-6 (Akulon® K123), EPM (Keltan® 740) and SMA (Stapron® S: 22.8 wt.% MA) produced by DSM, the Netherlands, were used. The 1-aminonaphtalene was supplied by Aldrich. In the case of the PA-6/EPM blend, 10 and 20 % concentrations of the disperse phase (EPM) were used. The reactive system consisted of a 2.5/0.5 w/w, SMA/1-aminonaphtalene mixture.

2.2.2 - Screw configuration and processing conditions

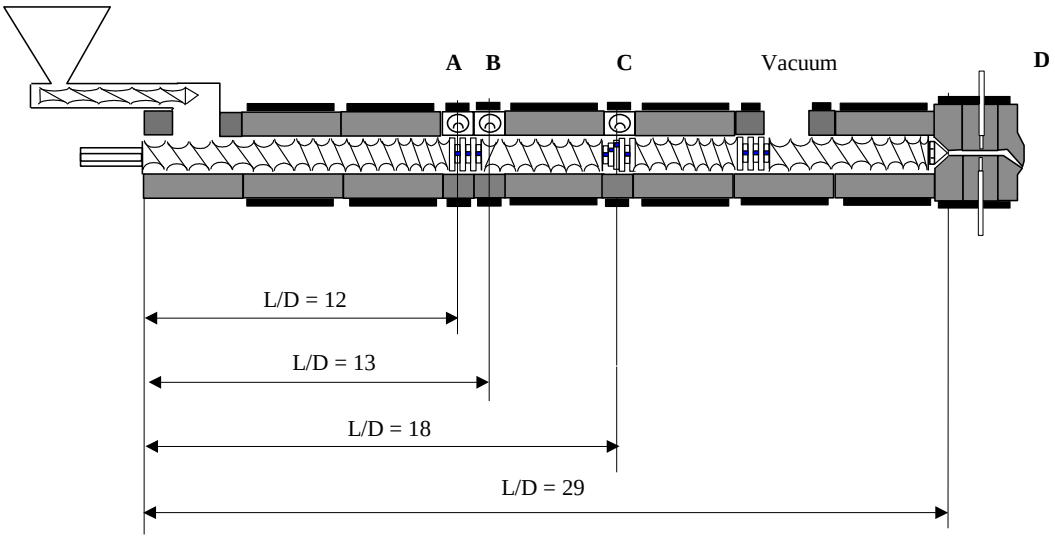

Figure 2.1 - Screw configuration and sampling locations.

The two systems were prepared in a laboratory modular Leistritz LSM 30.34 intermeshing co-rotating twin-screw extruder coupled to the relevant accessories. The configuration of the screws (L/D=29) and the locations of the sampling devices are depicted in Figure 2.1.

The blends were prepared using a barrel set temperature of 230 ºC and feeding the premixed components at a flow rate of 6 kg/h. The intensity of mixing was varied by selecting screw rotation speeds of 100, 150 and 200 rpm. In the case of the reactive system, a barrel set temperature of 210 ºC, screws rotating at 150 rpm and a flow rate of 6 kg/h of premixed SMA/1-aminonaphtalene were selected.

Sampling for the determination of the morphological evolution, or of the chemical conversion, was carried out at identical locations along the screws, when using either the sampling devices or when pulling the screws with the dedicated tool supplied by Leistritz. Samples of similar sizes were cooled in liquid nitrogen in order to ensure identical thermal histories. This was particularly easy with the new device, as it collects matching nut shaped specimens.

2.2.3 - Sampling device

The working principle of the sampling device is illustrated in Figure 2.2. The circular aperture in the barrel wall (1) allows the flow of material out of the extruder. The occurrence of this flow is controlled by the cylindrical valve (2), containing two cavities (3) and (4). When the valve is positioned as shown in Figure 2.2, there is no flow out of the extruder. However, accumulation of polymer material in hole (1) will take place. For collecting a portion of material from inside the extruder, the valve is rotated sequentially to expose hole (1) to cavity (3), where the accumulated material can be discarded. Upon further rotation, hole (1) is now exposed to cavity (4), which is rapidly filled with fresh material. The valve is rotated again to the position shown in Figure 2.2, where the sample is removed and quenched, for subsequent analysis. Collecting *circa* 2 g of polymer melt takes typically between 3 to 5 seconds (depending on flow rate and degree of filling).

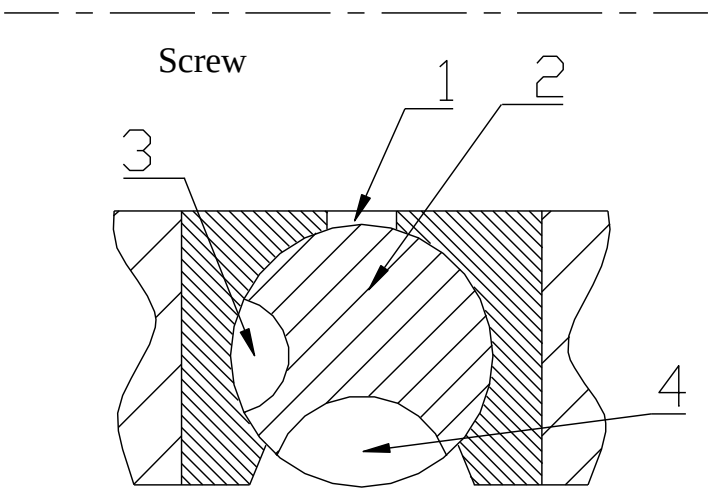

Figure 2.2 – Sampling device.

2.2.4 - Residence time

Upon reaching steady state during an extrusion experiment a small amount of tracer (silicon dioxide with specific surface of 175 m^2/g) was added instantaneously to the feed stream at t = 0. Samples of polymer plus tracer were then collected from each location along the extruder at various time intervals. The relative amount of silica present in each sample determined by ashing the sample is a straightforward measure of concentration with time. From this information it was possible to compute conventional residence time parameters, such as the cumulative residence time distribution, $F(\theta)$ and the mean residence time, $\bar{t}$ [16].

2.2.5 - Materials Characterization

The morphology of the systems under study was determined using a Jeol JSM 6310F Scanning Electron Microscope. The samples were fractured in liquid nitrogen and gold plated. An automatic method of image analysis (Leica Quantimet 550) was used to quantify the size of the disperse phase. As in other studies [9,17-21], equivalent circle diameters were computed from individual particle areas. The distribution width was estimated from the variance, i.e. the square of the standard deviation of the log-normal function.

The SMA/1-aminonaphtalene samples were dissolved in tetrahydrofuran (THF) and the IR spectra were recorded from the solutions using a liquid cell on a Perkin Elmer 1720 FT-IR spectrometer. The residual MA content of the SMA products was determined using the anhydride carbonyl signal at 1850 cm^{-1}. The FT-IR procedure was calibrated via titration of a set of SMA copolymers with MA contents of 10 to 40 wt.% MA. Some SMA/1-aminonaphtalene samples were dissolved in acetone and precipitated in n-hexane to remove unreacted 1-aminonaphtalene. Nitrogen contents of the SMA residues were determined after drying at 180 ºC under vacuum for 1 hour using a LECO FP-428 Nitrogen Analyser.

2.3 - RESULTS AND DISCUSSION

2.3.1 - PA-6/EPM Blends

Figure 2.3 shows a direct comparison of the morphologies of the PA-6/EPM blend (80/20 w/w, 150 rpm) at various positions along the screw (A, B and C), as obtained by the two sampling techniques, as well as the morphology of the final extrudate (D). Samples collected with the sampling device in location A (Figure 2.3a) exhibit sheets of PA-6 and rubber. After the first kneading zone, at location B (Figure 2.3c), droplets of the disperse EPM phase distributed in the PA-6 matrix can be observed. This morphological change can be related to the local mixing mechanism, involving a significant dispersive action [17] with rupture and distribution of the minor phase in the matrix. Samples collected in location C present a similar morphology, although the size of the disperse phase has decreased (Figure 2.3e), the process continuing up to the die (Figure 2.3g). These results show that the most significant evolution of morphology occurred in the initial zone of the extruder. In fact, after the first kneading section, only a moderate decrease in the average particle size of the minor phase can be detected. The final EPM dispersion is still rather coarse, since no compatibilizer was incorporated.

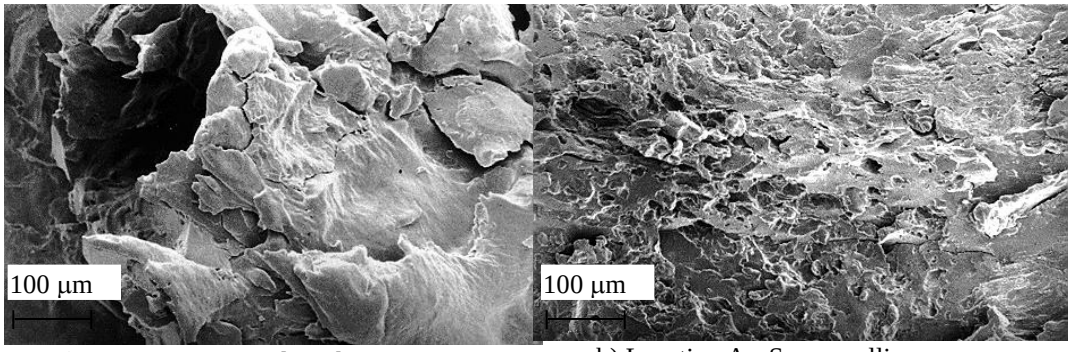

a) Location A- Sampling device; b) Location A - Screw pulling;

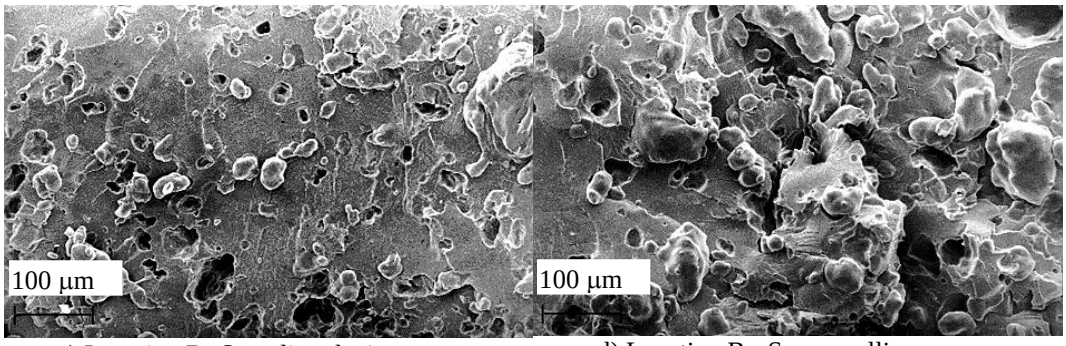

c) Location B- Sampling device; d) Location B - Screw pulling;

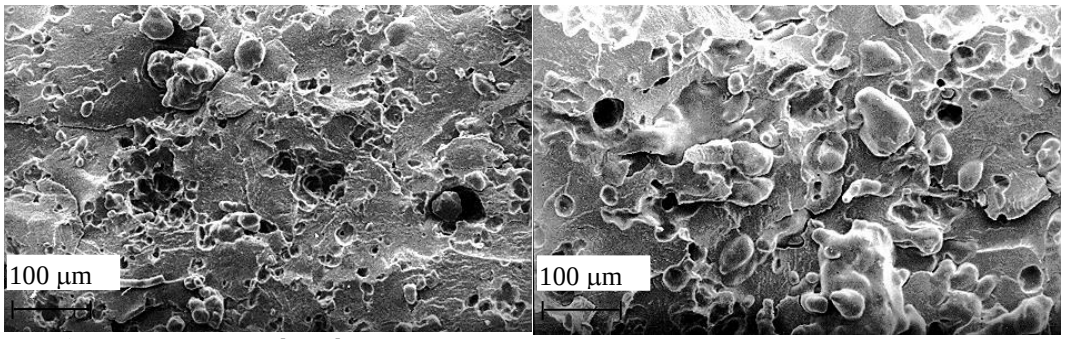

e) Location C- Sampling device; f) Location C - Screw pulling;

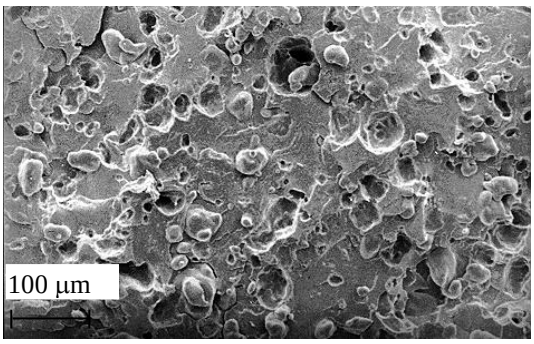

g) Location D.

Figure 2.3 - SEM micrographs of PA-6/EPM (80/20 w/w, 150rpm) removed from the extruder using the sampling device and collected after screw pulling; a) Location A- Sampling device; b) Location A - Screw pulling; c) Location B- Sampling device; d) Location B - Screw pulling; e) Location C- Sampling device; f) Location C - Screw pulling; g) Location D.

Samples collected using the screw pulling technique show the same type of evolution (Figure 2.3b, 3d and 3f). Nevertheless, differences in the morphology of equivalent samples obtained with the two methods are evident. The EPM particles shown in Figures 3a, 3c and 3e are smaller and more regular than those in Figures 3b, 3d and 3f respectively. This is attributed to particle coalescence in samples remaining molten for longer periods (*circa* 5 minutes), which is the case for those taken using the screw pulling technique [5,8,18,20].

The differences in the particle size of the two series of samples (i.e., with 10 and 20 % concentration of EPM) are also obvious in Tables 2.1 and 2.2, where the evolution of the average particle size in terms of equivalent circle diameter at various screw speeds is presented. The variance values show that the particle size distribution is broad when samples were collected after screw pulling. Samples collected with the new device show a narrower distribution in locations B and C.

Table 2.1 - Particle size of the disperse EPM phase in PA-6/EPM (80/20) blend [a].

Sampling location	Sampling method	100 rpm			150 rpm		
		Particle size			Particle size		
		Average (μm)	*Range* (μm)	*Variance* (μm^2)	*Average* (μm)	*Range* (μm)	*Variance* (μm^2)
B	device	49	26-70	196	40	18-66	169
	screw	69	25-106	484	56	23-162	900
C	device	43	21-109	289	35	20-71	144
	screw	53	28-118	576	54	23-80	324
D	extrudate	38	18-101	324	36	20-60	121

[a] Data for location A is not given since a lamellar morphology is obtained

Table 2.2 - Particle size of the disperse EPM phase in PA-6/EPM (90/10) blend [a].

Sampling location	Sampling method	100 rpm			150 rpm			200 rpm		
		Particle size			Particle size			Particle size		
		Average (μm)	*Range* (μm)	*Variance* (μm^2)	*Average* (μm)	*Range* (μm)	*Variance* (μm^2)	*Average* (μm)	*Range* (μm)	*Variance* (μm^2)
B	device	40	20-80	324	37	16-86	225	34	18-72	100
	screw	55	17-113	676	47	17-79	289	36	18-77	169
C	device	39	19-72	169	36	16-68	144	30	18-56	100
	screw	53	17-108	529	43	19-90	361	35	18-60	361
D	extrudate	41	17-76	144	32	16-75	169	32	17-60	121

[a] Data for location A is not given since a lamellar morphology is obtained

Tables 2.1 and 2.2 also show the evolution of the average particle size along the extruder, including the effect of the concentration of the dispersed phase and of the screw rotation speed on the particle size. An increase in EPM concentration results in an increase of the particle size, since particle interactions become more significant. An increase in screw speed leads to a reduction of the average particle size, which can be attributed to the higher shear stresses inducing significant droplets break up. These observations are in agreement with other studies [18,19,22-25].

2.3.2 - SMA imidation

The reaction of SMA with 1-aminonaphtalene at temperatures above 200 ºC results in the formation of cyclic imide:

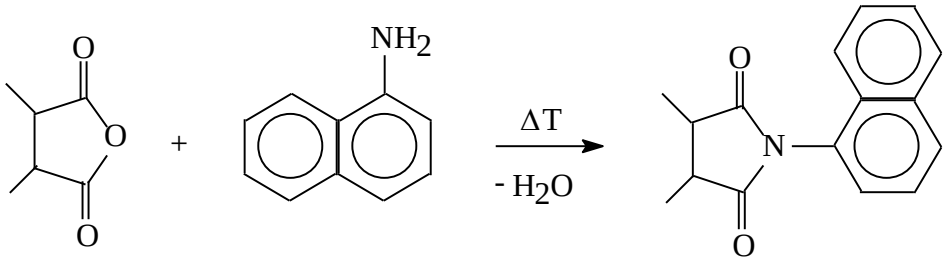

It was checked that 1-aminonaphtalene does not react with SMA at room temperature in the solid state, nor during preparation of the THF solution. Upon processing, the unreacted 1-aminonaphtalene was not devolatized (it has a boiling point of 306 ºC), but remained in the SMA product.

The residual MA contents of the various SMA samples, as determined with FT-IR, are given in Table 2.3. The evaluation of the nitrogen content of some samples allowed the calculation of the imide content and, consequently, of the residual MA content (Table 2.3, between brackets). They are in excellent agreement with the FT-IR data.

Table 2.3 - MA content (mol% ± 0.5mol%) determined by FT-IR for imidation of SMA[1] with 1-aminonaphtalene (2.5/0.5 w/w) as a function of the screw position.

Sampling location	Sampling device	Screw pulling
A	17.6 (17.4)[2]	14.9 (14.6)[2]
B	17.5	14.8
C	18.0	14.2
D	18.0 (17.4)[2]	

[1] MA content of starting material: 22.8 wt.% ≅ 23.9 mol%

[2] MA contents as determined via % N between brackets

In the first part of the extruder up to the first kneading zone (location A; $\bar{t}$ = 38 s) the MA content of SMA decreases from 23.9 to 17.6 mol%. Further on the screw (locations B, C and D, corresponding to $\bar{t}$ = 53, 73 and 145 s, respectively) the MA content hardly changes (the experimental error is ± 0.5 mol% MA). These results evidence that imidation occurs mainly in the melting zone and that additional reaction proceeds slowly. Since pulling the screws allows for further reaction for 5 minutes, it is not surprising that the residual MA contents show a small, but significant, decrease to about 14.5 mol%. As shown in Figure 2.4, the data obtained via the sampling device and screw pulling experiments fit satisfactorily a single curve. According to the recipe (SMA/aminonaphtalene = 2.5/0.5 w/w) the lowest residual MA content is 9.5 mol%, which is an indication that the imidation reaction is far from complete. The main conclusion from this part is that pulling the screws allows for further reaction and does not provide the correct chemical data.

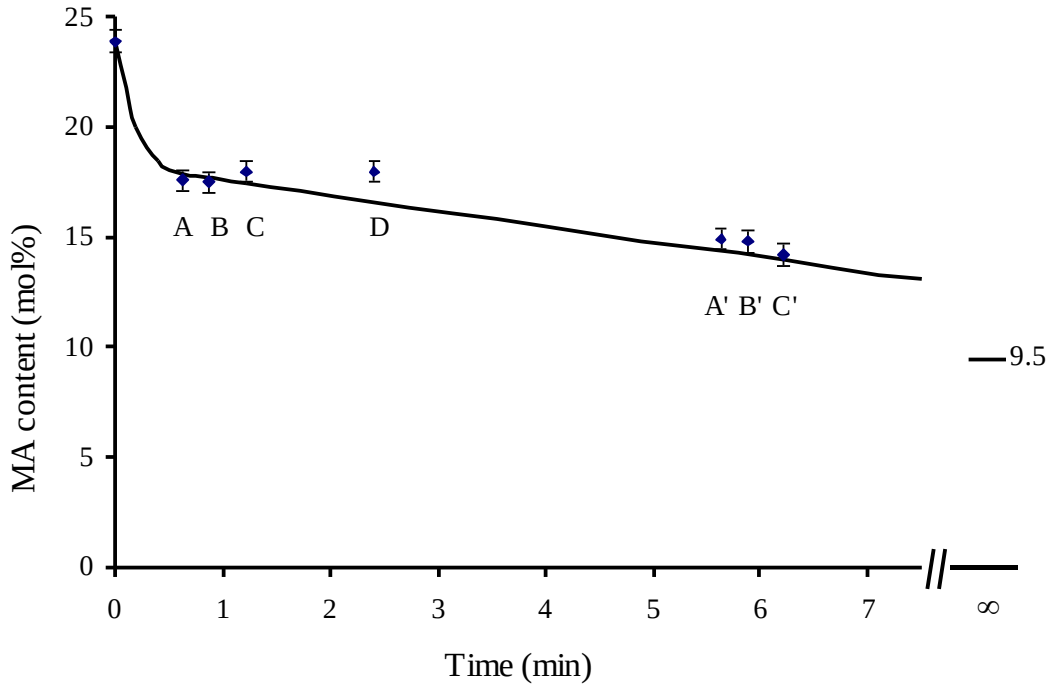

Figure 2.4 – Chemical conversion of SMA/1-aminonaphtalene imidation reaction as a function of the residence time (A, B, C and D - sampling device; A', B' and C' - screw pulling).

2.4 - CONCLUSIONS

The available sampling device enabled the pursuit of nearly real-time investigations of processes developing inside twin-screw extruders. Both blending and chemical modification of polymers could be studied, as illustrated by the PA-6/EPM blending and SMA imidation experiments reported in this work. It is clearly shown that screw pulling experiments can result in experimental artifacts and thus induce erroneous conclusions on physical/chemical mechanisms. In the near future, we will publish studies on "in-situ" compatibilization of PA-6/EPM/EPM-g-MA blends and grafting of MA using the sampling device described.

2.5 - REFERENCES

[1] – U. Sunsararaj and C. W. Macosko, *Polym. Eng. Sci*., **32,** 1814 (1992).

[2] – V. Bordereau, Z. H. Shi, L. A. Utracki, P. Sammut, and M. Carrega, *Polym. Eng. Sci*., **32**, 1846 (1992).

[3] – D. Paul and S. Newman, *Polymer Blends*, Academic Press, New York, 1978.

[4] – L. A. Utracki, *Two-Phase Polymer Systems*, Hanser Publishers, New York, 1991.

[5] – M. Xanthos, *Reactive Extrusion*, Hanser Publishers, New Jersey, 1992.

[6] – M. Lambla, *Comprehensive Polymer Science*, Pergamon Press, New York, 1993.

[7] – B. Maddock, *SPE J*., **15**, 383 (1959).

[8] – M. A. Huneault, M. F. Champagne, and A. Luciani, *Polym. Eng. Sci*., **36**, 1694 (1996).

[9] – M. Stephan, O. Franzheim, T. Rische, P. Heidemeyer, U. Burkhardt, and A. Kiani, *Adv. Polym. Tech.*, **16**, 1 (1997).

[10] – M. A Huneault, M. F. Champagne, L. E. Daigneault, and M. M. Dumoulin, SPE ANTEC Tech. Papers, **41**, 2020 (1995).

[11] – O. Chung and A. Y. Coran, American Chemical Society Rubber Division, Kentucky, 1996.

[12] – T. Sakai, *Adv. Polym. Tech.*, **14**, 277 (1995).

[13] – M. Stephan, L. Jakisch, and D. Fischer, PPS European Meeting, Stuttgart, Germany, 1995.

[14] – J.A. Covas, Patent Pending (1996).

[15] – O. S. Carneiro, G. Caldeira, and J. A. Covas, Proc. Adv. Mat. Proc. Technologies, Guimarães, Portugal, 1997.

[16] – D. Wolf and D. H. White, *AIChe Journal*, **22**, 123 (1976).

[17] – Z. H. Shi and L. A. Utracki, *Polym. Eng. Sci*., **32**, 1834 (1992).

[18] – C. Scott and C. W. Macosko, *Polymer*, **35**,5422 (1994).

[19] – B. Majumdar, D. R. Paul, and A. J. Oshinski, *Polymer*, **38**, 1787 (1997).

[20] – B. D. Favis and *J. App. Polym. Sci*., **39**, 285 (1990).

[21] – L. Yang and T. G. Smith, *Intern. Polym. Proc.*, **XII**, 11 (1997).

[22] – N. Chapleau and B. D. Flavis, *J. Materials Sci*., **30**, 142 (1995).

[23] – J. M. Willis and B. D. Favis, *Polym. Eng. Sci*., **30**, 1073 (1990).

[24] – B. D. Favis and J. P. Chalifoux, *Polymer*, **29**, 1761 (1988).

[25] – B. D. Favis and D. Therrien, *Polymer*, **32**,1474 (1991).

Part II

Polyolefin Modification

3.1 - INTRODUCTION

Considerable efforts have been made for producing new polymer materials with an improved performance/costs balance. This can be achieved by (co)polymerization of new monomers or by modification or blending of existing polymers. From a research and development point of view, the latter routes are usually more efficient and less expensive [1,2]. Free radical grafting of monomers is one of the most attractive ways for the chemical modification of polymers. It involves the reaction between a polymer and a vinyl-containing monomer, which is able to form grafts onto the polymer backbone in the presence of free radical generating chemicals, such as peroxides [1,2]. Such reactions can be performed in solution, yielding a relatively homogeneous medium because the reactants are easily mixed and the polymer and monomer are usually soluble. However, carrying out these reactions in the melt, i.e., via reactive extrusion, has economic advantages, as the modification is very fast and the need for solvent recovery is avoided.

Free radical grafting of maleic anhydride (MA) onto polyolefins has gained wide industrial application. MA modified polyolefins are an essential part of many plastics formulations. They are used as chemical coupling agents, impact modifiers, and compatibilizers for blends and filler reinforced systems [1-3]. Despite the large number of studies on MA grafting and the commercial success of MA grafted polyolefins, the chemical mechanism involved in the functionalization process is not fully understood. Several studies have shown that the reaction pathways depend on the polyolefin molecular structure. When a peroxide is used as initiator, crosslinking or chain scission may occur simultaneously with the grafting reaction. The dominant side reaction for polyethene (PE) is crosslinking [4-12], for polypropene (PP) is chain scission [13-17] and in the case of ethane/propene rubber (EPM) both crosslinking and chain scission may occur [18-24]. Grafting levels of PE are substantially higher than those of EPM and PP [25,26]. More subtle effects have been demonstrated. For example, Avella *et al*. [27] and Martinez *et al*. [20] showed that tacticity is also an important parameter and they found that the grafting level for atatic polypropene (aPP) was significantly higher

than that of isotatic polypropene (iPP). Recently, considerable progress has been made in elucidating the structure of MA grafted polyolefins. It was shown unambiguously that the MA graft structure consists of single saturated MA units [27]. Grafting occurs on secondary and/or tertiary carbons depending on the polyolefin composition. When long methylene sequences are present, grafting occurs mainly on secondary carbons. Actually, MA units seem to be attached to the polyolefin chain in close proximity of each other [28]. Despite the progress that has been made, the effect of the polyolefin composition on MA grafting is still not fully understood, due to the lack of true insight into the reaction mechanism. Actually, most grafting studies have been carried out using different grafting recipes (type and amount of peroxide and MA content) and different processing conditions (type of reactor, screw speed and temperature). As a result, a fair comparison of the experimental data in order to establish the true effect of the structure on grafting and crosslinking or degradation can not be made. This work aims at investigating the effect of the polyolefin structure on grafting and crosslinking or degradation both in the melt and in solution. A series of polyolefins with different ethene/propene ratios was modified with MA under similar conditions. The grafting yield was determined by FT-IR and the extent of crosslinking/degradation by dynamic rheological measurements.

3.2 - EXPERIMENTAL PROCEDURE

3.2.1 - Materials

The materials used together with their main characteristics are listed in Table 3.1. Maleic anhydride (MA) from Aldrich, 2,5–bis(tert-butylperoxy)-2,5-dimethylhexane (DHBP) from Akzo Nobel and biphenyl from Acros were used as monomer, initiator and solvent, respectively. The recipe used (5 phr of MA and 1 phr of peroxide) was identical in all the experiments.

Table 3.1 – Characteristics of the polyolefins used.

Polyolefin	Grade	Propene (wt.%)	Dynamic viscosity ($7x10^{-3}$ Hz at 200 ºC) (Pa.s)
HDPE1	DSM Stamylan HD 2H280	0	$4.3x10^2$
HDPE2	DSM Stamylex 7359	0	$2.0x10^2$
LDPE	DSM Stamylan LD 1922T	0	$4.4x10^2$
LLDPE1	DSM Stamylex LL 09-258	10[a]	$3.5x10^2$
LLDPE2	DEX Plastomers Exact 2M009	28[a]	$7.4x10^2$
EPM1	Exxon PE 805	22	$3.5x10^4$
EPM2	Exxon EPM X1703 F2	27	$1.2x10^4$
EPM3	DSM Keltan 740	40	$2.0x10^5$
EPM4	Exxon VA 404	55	$4.5x10^4$
EPM5	Shell non-commercial hydrogenated polyisoprene	60	$2.5x10^3$
EPM6	DSM Stamylan P 83E10	90	$3.6x10^4$
EPM7	DSM Stamylan P RA12MN40	95	$8.4x10^2$
iPP	DSM Stamylan P 13E10	100	$1.7x10^4$
aPP	Borealis non-commercial product	100	5
sPP	R & D sample DSM	100	$6.0x10^3$

a) octene instead of propene.

3.2.2 - Modification

Modification of the polyolefins was carried out both in the melt and in solution. Melt grafting was carried out in a modular Leistritz LSM 30.34 intermeshing co-rotating twin-screw extruder. Figure 3.1 shows the extruder layout. The screw configuration adopted, with three mixing zones consisting of sequences of kneading blocks and/or left hand elements, ensures efficient melting and homogenisation. In all experiments, the

barrel set temperature was 200 ºC, the screw speed 75 rpm and the throughput 5kg/h. The premixed materials were fed in the hopper. In order to collect small amounts of material during processing, six sampling devices were inserted in the barrel of the machine (for more details see reference 29). The evolution of grafting along the extruder could, therefore, be carried out and is reported separately [30]. Since the present study involves a significative number of polymers, material sampling from the extruder was only done at the location identified in Figure 3.1. Consequently, samples collected from the freshly molten material at the first kneading zone and from the extrudate were quenched in liquid nitrogen in order to prevent further reaction. In the case of atactic polypropene (aPP) and syndiotatic polypropene (sPP), melt modification was done in a Haake (Rheocord 90 equipped with a Rheomix 600) batch kneader under similar conditions, since only limited amounts of material were available.

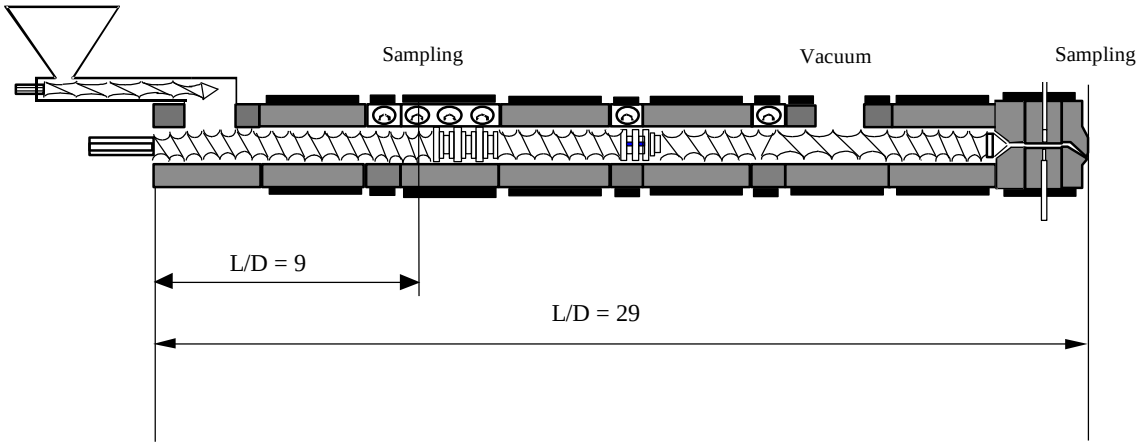

Figure 3.1 – Extruder layout and sampling locations.

Solution modification was performed in a glass reactor heated in an oil bath (180 ºC). Polymer, solvent and MA were added simultaneously in a 10/90/0.5 (w/w/w) ratio and the flask was purged with nitrogen. The materials were mixed with a glass stirrer until a clear solution was obtained. Then, the peroxide was added to start the grafting reaction. After 20 minutes (approximately 35 times the half life time of DHBP) the hot solution was precipitated in acetone (1/10; v/v) and the polymer was recovered for further characterization.

3.2.3 - Characterization

The materials modified in the melt were dissolved in toluene (PE and EPM) or xylene (PP) under reflux until a clear solution was obtained. Then, these solutions were precipitated in acetone and filtered in order to obtain the purified products. The precipitated products obtained in the melt and in solution were dried in a vacuum oven for 1 hour at 180 ºC. Thin films were prepared by compression-moulding and FT-IR spectra were recorded on a Perkin-Elmer 1600 spectrometer. The grafted MA content is expressed as the extinction of the anhydride peak at 1785 cm^{-1} normalized by the film thickness (E/f).

For rheological measurements, the original and modified polyolefins were compression-moulded as discs of 4 cm in diameter and 2 mm in thickness for 10 minutes, at 200 ºC, under a pressure of 30 ton. Oscillatory measurements were carried out in a TA Instruments Weissenberg rotational rheometer with parallel-plate geometry. The gap and diameter of the plates was 1.8 mm and 4.0 cm, respectively. The linear viscoelastic material's response was measured at 200 ºC, imposing a constant strain of 0.01, and carrying out a frequency sweep from $4x10^{-3}$ to 40 Hz .

3.3 - RESULTS

The MA graft content and the dynamic viscosity (at constant frequency) of the different polyolefins modified in the melt and in solution are presented in Table 3.2. Data for melt modification for both the material collected from inside the extruder and from the extrudate are included. At the first kneading zone the conversion of the grafting reaction is significant, viz.15-70 % of the final conversion of the extrudate. The dynamic viscosity of the samples collected at the kneading zone is quite similar to that taken from the extrudate. Thus, a considerable part of the various modification reactions occurs already in the first kneading zone, i.e., upon melting. The evolution of the reactions along the extruder axis will be discussed in a separate paper [30].

Table 3.2 –MA graft content (E/f) and dynamic viscosity ($7x10^{-3}$ Hz at 200 ºC) of the various polyolefins after melt and solution modification.

Polyolefin	Melt modification				Solution modification	
	Kneading zone		Extrudate			
	E/f ($1x10^{-3}$)	Viscosity (Pa.s)	E/f ($1x10^{-3}$)	Viscosity (Pa.s)	E/f ($1x10^{-3}$)	Viscosity (Pa.s)
HDPE1	3	$1.5x10^5$	18	$1.2x10^5$	14	$1.5x10^5$
HDPE2	6	$1.1x10^5$	21	$9.3x10^4$	13	$5.1x10^4$
LDPE	7	$3.2x10^4$	12	$5.0x10^4$	18	$2.2x10^4$
LLDPE1	12	$5.3x10^4$	18	$6.0x10^4$	15	$5.0x10^4$
LLDPE2	9	$1.0x10^5$	17	$1.5x10^5$	18	$4.1x10^4$
EPM1	a	$2.1x10^5$	a	$4.5x10^5$	-	-
EPM2	13	$4.0x10^5$	20	$3.0x10^5$	17	$1.4x10^5$
EPM3	a	$2.0x10^5$	a	$1.8x10^5$	12	$1.5x10^5$
EPM4	8	$1.3x10^5$	20	$1.7x10^4$	13	$8.2x10^3$
EPM5	14	$1.2x10^4$	23	$1.9x10^4$	18	$1.2x10^4$
EPM6	1	$1.1x10^4$	7	$3.9x10^3$	9	$3.9x10^3$
EPM7	1	230	4	150	6	70
iPP	1	$3.7x10^3$	3 (3)	25	4	20
aPP			(3)		5	-
sPP			(3)		6	$4.2x10^2$
EPM3/iPP (50/50)	4	$1.9x10^4$	6	$4.5x10^3$	8	$1.9x10^3$

a) could not be determined due to extensive crosslinking.
b) data between brackets for products grafted in a batch kneader.

MA graft contents of the modified polyolefins both in the melt and in solution clearly depend on the initial polyolefin structure (Table 3.2 and Figure 3.2), which is in agreement with the results of Hogt *et al.* and Avela *et al.* [25, 26]. The MA content has a constant level until ~50 wt.% propene, it decreases to E/f~0.020-0.015 as the propene content increases and is low (E/f~0.004) for polymers with a high propene content. PPs

with different tacticity (iPP, aPP and sPP) show similar values of grafted MA, which is in contrast with the results obtained by Martinez *et al.* [20].

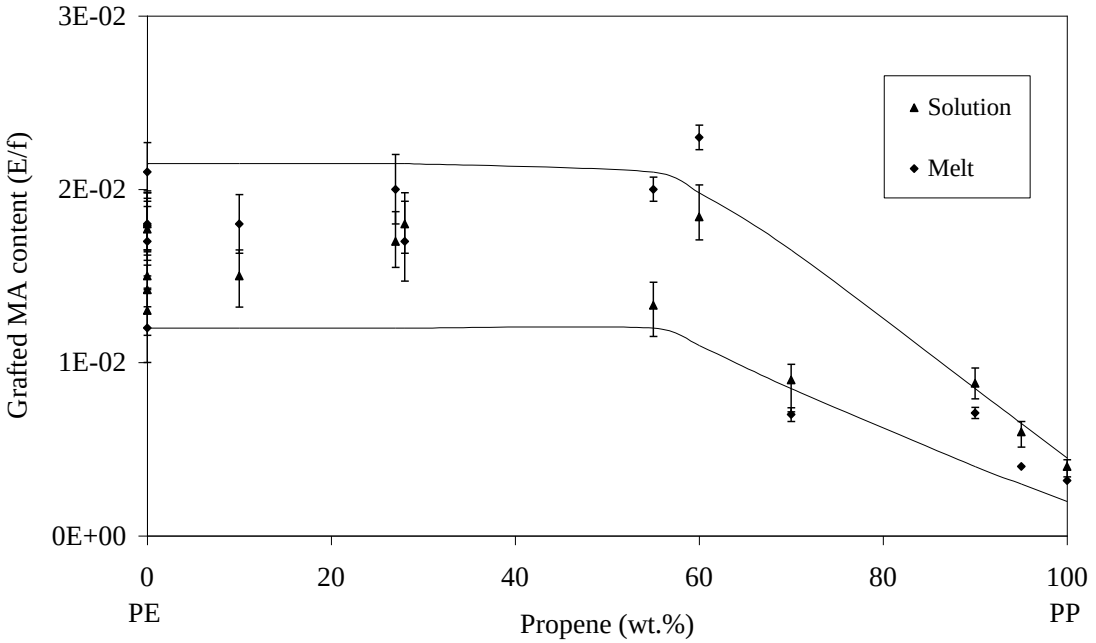

Figure 3.2 – Maleic anhydride graft level expressed as FT-IR extinction of anhydride band at 1785 cm-1 normalize to film thickness (E/f) as a function of propene content.

Within the experimental error (circa 10% of the measured value), the MA graft contents acquired both in the melt and in solution are similar. As shown in Figure 3.2 all the experimental values are contained within a range, except for EPM5, which has a somewhat higher MA graft content. For HDPE variation of the molecular weight does not have a significant effect on the degree of grafting. For EPM3/iPP blend MA grafted content levels are determined, which fall in the band.

Figures 3.3 show the change of viscosity as a function of propene content. Since the rheology of the modified polyolefins should be not only dependent on the chemical reaction but also on the rheology of the original polymer, the ratio of the two seems more relevant. The modified polymers with low propene content (less than 20 wt.%) have a high viscosity. The viscosity decreases significantly when the propene content is approximately 50 wt.% and the lowest viscosity is observed for PP (100 wt.% propene). Thus, branching/crosslinking dominates at low propene contents and degradation at high propene contents.

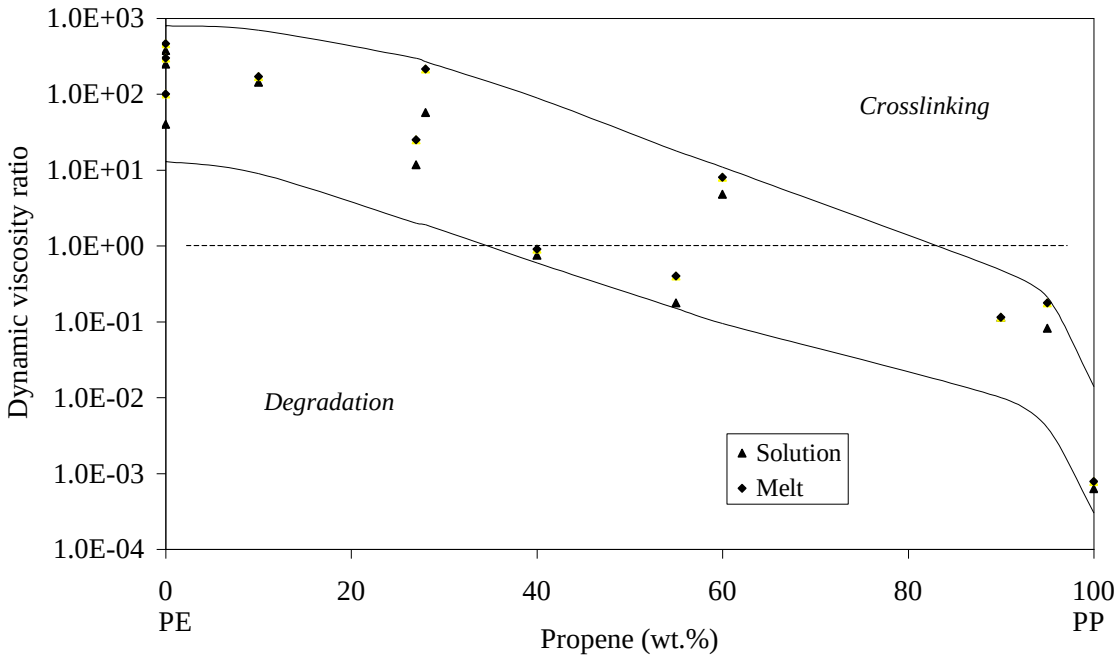

Figure 3.3 – Ratio of dynamic viscosities ($7x10^{-3}$ Hz) of modified and original polyolefins as a function of propene content.

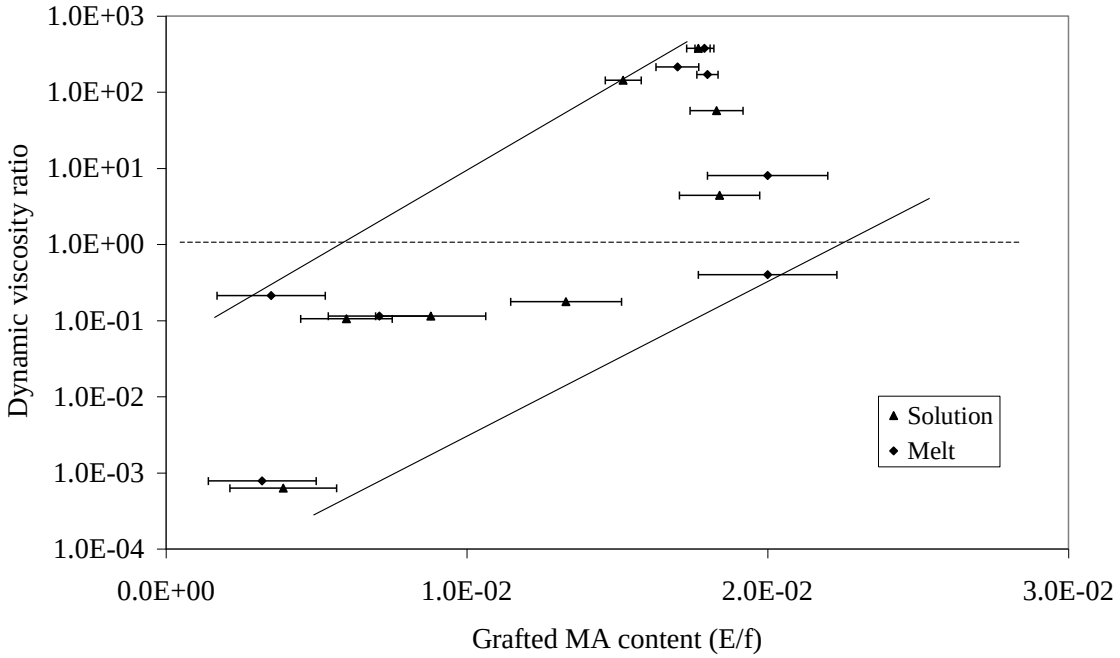

Figure 3.4 – Ratio of dynamic viscosities ($7x10^{-3}$ Hz) of modified and original polyolefins as a function of the maleic anhydride graft level.

The variation of the ratio of the dynamic viscosities with the MA graft content is given in Figure 3.4. A relationship between these two parameters is observed, viz. low MA graft contents are associated with low viscosities.

3.4 - DISCUSSION

The above results will be discussed on the basis of a mechanism for the free radical grafting of unsaturated monomers onto polyolefins (Figure 3.5). Although this mechanism is not proven in a truly scientific way, it is an adapted version of the free radical polymerization mechanism and is generally accepted and used [1-3]. Graft copolymerisation is initiated by the generation of free radical species, for instance, by the thermal decomposition of a peroxide, ROOR, into primary alkoxy radicals RO•, which may subsequently decompose to secondary radicals. A peroxide derived radical abstracts a H-atom from the polyolefin backbone, producing a macromolecular radical P•. Next, a first monomer (M) adds to the polymer radical forming P-M• which, depending on the structure of the monomer and/or the experimental conditions, may be followed by propagation to P-$(M)_n$•. When H-transfer occurs, the final graft structure is obtained P-$(M)_n$-H and a new polymer radical is formed, which may start up a new grafting cycle. Propagation usually does not occur for MA, hence P-MA-H is the final graft structure [27]. It has been shown that substantial intramolecular H-transfer occurs for MA, yielding multiple MA grafts in close proximity [28]. Polymerization of the monomer can be initiated not only by the macromolecular radical, but also by a peroxide derived radical, which will eventually result in the formation of free polymer. For MA it is believed that free oligomers are only formed when the MA added is not fully dissolved in the polymer melt or in the solvent. Termination of the various free radical species may in principle occur via combination to P-P or disproportionation to P'$^{=}$ and P'-H. The polymer radical may also undergo degradation via β-scission, yielding P"$^{=}$ and P"•. Termination products derived from P-MA• are not formed [27].

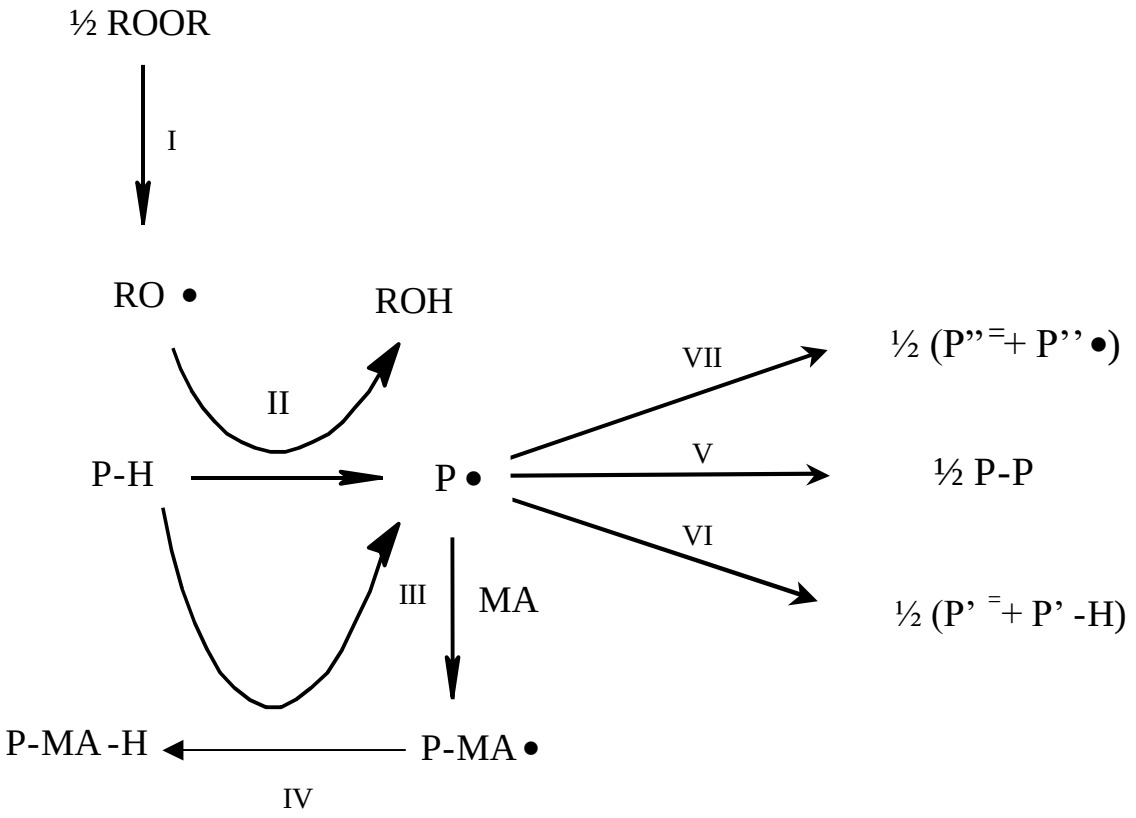

Figure 3.5 – Simplified mechanism of maleic anhydride free radical grafting I: peroxide decomposition; II: H-abstraction; III: monomer addition; IV: H-transfer to polyolefin; V: combination; VI: disproportionation and VII: β-scission.

In our study it was shown that the presence of a very large amount of biphenyl does not affect the degree of MA grafting, nor the rheological properties of the modified polyolefin. Biphenyl only contains aromatic H-atoms, which in comparison to aliphatic H-atoms present in the polyolefins, are hardly susceptible for H-abstraction. As a result, H-abstraction in a polyolefin solution in biphenyl will only yield polyolefin radicals and, thus, grafting just occurs on the polyolefin. Obviously, when a solvent with more labile H-atoms is used, such as an alkane, the solvent will also be grafted, resulting in a decrease of the polymer MA graft content. This is supported by the demonstration of grafting onto n-alkanes, which are used as low molecular models for polyolefins [28].

The alkyl radicals obtained by H-abstraction from polyolefins will have a planar structure and there will be hardly any preference for the monomer to approach the carbon centered radical either from above or below the plane. Whether starting with

iPP, aPP or sPP, after H-abstraction the tacticity is lost and grafting will proceed independently of the original tacticity. Therefore, the degree of grafting of iPP, aPP and sPP should be equal as it was shown for both grafting in the melt and in solution. The effects of tacticity as observed by Martinez *et al.* [20] can not be explained.

PE termination clearly occurs via combination of two P• radicals. Branched or even crosslinked PE is formed during processing of PE in the presence of peroxides both in the absence [31-35] or in presence of MA (Table 2; [4-12]). It is well-established that in the presence of peroxides, n-alkanes form dimmers [36]. It is assumed that the structure of peroxide crosslinked PE is similar, i.e., that exists linkages between tertiary C-atoms, as it was demonstrated with Solid state ^{13}C NMR for PE crosslinked via radiation [37]. It is noted that crosslinking does not occur via combination of P• with P-MA• radicals or of two P-MA• radicals [27]. The competition between the propagation and combination reactions determines the number of propagation cycli and, thus, is one of the main parameters determining the graft efficiency. Assuming a peroxide efficiency of 50%, one can calculate from the MA graft content usually obtained for PE (~1 wt.%) and from the amount of peroxide usually applied, that the number of propagation cycli is in the order of magnitude of ~10 mol MA grafted per 1/2 mol of peroxide.

In the case of PP, degradation via β-scission of P• radicals occurs. This is used on a commercial scale for producing controlled rheology PP [1,38-40]. It has been stated that the relatively low degree of grafting for PP is the result of β-scission. However, this is an oversimplification, since β-scission is not a termination reaction, but produces an equivalent of secondary P"• radicals. MA grafts derived from P"• radicals have not been identified [27], which indicates that for some reason the P"• radicals terminate relatively rapidly. The latter, in combination with a rate of β-scission of P• radicals slightly above that of the addition of MA to P• radicals, probably explains why the MA graft content of PP is lower than that of PE. Typical PP grafting studies involve a peroxide range from 0.23 to 1.25 wt.% and results in 0.15-1.08 wt.% MA grafted. The order of magnitude for the number of grafting cycli for PP is calculated to be about 3.

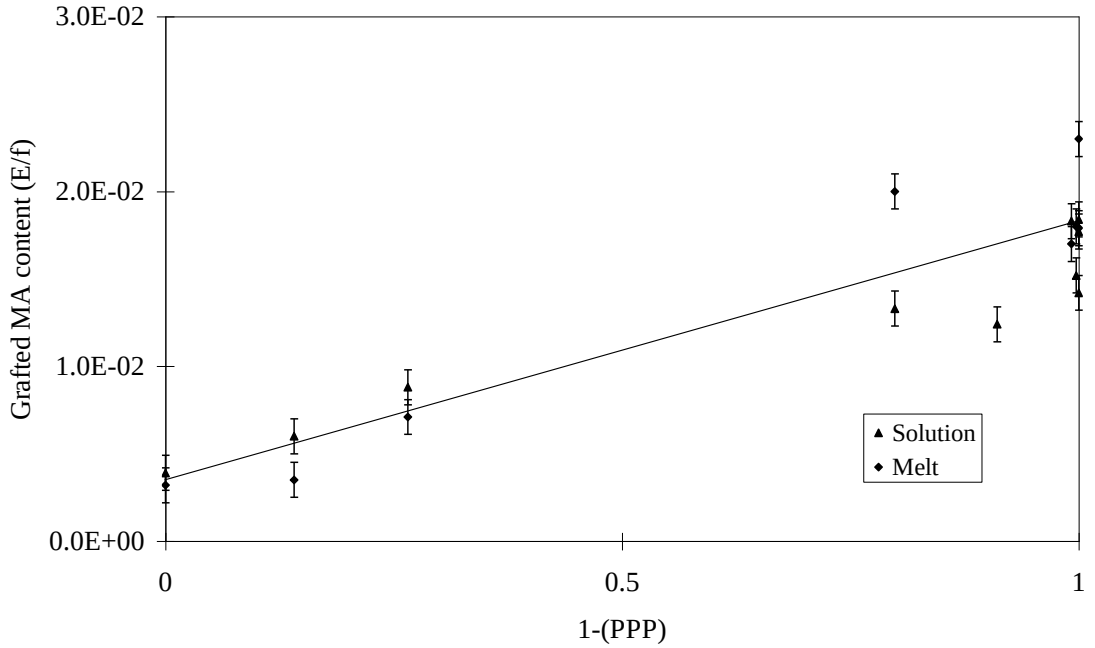

Figure 3.6 – Maleic anhydride graft level as a function of calculated fraction of non-PPP triads (1-[PPP]).

One would anticipate that EPMs will have a behaviour between those of PE and PP. However, the MA graft level of EPM with up to 50 wt.% propene is more or less similar to that of PE. Only when the propene content is above 50 wt.%, the MA graft content starts to decrease with minimum levels for PP. At closer inspection of Figure 3.3, it seems that both in the melt and in solution, the MA graft content of EPM5 (hydrogenated polyisoprene) is slightly above that of random EPMs. This suggests a specific effect of the ethene/propene sequence distribution. If the MA graft content is plotted not against the propene content (Figure 3.2), but against the calculated number of propene centred triades different from the PPP sequence, i.e. 1-[PPP], a linear correlation is obtained (Figure 3.6). For EPM5, 1-[PPP] is zero and, thus, equal to that of PE. The MA content of EPM5 is indeed close to those determined for HDPE and LDPE. In addition, it was shown that grafting of MA onto EPM5 occurs on methylene C-atoms only [27], which again demonstrates that EPM5 behaves similarly to PE. It is not clear why the presence of PPP-triades is decisive for the MA graft content. Probably, β-scission of a PPP sequence is faster than that of EPP or EPE sequences, since in the former case always P”$^{=}$ with a dialkyl-substituted and, thus, a relatively

stable unsaturation, is formed. The dynamic viscosity ratio depends on the propene content over the whole propene range from PE to PP (Figure 3.3) and does not level off like the MA graft content. Since the logarithm of the dynamic viscosity is proportional to the molecular weight, the actual number of chain scissions per chain is exponentially increasing with the propene content and eventually may produce an improved correlation with 1-[PPP].

3.5 - CONCLUSIONS

Significant differences in MA grafting and rheological behaviour were obtained depending on the original polyolefin structure. The MA graft content was low for polyolefins with high propene content and high when the propene content was below 50 wt.%. The degree of grafting was independent of the method used, i.e. solution or melt grafting. A decrease of the propene content of the polyolefin results in a transition from degradation to branching/crosslinking. The experimental data can be explained by using a general scheme for free radical grafting onto polyolefins.

3.6 - REFERENCES

[1] – Reactive Extrusion, M. Xanthos (Ed.), Hanser Publishers, New York, 1992.

[2] –Reactive Modifiers for Polymers, S. Al-Malaika (Ed.), Blackie Academic & Professional, London, 1997.

[3] – G. Moad, *Prog. Polym. Sci.*, **24**, 81 (1999).

[4] – S. Porejko, W. Gabara and J. Kulesza, *J. Polym. Sci.: Part A-1*, **5**, 1563 (1967).

[5] – S. Porejko, W. Gabara, T. Blazejewicz and M. Lecka, *J. Polym. Sci.: Part A-1*, **7**, 1617 (1969).

[6] – R. Greco, P. Musto, F. Riva and G. Maglio, *J. Appl. Polym. Sci*., **37**, 789 (1989).

[7] – A. E. Hamielec, P. E. Gloor, S. Zhu and Y. Tang, Proc. Compalloy'90, New Orleans, USA, 1990.

[8] – R. M. Ho, A. C. Su, C. H. Wu and S. I. Chen, *Polymer*, **34**, 3264 (1993).

[9] – Y. H. R. Jois and J. M. Bronk, *Polymer*, **37**, 4345 (1996).

[10] – D. H. Roberts, R. C. Constable and S. Thiruvengada, *Polym. Eng. Sci.*, 3**7**, 1421 (1997).

[11] – T. Bray, S. Damiris, A. Grace, G. Moad, M. O'Shea, E. Rizzardo and G. V. Diepen, *Macromol. Symp.*, **129**, 109 (1998).

[12] – C. Rosales, R. Perera, M. Ichazo, J. Gonzalez, H. Rojas, A. Sánchez and A. Barrios, *J. Appl. Polym. Sci*., **70**, 161 (1998).

[13] – H. Chiu and W. Chiu, *J. Appl. Polym. Sci*., **68**, 977 (1998).

[14] – N. G. Gaylord, M. Mehta and R. Mehta, *J. Appl. Polym. Sci*., **33**, 2549 (1987).

[15] – C. H. Wu and A. C. Su, *Polym. Eng. Sci.*, **31**, 1629 (1991).

[16] – R. Greco and P. Musto, *J. Appl. Polym. Sci*., **44**, 781 (1992).

[17] – A. J. Oostenbrink and R. J. Gaymans, *Polymer*, **33**, 3086 (1992).

[18] – C. H. Wu and A. C. Su, *Polymer*, **33**, 1989 (1992).

[19] – C. Wu, C. Chen, E.Woo and J. Kuo, *J. Polym. Sci.: Part A: Polym. Chem.*, **31**, 3405 (1993).

[20] – J. M. García-Martínez, O. Laguna and E. P. Collar, *Intern. Polym. Processing IX*, 246 (1994).

[21] – J. M. García-Martínez, O. Laguna and E. P. Collar, *Intern. Polym. Processing IX*, 346 (1994).

[22] – B. J. Kim and J. L. White, *Intern. Polym. Processing X*, 213 (1995).

[23] – A. K. Ray, A. Jha and A. K. Bhowmick, *J. Elast. Plast.*, **29**, 201 (1997).

[24] – J. M. García-Martínez, O. Laguna and E. P. Collar, *J. Appl. Polym. Sci*., **68**, 483 (1998).

[25] – A. H. Hogt, Proc. Compalloy'90, New Orleans, USA, 1990.

[26] – M. Avela, N. Lanzetta and G.Maglio, Polymer Blends (M. Kryszewski, A. Galeski and E. Martuscelli, Eds.), vol.2, Plenum, New York, 1984.

[27] – W. Heinen, C. H. Rosenmöller, C. B. Wenzel, H. J. M. de Groot, J. Lugtenburg and M. van Duin, *Macromolecules*, **29**, 1151 (1996).

[28] – S. Ranganathan, W. E. Baker, K. E. Russel and R. A Whitney, *J. Polym. Sci.: Part A: Polym. Chem.*, **37**, 3817 (1999).

[29] – A. V. Machado, J. A. Covas and M. van Duin, *J. Appl. Polym. Sci.,***71**, 136 (1999).

[30] – A. V. Machado, J. A. Covas and M. van Duin, submitted to J. Polym. Sci.: Part A: Polym. Chem..

[31] – S. Suyama, H. Ishigaki, Y. Watanabe and T. Nakamura, *Polymer*, **27**, 503 (1995).

[32] – P. Ghosh, D. Dev and A. Chakrabarti, *Polymer*, **38**, 6175 (1997).

[33] – A. Harlin and E. Heino, *J. Polym. Sci.: Part B: Polym. Phys*., **33**, 479 (1995).

[34] – A. Smedberg, T. Hjertberg and B. Gustafsson, *Polymer*, **38**, 4127 (1997).

[35] – A. V. Machado, J. A. Covas and M. van Duin, submitted to J. Appl. Polym. Sci..

[36] – J. D. van Drumpt and H. J Oosterwijk, *J. Polym. Sci.: Part A: Polym. Chem.*, **14**, 1495 (1976).

[37] – F. Horil, Q. Zhu, R. Kitamaru and H. Yomaoka, *Macromolecules*, 2**3**, 977 (1990).

[38] – K. Ebner and J. L. White, *Intern. Polym. Proc. IX*, 233 (1994).

[39] – A. C. Kolbert, J. G. Didier and L. Xu, *Macromolecules*, 8598 (1996).

[40] – M. G. Lachtermacher and A. Rudin, *J. Appl. Polym. Sci*., **58**, 2077 (1995).

4.1 - INTRODUCTION

Polymer melt processing has been associated with the development of physical phenomena created by thermal energy and mechanical stresses. However, it is also known that the input of mechanical and thermal energy to polymers may result in chemical or mechanochemical effects [1-4]. Processing of polyolefins yields products with properties that can be related to the chemical reactions induced by the operating conditions, the high temperatures and the presence of oxygen [1]. If these reactions are uncontrolled, processed polymers with inferior properties may be obtained. These reactions are often referred to as "degradation". However, mechanochemical effects can also be used advantageously. For example, shear-induced polymer reactions with fillers can enhance filler dispersion and, consequently, improve the properties of the compounds. Crosslinking of polyethene (PE), controlled degradation of polypropene (PP) and hydrolysis of polycondensate polymers are used to produce materials with improved properties. Frequently, chemicals are added during melt processing in order to enhance these mechanochemical effects. For example, branching or crosslinking of PE using peroxides or silanes produces materials with improved heat and chemical resistance and lower stress cracking and shrinkage [3-17]. The degradation of PP initiated by peroxides yields grades with lower molecular weight and/or a narrower molecular weight distribution [2-6, 18-23]. These types of reactions only modify the physical structure of the polymers. In order to change the chemical structure of the polymer, other types of reactions by adding extra chemicals, such as grafting, transesterification, and imidization or by adding other polymers (i.e. reactive blending) may be performed [1-4]. In short, it may be useful to have reactions during processing for a wide range of applications.

It has been demonstrated that extruders are effective reactors in which the chemical modification of polymers can be achieved economically [1-4]. However, extruders have largely been used as black boxes, where the process and the product quality are improved by changing the operating conditions without having an actual insight into the chemical reactions developing along the screw axis. In order to change this situation

material sampling techniques have been developed [24, 25]. For example, sampling devices have been used to study the evolution of chemical conversion and morphology development in PA-6/EPM/EPM-g-MA blends along the screw [26]. These devices can be located along the barrel and samples can be collected, in a few seconds, for subsequent characterization. In the present work these devices are used to study the evolution of polyolefin structure upon processing in a twin-screw extruder in the absence or in the presence of peroxide. Various polyolefins with various ethene/propene ratios, such as PEs (0 wt.%), EPMs (22 to 55 wt.%) and PPs (100 wt.%), were studied.

4.2 - EXPERIMENTAL

4.2.1 - Materials

A series of polyolefins with varying ethene/propene ratio, supplied by DSM and Exxon, were selected. Their characteristics together with the amount of peroxide used in each experiment are presented in Table 1.

Table 4.1 – Polyolefins, characteristics and amounts of peroxide used.

Polyolefin	Manufacturer/Grade	Propene content (wt. %)	Molecular weight, $\bar{M}_w$, (kg/mol)	Amount of peroxide (phr)
PE1	HDPE - DSM Stamylan HD 2H280	0	60	0; 0.1; 1
PE2	HDPE - DSM Stamylex 7359	0	30	0
PE3	LDPE - DSM Stamylan LD 2100TN00	0	360	0; 0.1
EPM1	Exxon PE 805	22	120	0; 0.1
EPM2	Exxon EPM X1-703F2	27	80	0; 0.1
EPM3	Exxon VA 404	55	-	0; 0.1
PP	DSM Stamylan P 13E10	100	500	0; 0.1; 1

The peroxide, 2,5–bis(tert-butylperoxy)-2,5-dimethylhexane (Trigonox 101: DHBP), used as the initiator for crosslinking or degradation reactions was supplied by Akzo Nobel, the Netherlands. The half-life time of the peroxide at 200 ºC is 6.1 s.

4.2.2 - Processing

The polyolefins were tumble mixed with different concentrations of peroxide and processed in a laboratory modular Leistritz LSM 30.34 intermeshing co-rotating twin-screw extruder (Figure 4.1). No special precautions against the presence of oxygen were taken. For all experiments, the barrel set temperature was 200 ºC, the screw speed 75 rpm and the flow rate 5 kg/h. Samples for subsequent off-line characterization were quickly collected along the extruder axis using a series of sampling devices (see [24] for details) and were immediately quenched in liquid nitrogen in order to avoid further reaction. The location of these devices is also shown in Figure 4.1. Generally, locations where significant stresses develop were chosen for this purpose. The screw contains a series of transport elements separated by three mixing zones, consisting of staggered kneading disks and a left hand element, respectively. They produce intensive mixing, together with the development of local pressure gradients. Melting of the solid polymer is caused by the mechanical stresses developed by the mixing block upstream.

The melt temperature was also measured at the sampling points. A needle type thermocouple with a small time constant (1 s) was used. Immediately after rotating the sampling device in order to collect polymer material, the pre-heated needle was stuck into the molten volume and a measurement was made. The error associated with this simple procedure is estimated to be of only a few degrees Celsius, as shown in a separate work [27].

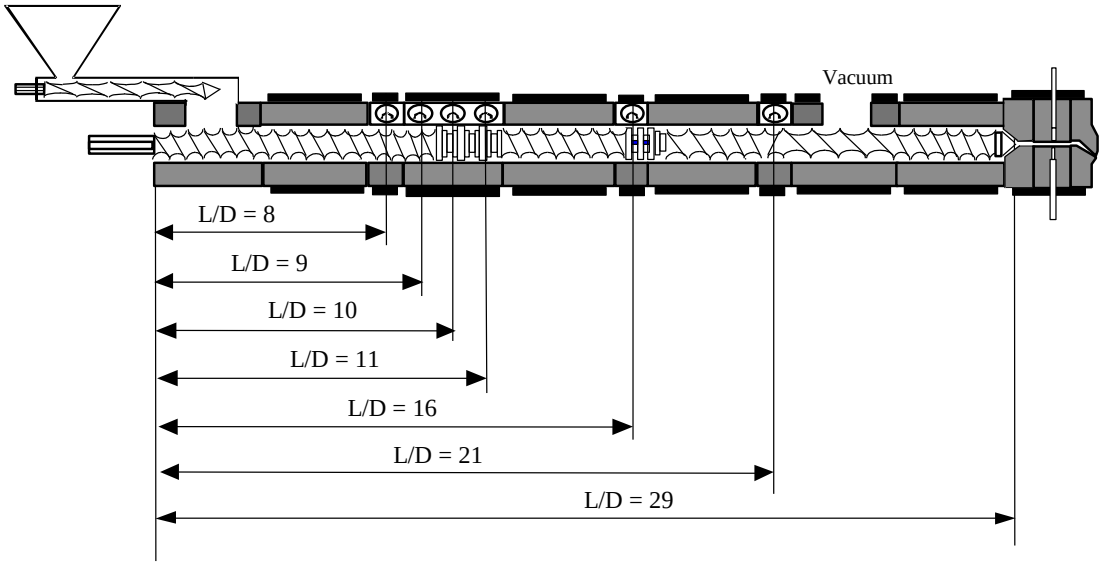

Figure 4.1 – Extruder layout and sampling locations.

4.2.3 - Residence time distribution

Residence time parameters at various locations along the extruder and upon exiting the die were determined using a simple procedure. After reaching steady state upon processing, a small amount of silicon dioxide tracer (with a specific surface of 175 m^2/g) was incorporated into the feed stream at time t = 0. Samples of polymer plus tracer were then collected from a specific sampling point at known time intervals. The technique was repeated for each sampling location. The relative amount of silica present in each sample was determined by ashing the sample and is a straightforward measure of concentration at a specific time. From this data it was possible to compute conventional residence time parameters, such as the cumulative residence time distribution, F(θ), and the mean residence time, $\bar{t}$ [28].

4.2.4 - Materials characterization

The materials were characterized in terms of their rheological behaviour and gel content. Samples for rotational oscillatory rheometry were compression-moulded as discs of 40 mm in diameter and 2 mm in thickness for 10 minutes at 200 ºC, under a pressure of 30 ton. Isothermal frequency sweeps from 0.004 to 40 Hz were performed

at 200 ºC in a TA Instruments Weissenberg rotational rheometer using parallel-plate geometry. The gap and diameter of the plates was 1.8 mm and 40 mm, respectively. In order to maintain the material behaviour within the linear viscoelastic domain, the applied strain was 0.01.

The possibility of error affecting the rheological data due to unwanted changes in chemistry during sample preparation must be considered. Thus, samples collected from the extruder were dissolved/precipitated, compressed and analysed under the same conditions. The results obtained were very similar to those without dissolution/precipitation.

For gel content weighted samples (about 1.5 g) were placed in 120 mesh stainless-steel cages and immersed in boiling toluene. The extractions were carried out under reflux for 24 hours with solvent change after 12 hours. After removal from the boiling solvent, the samples were dried in a vacuum oven during 5 hours at 80 ºC in a nitrogen atmosphere. Then they were weighted and the gel contents were calculated.

4.3 - RESULTS AND DISCUSSION

Since various polyolefins with different structure (ethene/propene ratio) were studied, the results obtained in each case will be presented and discussed separately. Then, a general correlation between branching/crosslinking and/or degradation reactions and peroxide decomposition will be established.

A simple observation of the polymer samples removed from the extruder with the sampling devices showed that, under the processing conditions selected, melting was not complete at L/D=8 (Figure 4.1). However, only one L/D downstream a more or less homogeneous melt had already developed. Therefore, data on samples from location L/D=8 will not be included in the following discussion.

4.3.1 – Polyethene

Figure 4.2 shows the rheological behaviour (dynamic viscosity and storage modulus versus oscillation frequency) of PE1, PE2 and PE3 along the extruder. The linear PE1

and PE2 (both HDPEs) exhibit a Newtonian plateau at the low frequency range while the long chain branched PE3 shows a significant decrease of viscosity with increasing frequency, and a relatively high elasticity. When these polymers are processed in the absence of peroxide, there is no evidence of mechanochemical effects taking place, i.e., the PEs are relatively stable under the operating conditions selected.

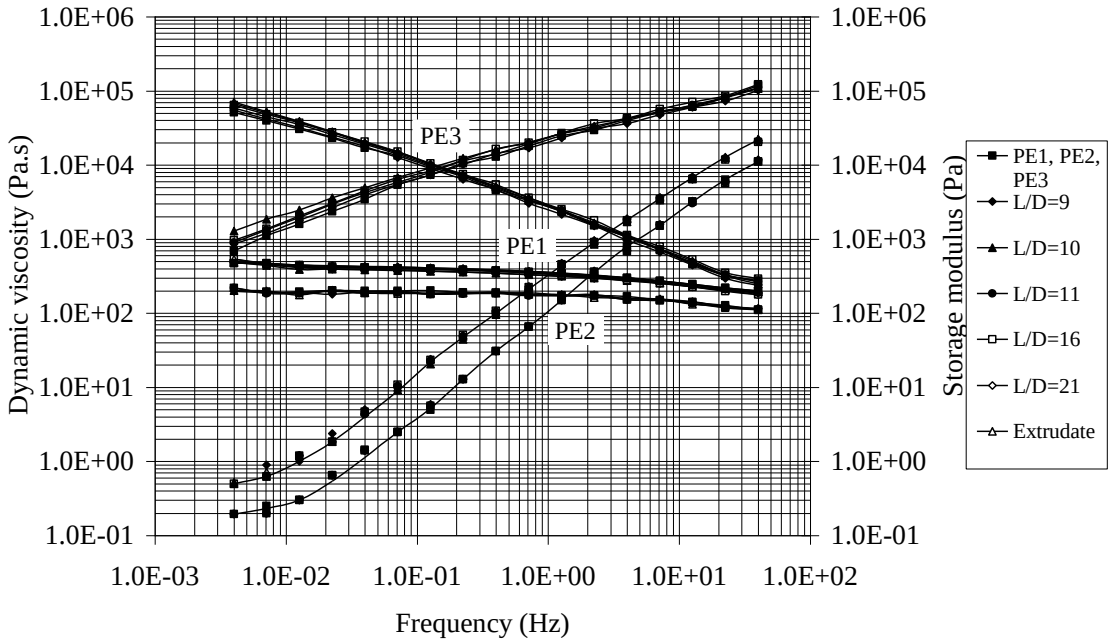

Figure 4.2 – Dynamic viscosity and storage modulus of PE1, PE2 and PE3 along the extruder.

When 0.1 phr of DHBP is added to PE1, both the viscosity and the storage modulus increase significantly upon melting as a result of branching/crosslinking. This is demonstrated in Figure 4.3, which compares the response of the original PE with that measured along the extruder and at the die exit. After melting little changes are perceived downstream. When using 1 phr DHBP the viscosity and elasticity increase is even larger (at $7x10^{-3}$ Hz : η': $4x10^{2}\rightarrow$~$6x10^{5}$ Pa.s and G': $6x10^{-1}\rightarrow1x10^{5}$ Pa), as depicted in Figure 4.4. This increase is significant up to L/D=11, then the values decrease slightly along the extruder.

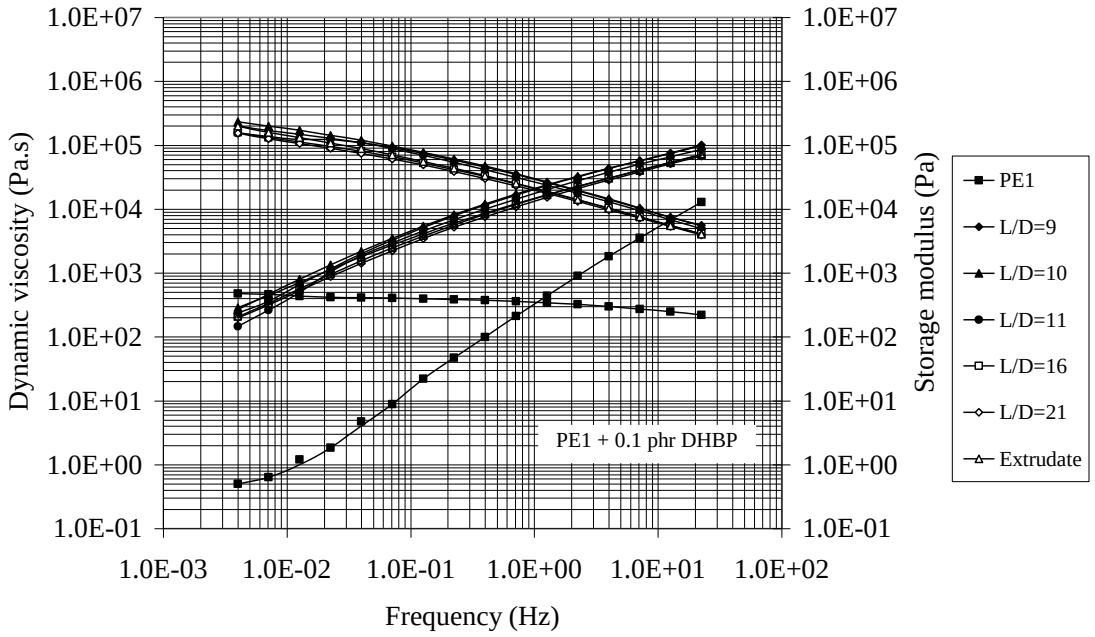

Figure 4.3 – Dynamic viscosity and storage modulus of PE1 along the extruder with 0.1 phr DHBP.

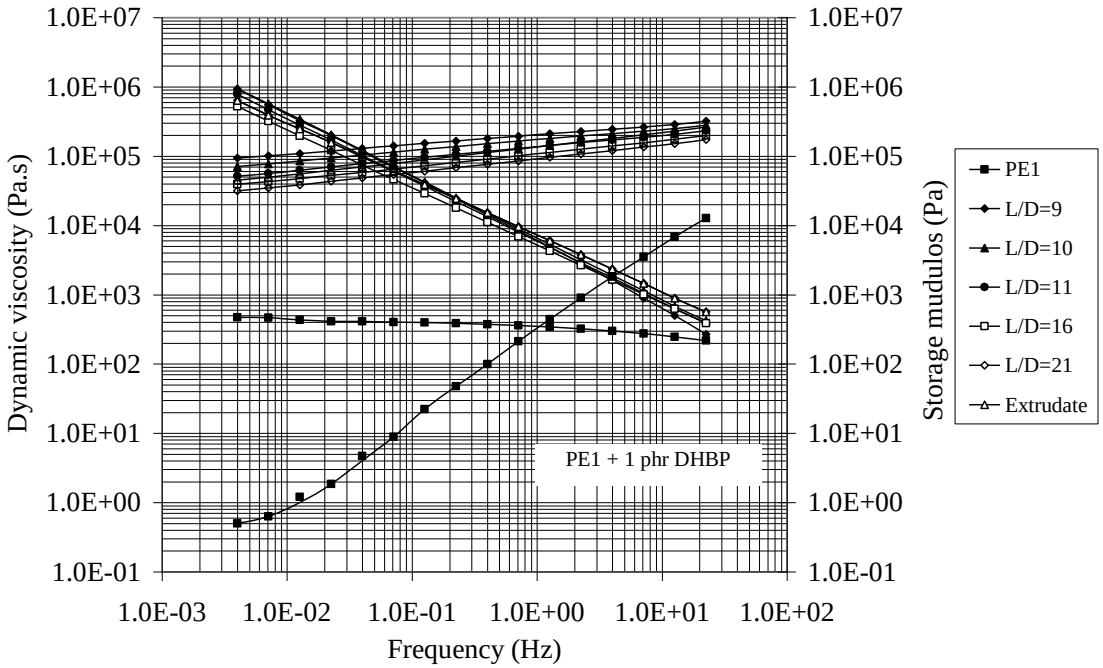

Figure 4.4 – Dynamic viscosity and storage modulus of PE1 along the extruder with 1 phr DHBP.

The variation of the gel content can eventually confirm the above results on the evolution of the branching/crosslinking reactions along the extruder. As shown in Figure 4.5, the gel content along the extruder remains low when 0.1 phr DHBP is used,

no differences being perceived from L/D=9 onwards. When 1 phr of peroxide is used, the gel content increases along the extruder until it reaches a plateau (55%) at L/D=16. These measurements show that branching/crosslinking reactions are not complete in the first part of the extruder, but they probably continue until all peroxide is decomposed, as it will be discussed later.

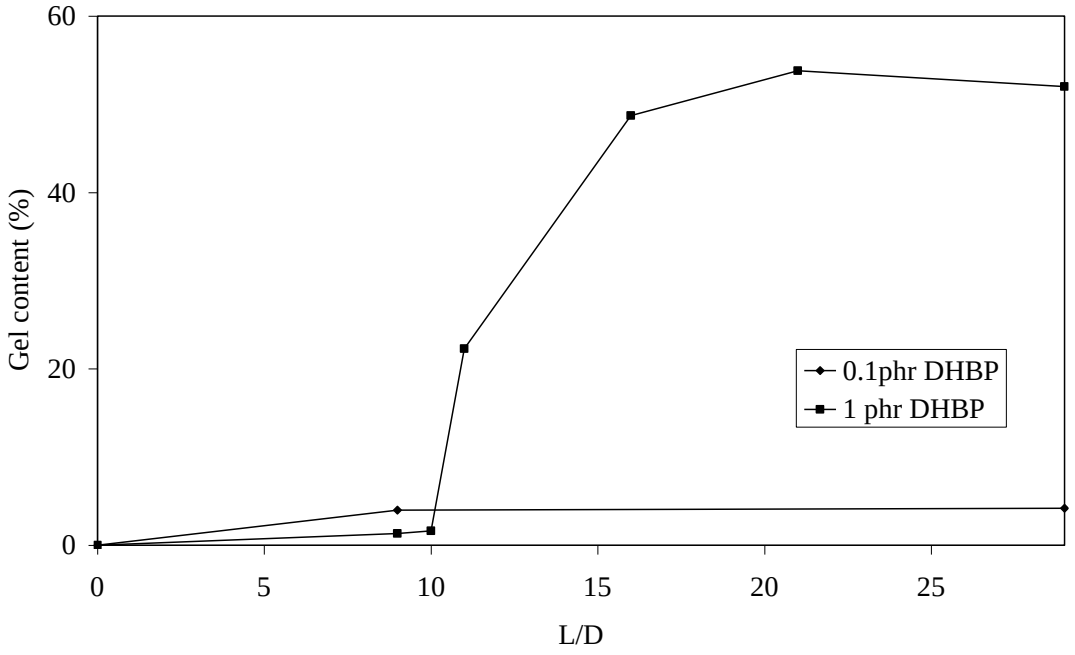

Figure 4.5 – Gel content of PE1 along the screw axis, with 0.1 and 1 phr DHBP.

When 0.1 phr peroxide is added to PE3, an increase in viscosity and storage modulus, particularly at the lower frequency range, is observed (Figure 4.6), again as a consequence of branching/crosslinking in the melting zone. Further downstream a small decrease in viscosity and storage modulus seems to take place, which is probably due to the degradation of the network formed earlier. The changes observed with PE3 when processed in the presence of peroxide are small when compared with those of PE1, which can be attributed to the differences in the initial molecular weight. An increased molecular weight facilitates the formation of a network, but on the other hand degradation effects are more likely to occur.

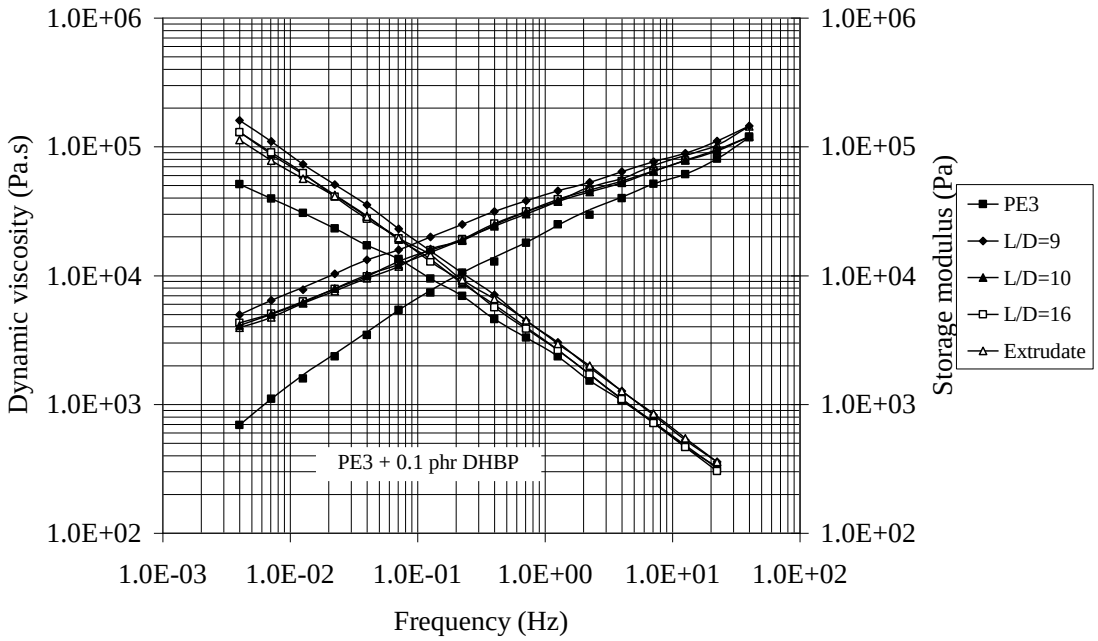

Figure 4.6 – Dynamic viscosity and storage modulus of PE3 along the extruder with 0.1 phr DHBP.

4.3.2 - Polypropene

Figure 4.7 shows the evolution of viscosity and storage modulus of PP samples taken along the extruder during processing with 0, 0.1 and 1 phr, respectively, at constant frequency ($7x10^{-3}$ Hz). In the absence of peroxide those parameters decreased slightly along the screw, i.e., some degradation occurred under these processing conditions. However, this decrease is much more important particularly in the melting zone when adding 0.1 phr DBHP is added (Figure 4.7). In the presence of 1 phr of peroxide a dramatic degradation occurs already at L/D=9 (the viscosity decreases from $1.8x10^{4}$ to 20 Pa.s at $7x10^{-3}$ Hz) and the process continues along the extruder. The degraded PP has very low viscosity and elasticity, indicating a relatively small average chain length and low entanglement density.

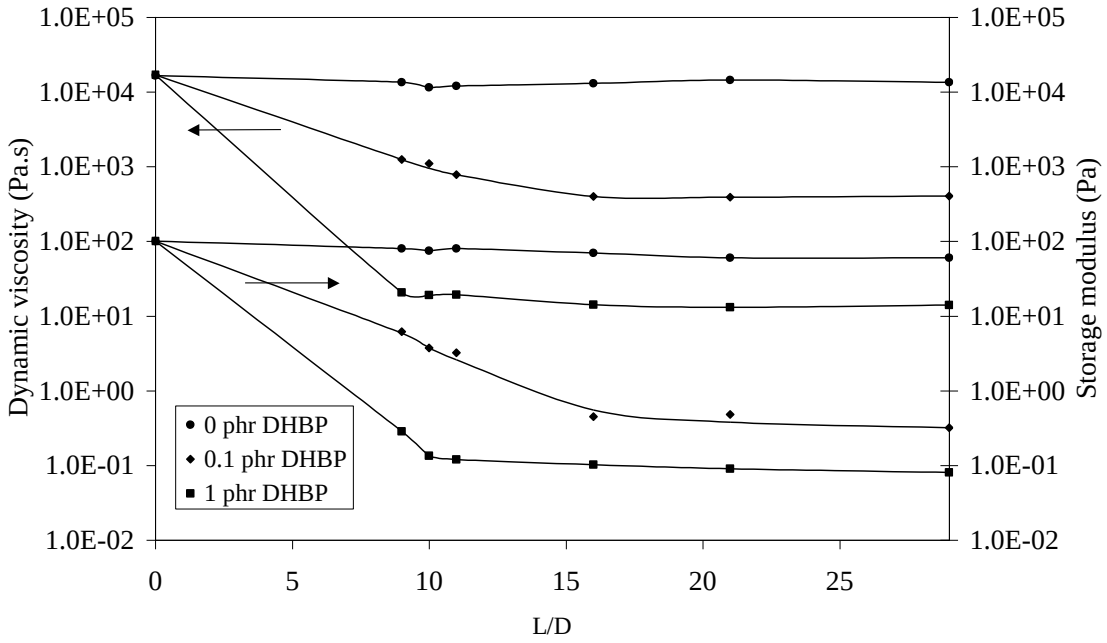

Figure 4.7 – Dynamic viscosity and storage modulus at 7x10-3 Hz of PP along the extruder with 0, 0.1 and 1 phr DHBP.

4.3.3 – Ethene/propene copolymers

The rheological measurements of the various EPM copolymers (Table 1) are depicted in Figures 4.8 to 4.10. At low frequencies, both the viscosity and elasticity of EPM1 increase along the extruder (Figure 4.8). In the presence of 0.1 phr peroxide (Figure 4.11) the dynamic viscosity and storage modulus increase significantly upon melting, but remain constant thereafter. Thus, branching/crosslinking occurs with this material. EPM2 processed by itself shows a small gradual increase in viscosity and storage modulus along the screw axis (Figure 4.9). In the presence of 0.1 phr peroxide, the values of the rheological parameters increase up to L/D=11 and then they decrease (Figure 4.11). Clearly, branching/crosslinking takes place, followed by degradation. EPM3 evidences a small decrease in viscosity along the extruder upon processing without peroxide (Figure 4.10). This decrease becomes much more important in the presence of 0.1 phr peroxide (Figure 4.11). The reported differences in behaviour are related to the ethene/propene ratio of each copolymer. EPM1 has the lower propene content (22 %), therefore only branching/crosslinking occurs. As the propene content

increases, both branching/crosslinking and degradation take place, degradation becoming the main reaction for a propene rich copolymer such as EPM3 (55wt.% propene). Differences in the molecular weight of EPM1 and EPM2 should also be relevant. Since EPM1 has a higher molecular weight more branching/crosslinking should occur than for EPM2.

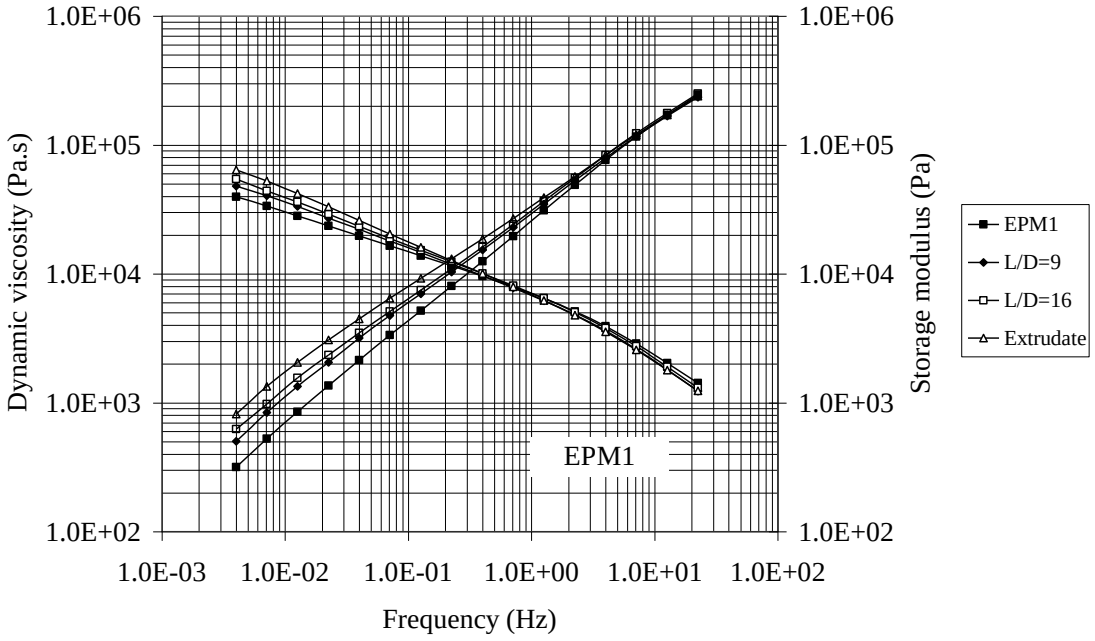

Figure 4.8 – Dynamic viscosity and storage modulus of EPM1 along the extruder.

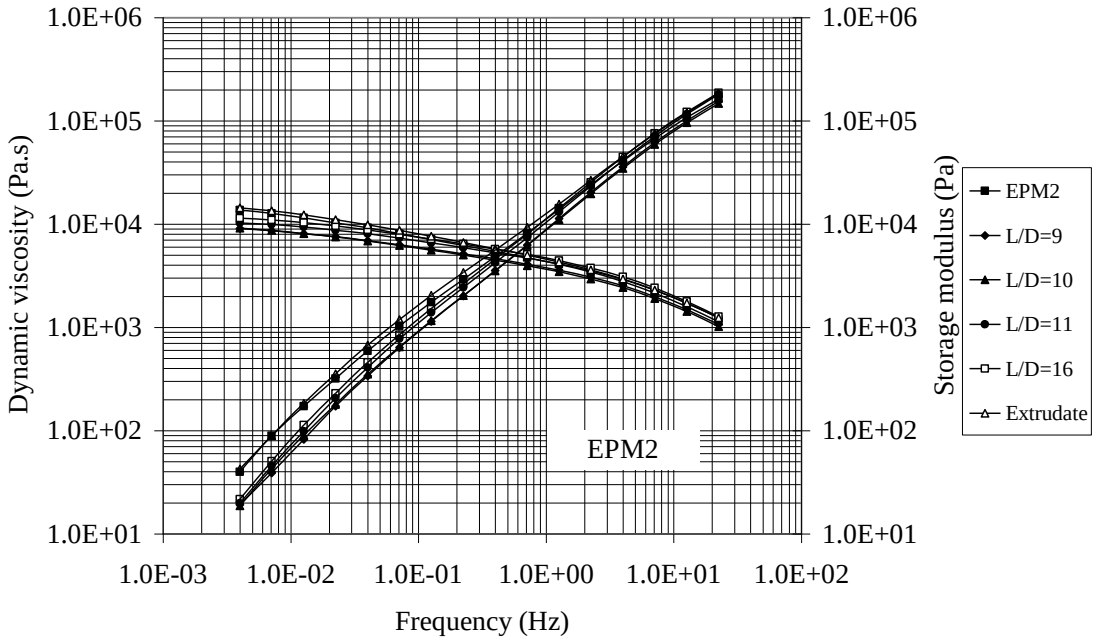

Figure 4.9 – Dynamic viscosity and storage modulus of EPM2 along the extruder.

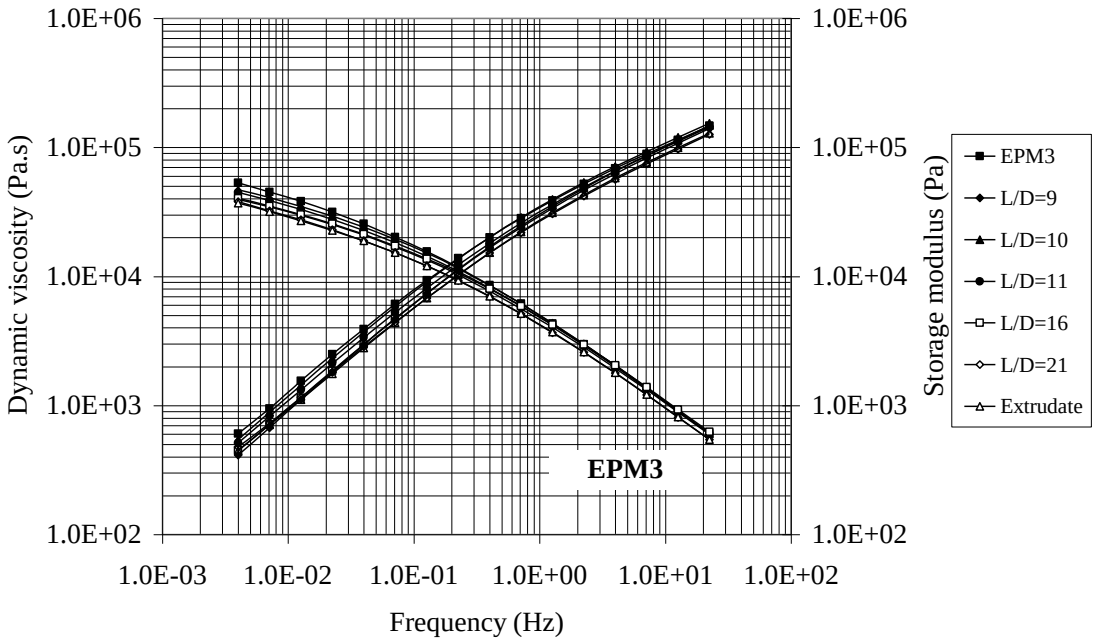

Figure 4.10 – Dynamic viscosity and storage modulus of EPM3 along the extruder.

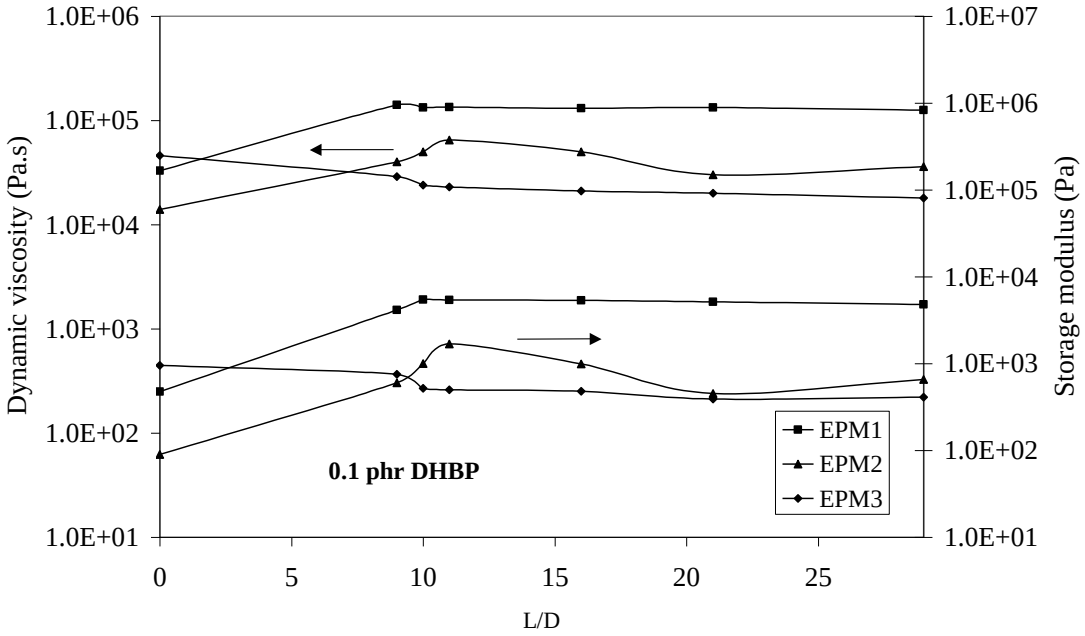

Figure 4.11 – Rheological properties of EPM1, EPM2 and EPM3 along the extruder with 0.1 phr DHBP (dynamic viscosity and storage modulus at $7x10^{-3}$ Hz).

4.3.4 - Correlation between crosslinking/degradation and peroxide decomposition

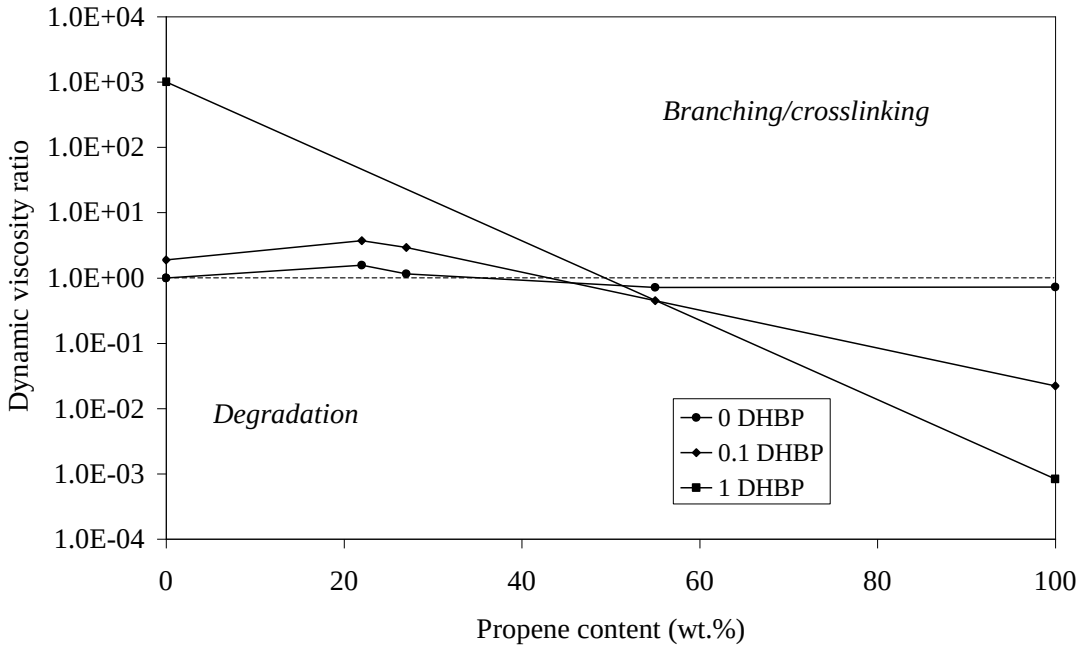

Figure 4.12 – Viscosity ratio of dynamic at $7x10^{-3}$ Hz of the modified (0.1 and 1 phr DHBP) and original polyolefins as a function of the propene content at L/D=29.

Figure 4.12 summarizes most of the previous results by depicting the relationship between the ratio of the dynamic viscosities of the modified (0.1 and 1 phr DHBP) and original polyolefins, at the die outlet, and their chemical composition (propene content). As expected, the viscosity ratio of the various materials decreases with increasing propene content from a value larger than unity for PE to a value far below 1 for PP. Figure 4.13 represents a simplified scheme of the reactions occurring during melt processing of polyolefins in the presence of peroxide [2-9, 19-23]. The decomposition of the peroxide yields free radicals, which abstract H-atoms from the polyolefin backbone. The subsequent reactions of the polyolefin radical depend on the chemical structure of the polyolefin. For example, since PE forms long chain branches when PE radicals terminate by bimolecular combination, a branched material with increased molecular weight, i.e., a material with higher viscosity and elasticity, is obtained [2-4, 10-17]. In the case of PP, chain scission of the PP radicals occurs, thus a material with a lower viscosity and elasticity is obtained [2-4, 16]. In the case of an ethene/propene

copolymer, the above reactions can take place simultaneously and the resulting structure will depend on the particular ethene/propene ratio and also on the original copolymer molecular weight.

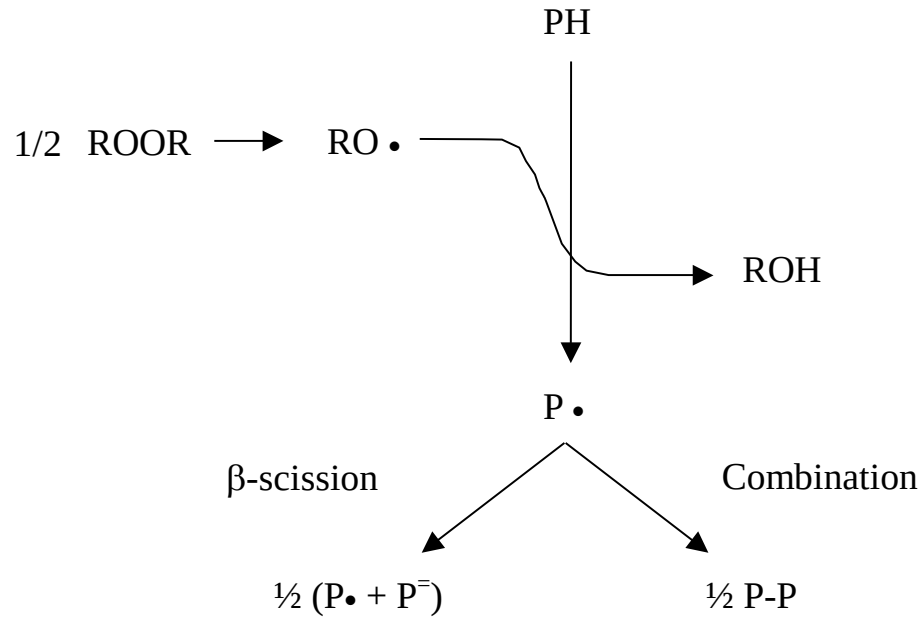

PE: combination → branching/crosslinking → viscosity and elasticity increase

PP: β-scission → degradation → viscosity and elasticity decrease

EPM: combination/β-scission → branching + degradation → viscosity similar to that of original material

Figure 4.13 – Simplified scheme of the reactions during melt processing of polyolefins in the presence of peroxide.

In the preceding discussion the rheological response of processed polyolefins in the absence and in the presence of peroxide has been discussed qualitatively (i.e., in terms of crosslinking versus degradation development). Finally, a more quantitatively correlation between the degree of crosslinking/degradation and the peroxide decomposition along the extruder will now be determined. The peroxide decomposition was calculated as the integral of a first order kinetics equation, using an Arrhenius law, peroxide decomposition data provided by Azko Nobel (k_0= $1.68x10^{16}$ s^{-1} and E_A= $155.49x10^3$ J/mole) and the melt temperature and residence time measured at each location (Table 4.2). The temperature profiles denoted as lower and higher correspond

to the lowest and highest temperatures measured at each location, considering all the materials.

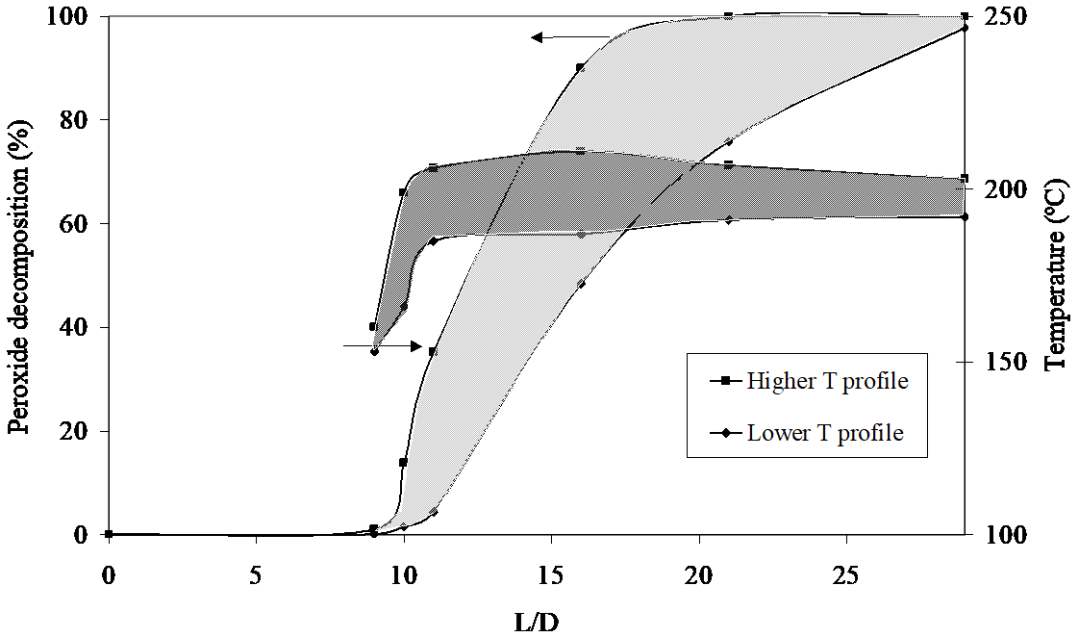

Figure 4.14 – Melt temperature and calculated peroxide decomposition along the screw axis.

Figure 4.14 shows the calculated evolution of the peroxide decomposition along the extruder using the two temperature profiles. According to the calculations, DHBP starts to decompose at L/D=9, and not before, simply because the temperature is too low. Then, decomposition becomes very fast because the melt temperature jumps to 190-200 ºC. Complete DHBP decomposition is achieved up to end of the extruder. Hence, according to the calculations, branching or degradation reactions are completed from L/D=21 to the end of the extruder, depending on the set temperature. Figure 4.15, which depicts the evolution of the PE1 gel content (1 phr peroxide) and the calculated peroxide decomposition along the extruder, confirms the validity of this prediction. The shapes of the curves are similar, demonstrating that there is a close correlation between the peroxide decomposition and crosslinking/branching.

Table 4.2 – Experimental mean residence times and temperatures profiles.

Sampling location (L/D)	Mean residence time, $\bar{t}$ (s)	Temperature along the axis (ºC)	
		Highest	Lowest
9	25	153	160
10	30	166	199
11	32	185	206
16	50	187	211
21	67	191	207
Extrudate	110	192	203

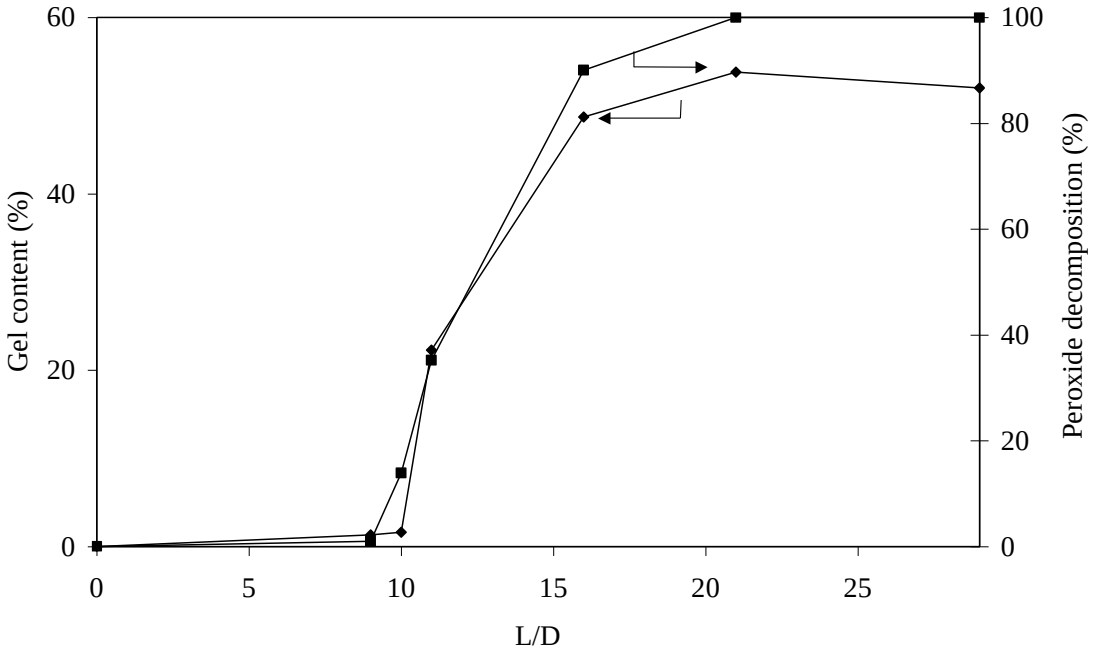

Figure 4.15 – Evolution of gel content (PE 1 with 1 phr DHBP) and calculated peroxide decomposition along the extruder.

4.4 - CONCLUSIONS

The evolution of the rheological response of PE, EPM and PP processed in a twin-screw extruder was monitored along the barrel.

Significant differences in viscosity were observed depending on the structure of the polyolefin being tested. In the absence of peroxide the rheological properties of the polyolefins were only moderately affected by the thermal/mechanical stresses inherent to processing. However, in the presence of peroxide branching/crosslinking and/or degradation occur along the extruder, until the peroxide is fully converted. The degree of branching/crosslinking and/or degradation depends essentially on the ethene/propene ratio, on the original molecular weight of the polymer and on the amount of peroxide added. In a quantitative approach the change in rheological behaviour could be correlated with the peroxide decomposition.

4.5 - REFERENCES

[1] – A. Casale and R. Porter, Polymer Stress Reactions, Academic Press, New York, 1978.

[2] – A. E. Hamielec, P. E. Gloor and S. Zhu, Canadian J. Chem. Eng., 69, 611 (1991).

[3] – M. Xanthos (Ed.), Reactive Extrusion, Hanser Publishers, New York, 1992.

[4] – S. Al-Malaika (Ed), Reactive Modifiers for Polymers, Blackie Academic & Professional, London, 1997.

[5] – A. Holmstrom and E. M. Sorvik, J. Polym. Sci., 57, 33 (1976).

[6] – G. R. Rideal and J. C. Padget, J. Polymer Sci.: Symp., 57, 1 (1976).

[7] – G. E. Hulse, R. James and D. R: Warfel, J. Polym. Sci.:Part A: Polym. Chem., 19, 655 (1981).

[8] – J. Boer and A. J. Pennings, Makromol. Chem., 2, 749 (1981).

[9] – A. K. Khitrin, J. Polym. Sci.: Part A: Polym. Chem., 33, 2413 (1991).

[10] – K. J. Kim, Y. S. Ok and B. K. Kim, Eur. Polym. J., 28, 1487 (1992).

[11] – J. Sohma, Colloid Polym. Sci., 27, 1060 (1992).

[12] – D. Suwanda and S. T. Balke, Polym. Eng. Sci., 33, 1585 (1993).

[13] – S. Suyama, H. Ishigaki, Y. Watanabe and T. Nakamura, Polymer J., 27, 371 (1995).

[14] – S. Suyama, H. Ishigaki, Y. Watanabe and T. Nakamura, Polymer J., 27, 503 (1995).

[15] – A. Harlin and E. Heino, J. Polym. Sci.: Part B: Polym. Physics, 33, 479 (1995).

[16] – P. Ghosh, D. Dev and A. Chakrabarti, Polymer, 38, 6175 (1997).

[17] – A. Smedberg, T. Hjertberg and B. Gustafsson, Polymer, 38, 4127 (1997).

[18] – K. Ebner and J. L. White, Intern. Polym. Processing IX, 233 (1994).

[19] – M. G. Lachtermacher and A. Rudin, J. Appl. Polym. Sci., 58, 2077 (1995).

[20] – M. G. Lachtermacher and A. Rudin, J. Appl. Polym. Sci., 58, 2433 (1995).

[21] – A. C. Kolbert, J: G. Didier and L. Xu, Macromolecules, 8598 (1996).

[22] – M. G. Lachtermacher and A. Rudin, J. Appl. Polym. Sci., 59, 1775 (1996).

[23] – M. G. Lachtermacher and A. Rudin, J. Appl. Polym. Sci., 59, 1213 (1996).

[24] - A.V. Machado, J. A. Covas and M. van Duin, J. Appl. Polym. Sci., 71, 135 (1999).

[25] – O. Franzheim, M. Stephan, T. Rische, P. Heidemeyer, U. Burkhardt and A. Kiani, Polym. Adv. Tech., 16, 1 (1997).

[26] – A. V. Machado, J. A. Covas and M. van Duin, J. Polym. Sci.: Part A: Polym. Chemistry, 31, 1311 (1999).

[27] – O. S. Carneiro, J. A. Covas and B. Vergnes, submitted to J. Appl. Polym. Sci..

[28] - O. S. Carneiro, G. Caldeira, and J. A. Covas, Mat. Proc. Tech., 92-93, 309 (1999).

5.1 - INTRODUCTION

One of the most common examples of polymer modification, both from an academic and a commercial point of view, is grafting of maleic anhydride (MA) onto polyolefins [1-10]. Maleated polyolefins have found widespread application as "in-situ" compatibilizers for blends, adhesives for multilayer systems and coupling agents for glass fibres [1-4]. Grafting involves the reaction of a polymer with a monomer or a mixture of monomers yielding side groups or polymer chains attached to the polymer backbone. Free radical initiators, such as peroxides, have been used to initiate the reaction [1-15]. The grafting process is usually performed in the melt in an extruder, i.e. via reactive extrusion (REX) [1,2]. It is carried out at elevated temperatures with highly viscous and probably heterogeneous systems. The extruders used should therefore contain intensive mixing zones, since efficient mixing of the monomer with the polymer is essential for minimizing the formation of free homopolymer.

Extruders have been used as chemical reactors in academic studies and on a commercial scale for over 30 years [16]. Their use has advantages over alternative processes, for instance the absence of solvents avoiding product isolation, short residence times and a continuous operation. However, important functional characteristics, such as the temperature profile, the screw speed, the degree and the type of mixing and the residence time distribution should be taken into account [17].

Combining processing and chemical reactions makes REX very complex and, in the case of free radical grafting in the melt, gives rise to a tremendous challenge in terms of reactivity, selectivity, processing and product optimisation and control. Much effort has been made in order to establish the kinetics of free radical grafting and model the process. Some authors [18,19] developed a general kinetic model and combined it with generally accepted models for melting in a single screw extruder. The required input consists of data on the extrudate, such as molecular weight, grafting content, residence time and temperature. However, the actual process development inside the extruder has remained largely unknown, which is mainly due to difficulties in collecting representative samples from the extruder during processing. Recently, we have

developed an experimental technique that allows fast and representative sampling of the melt along the screw axis for subsequent off-line characterization [20]. These sampling devices have been used to investigate in detail the "in-situ" compatibilization of blends of polyamide 6 (PA-6) with ethylene-propylene rubber (EPM) in the presence of EPM grafted with MA (EPM-g-MA) [21], as well as the processing of polyolefins in the absence and in the presence of peroxide [22]. The latter can be considered as a starting point of the current investigation. In the present study a series of such sampling devices was used in order to follow the physico-chemical phenomena (i.e., the degree of MA grafting and the rheological behaviour), developing along the screw axis during grafting of MA onto polyethylene (PE), EPM and polypropylene (PP). Melt temperature and average residence time were measured at various locations. By combining all these data a descriptive model could be implemented, which might serve as the basis for future quantitative approaches.

5.2 - EXPERIMENTAL

5.2.1 - Materials

Stamylan HD 2H280 (PE1: HDPE; M_w = 60 kg/mol), Stamylex 7359 (PE2: HDPE; M_w = 30 kg/mol) and Stamylan P 13E10 (PP; M_w = 500 kg/mol) were supplied by DSM; Exxon VA 404 (EPM: 45 wt.% ethene) was produced by Exxon. Maleic anhydride (MA) was obtained from Aldrich, while 2,5–bis(tert-butylperoxy)-2,5-dimethylhexane (Trigonox 101: DHBP), di-tert-butyl peroxide (Trigonox B: DBP) and 2,2-bis(tert-butylperoxy)butane (Trigonox D: BBP) were supplied by Akzo Nobel. The half-life time of these peroxides at 200 ºC is 6.1, 14.4 and 0.8 s, respectively.

5.2.2 - Grafting

The recipes and experimental conditions used in each experiment are given in Table 5.1. For PE1 the recipe was varied in order to have different initial amounts of MA and/or peroxide. When using different peroxides, the number of moles of the peroxide

was kept constant in all experiments (the mono or bifunctionality and the molecular weight of the various peroxides was taken into account).

Table 5.1 – Grafting recipes.

Polyolefin	Experiment	Recipe		Comments
		MA (phr)	DHBP (phr)	
PE1	1	5	1	
	2	5	0.5	
	3	5	0	Thermal grafting
	4	1	1	
	5	1	0.5	
	6	0	1	
	7	5	1	Separate feed
	8	5	-	0.95 phr DBP
	9	5	-	1.5 phr BBP
PE2	10	5	1	
EPM	11	5	1	
PP	12	5	1	
	13	5	1	Separate feed
	14	0	1	

The grafting reactions were carried out in a modular Leistritz LSM 30.34 intermeshing co-rotating twin-screw extruder. Most experiments were performed using the same processing conditions, i.e., a barrel set temperature at 200 ºC, a screw rotation of 75 rpm and a throughput of 5kg/h. Figure 5.1 shows the extruder layout and the sampling locations (denoted as A to F). The screw configuration was identical to that used in Part I of this work [22], and contains a series of transport sections separated by three mixing zones, consisting of staggered kneading disks and a left hand element, respectively. Generally, the polyolefin, monomer and peroxide were tumble mixed and fed through

the hopper. However, in experiments 7 and 13 a mixture of the polymer and monomer was fed to the hopper while the peroxide, previously dissolved in acetone, was injected at the end of the first kneading zone (location C in Figure 5.1) by means of a HPLC pump.

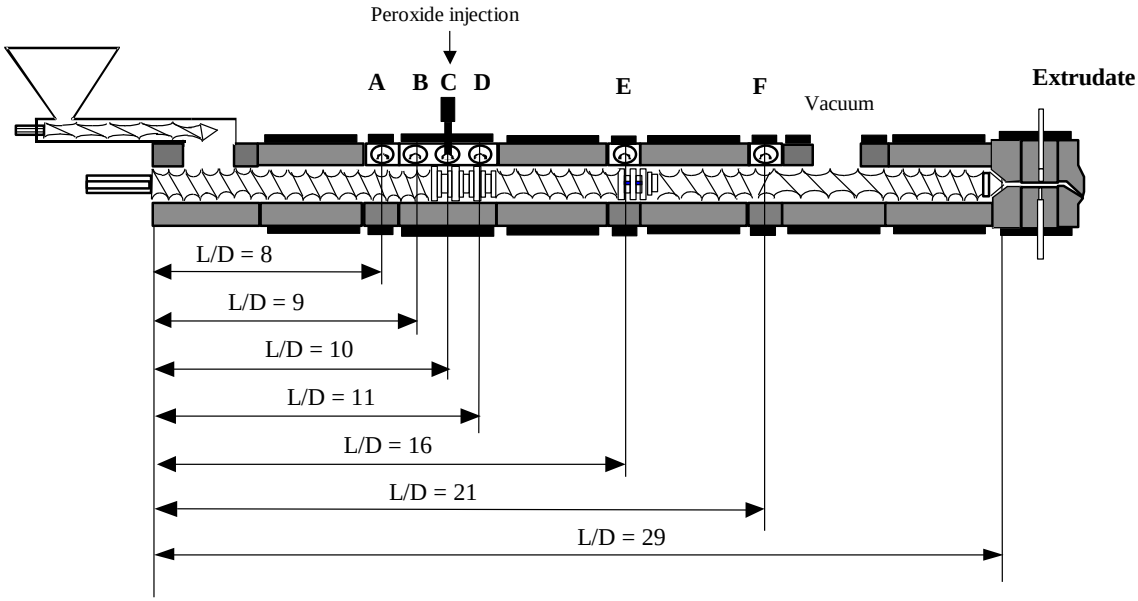

Figure 5.1 – Extruder layout and sampling locations.

In all the extrusion experiments molten polymer samples were collected along the screw axis and from the extrudate and were quenched in liquid nitrogen in order to avoid further reaction. The average melt temperature was measured at various locations along the extruder by sticking a pre-heated needle type fast response thermocouple (penetration probe, type K, Coleparmer, time constant ~ 1s) into the freshly collected material.

5.2.3 - Residence time distribution

The average residence time at the various sampling locations along the extruder, under the selected operating conditions, was estimated using a tracer impulse technique. Upon reaching a steady state, a small amount of silicon dioxide (specific surface of 175 m^2/g) was added instantaneously to the feed stream at t = 0. Samples of the modified polymer plus tracer were then collected from one sampling point at various time intervals, the

procedure being repeated for all the sampling locations. The relative amount of silica was determined by ashing the sample. From this data the conventional residence time parameters, such as the cumulative residence time distribution, F(θ), and the mean residence time, $\bar{t}$, were computed [23].

5.2.4 - Characterization

Since under the processing conditions selected melting was not complete at L/D=8 (Figure 5.1) – as observed previously - samples at this location were not characterized.

The modified polyolefins were dissolved in toluene (PE and EPM) or xylene (PP) under reflux until a clear solution was obtained. The warm solutions were precipitated in acetone and filtered in order to obtain the purified polymers, which were dried in a vacuum oven for 1 hour at 180 ºC. Then, thin films were prepared by compression-moulding and FT-IR (Perkin-Elmer 1600) spectra were recorded. For a quantitative determination of the MA content, the 1785 cm^{-1} peak was used considering the film thickness. FT-IR calibration was carried out by imidization of some of the MA grafted polyolefins with NH_3, followed by N-content determination.

Oscillatory rheological measurements were carried out in a TA Instruments Weissenberg rotational rheometer at 200 ºC using a parallel-plate geometry. The gap and diameter of the plates was 1.8 mm and 4.0 cm, respectively. A frequency sweep from 0.04 to 40 Hz was performed for each sample, applying a strain of 0.01 in order to maintain the material's response in the linear viscoelastic regime.

Gel content determinations were performed by weighing samples (about 1.5 g), placing them in 120 mesh stainless-steel cages and immersing these in boiling toluene. The extractions were run under reflux for 24 hours. The solvent was renewed once after about 12 hours. After removal of the boiling solvent, samples were dried in a vacuum oven for 5 hours at 80 ºC in a nitrogen atmosphere. Then they were weighed again.

5.3 - RESULTS AND DISCUSSION

In Part I of this work [22] the evolution of chemical reactions (branching/crosslinking and/or degradation) along the extruder for various polyolefins in the absence or in the presence of peroxide was studied. In the presence of peroxide branching/crosslinking or degradation occurs along the extruder until the peroxide is fully converted. The degree of branching/crosslinking or degradation depends on the ethene/propene ratio, on the original molecular weight of the polymer and on the amount of peroxide added. Here, the evolution of grafting MA onto various polyolefins (having different ethene/propene ratios, i.e., 0 wt.% propene for PE1 and PE2, 55 wt.% propene for EPM and 100 wt.% for PP) along the extruder, in terms of grafted MA and rheological changes, will be discussed. As several variables were investigated, the results obtained in each case will be presented and discussed separately.

5.3.1 – Reproducibility

In order to determine whether unavoidable temperature fluctuations during processing could have an effect on grafting, various samples of modified PE1 (experiment 1 in Table 5.1) were collected at location C of the extruder at random time intervals. The temperature of each sample was measured and the grafting MA content was determined. During temperature measurements a systematic error is made due to heat transfer from the metal to the sample and from the sample to the air. The former will result in an increase of the temperature of the sample while the latter would lower the sample temperature. Nevertheless, the effect of these errors on the measured temperature will be rather small since the measurements are very fast (2 s). For a barrel set temperature of 200 ºC the average temperature (at location C) remained as 187±2 ºC. The experimental error associated to the determination of the MA graft content is typically ± 0.1 wt.% MA, as estimated from different measurements carried out on films prepared from the same polymer sample. Figure 5.2 relates the MA content with the temperature of the various samples. Within the experimental error, the MA content is essentially constant, i.e., it is insensitive to temperature fluctuations.

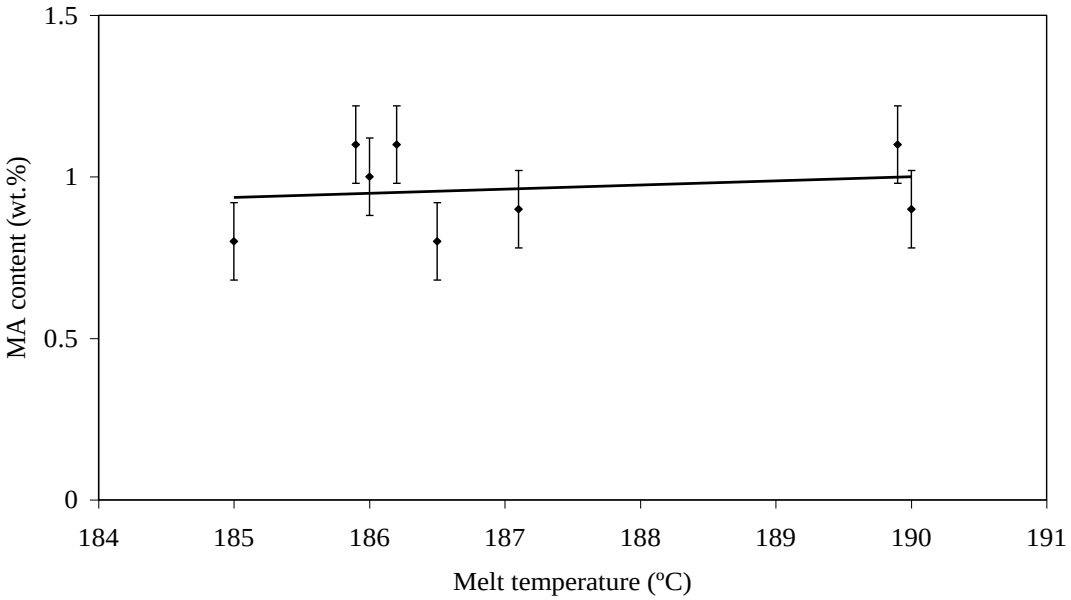

Figure 5.2 – MA content of PE1 versus melt temperature at location C (5 phr MA, 1 phr DHBP, 200 ºC).

5.3.2 - Grafting along the extruder

The MA contents along the extruder axis (locations B to F) for the various grafting experiments are presented in Table 5.2. The data for the various polymers upon grafting with 5phr MA and 1 phr DHBP at 200 ºC (barrel set temperature) - experiments 1, 10, 11 and 12 - are plotted in Figure 5.3. Regardless of the polyolefin structure, there is a strong increase in the grafting level in the first part of the extruder up to location E, followed by a plateau.

The measured average temperature and residence time (Table 5.3) at each location were combined with an algorithm that integrates numerically the peroxide decomposition for a given temperature and time. This algorithm uses a first order equation for peroxide decomposition in combination with the Arrhenius equation (data for DHBP, as provided by Akzo-Nobel: $k_0 = 1.68 \times 10^{16}$ s^{-1} and $E_A = 155.49 \times 10^3$ J/mole). The use of the average residence time provides a qualitative approach to understanding the MA grafting profile, since a truly quantitative model would require the use of the residence time distribution. Anyway, a small difference of 3-4 seconds in the average residence time will result in a significant change of the peroxide decomposition profile along the extruder, especially in the first part.

Table 5.2 – Grafted maleic anhydride content along the extruder for the various grafting experiments at the various sampling locations.

Polyolefin	Experiment	Grafted MA content (wt.%)					
		B	C	D	E	F	Extrudate
PE1	1	0.28	0.71	1.23	1.66	1.75	1.72
	2	0.20	0.36	1.01	1.54	1.55	1.58
	3	0.06	0.11	0.12	0.11	0.12	0.12
	4	0.22	0.28	0.37	0.40	0.40	0.40
	5	0.19	0.23	0.46	0.45	0.46	0.46
	7	0.05	0.05	0.38	0.93	1.94	1.96
	8	0.24	0.29	0.80	1.10	1.34	1.62
	9	0.07	0.07	0.08	0.11	0.11	0.12
PE2	10	0.57	1.44	1.79	1.85	1.93	1.93
EPM	11	0.26	0.64	1.16	1.56	1.57	1.57
PP	12	0.19	0.25	0.41	0.64	0.64	0.64
	13	0.01	0.01	0.11	0.48	0.51	0.53

Table 5.3 – Measured mean residence time and temperatures profiles.

Sampling location	Mean residence time, $\bar{t}$, (s)	Average temperature along the axis (ºC)			
		PE1	PE2	EPM	PP
B	25	160	179	199	153
C	30	187	194	208	166
D	32	204	206	212	185
E	50	211	207	216	187
F	67	207	203	219	191
Extrudate	110	200	201	207	192

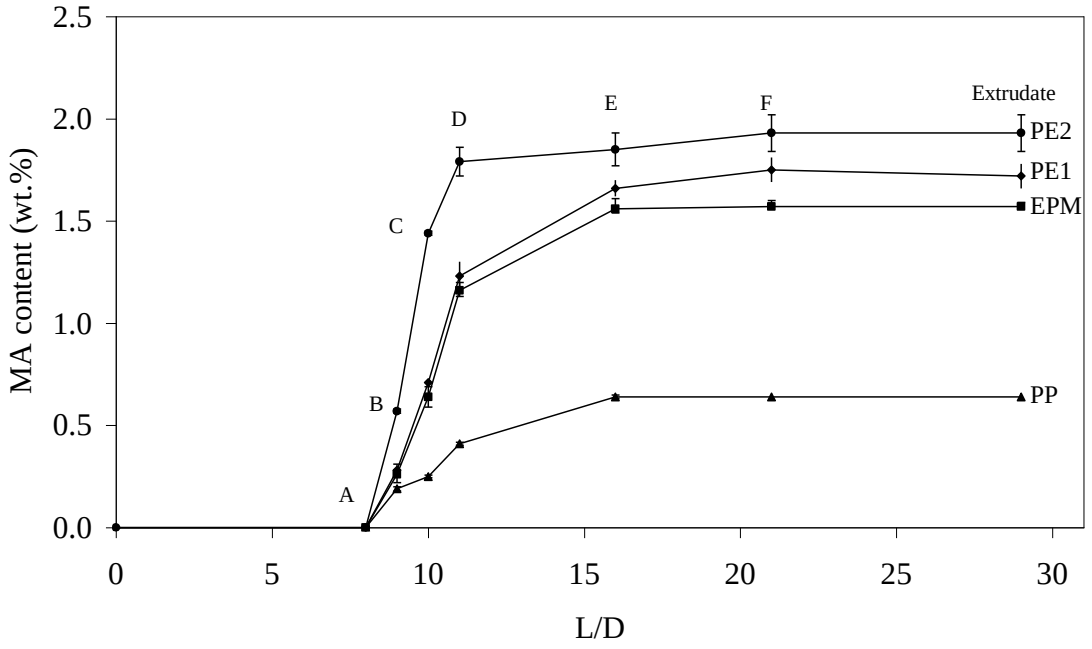

Figure 5.3 – MA content along the extruder for modification of PE1, PE2, EPM and PP with 5phr MA and 1 phr DBHP at 200 ºC.

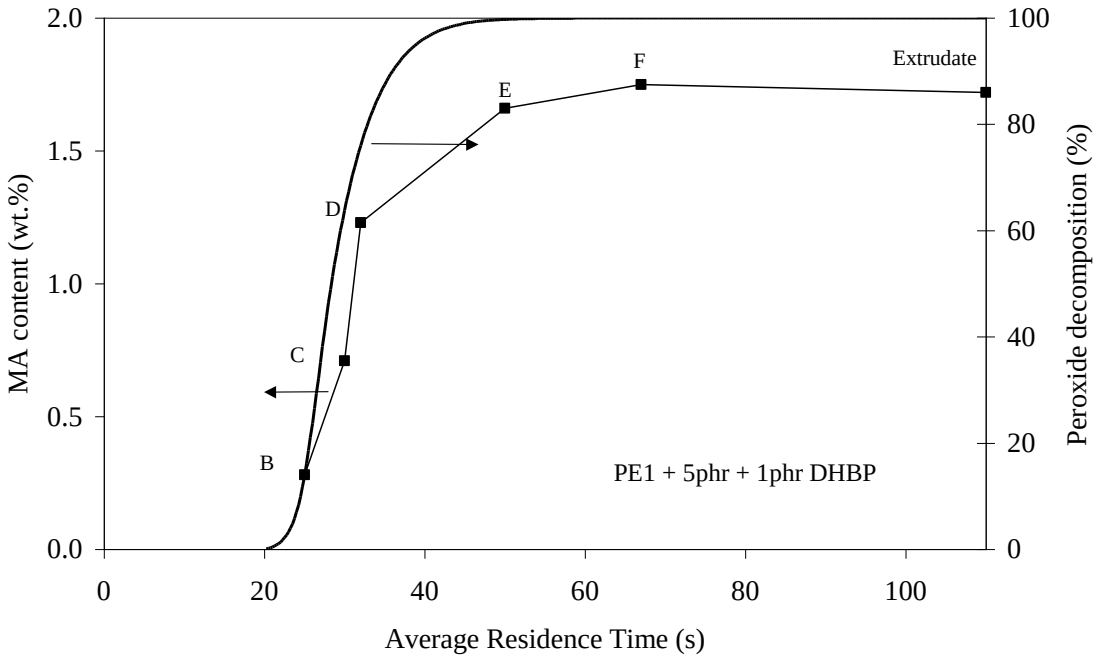

Figure 5.4 – MA graft content for PE1 and calculated peroxide decomposition, with 5phr MA and 1 phr DHBP at 200 ºC, as a function of average residence time.

For example, the experimental MA content and the calculated peroxide decomposition for PE1 with 5 phr MA and 1 phr DHBP at 200 ºC (experiment 1) are plotted in Figure 5.4 as a function of the average residence time. The experimental grafting data follows closely the calculated peroxide decomposition. When the peroxide starts to decompose (at about 160 ºC at location B, as shown in Table 5.2), the grafting reaction begins. Between B and D the temperature increases sharply from 160 to 204 ºC, which results in an acceleration of the peroxide decomposition and, consequently, of MA grafting. At location E the peroxide is completely decomposed and the degree of grafting has almost reached a constant level. Thus, the grafting profile along the extruder is explained by the peroxide decomposition.

5.3.3 - Effect of polyolefin structure on grafting

Table 5.4 – Gel contents for MA grafted PE1, PE2 and EPM along the extruder.

Polyolefin	Experiment	Gel content (%)					
		B	C	D	E	F	Extrudate
PE1	1	5	7	23	29	15	6
	2	1	3	-	5	-	7
	4	1	2	13	52	53	54
	5	1	2	3	15	13	10
	6	1	2	22	49	54	52
	7	-	2	8	20	25	24
PE2	10	0	0	-	-	-	0
EPM	11	3					2

Even though the MA graft profiles for EPM and PP are similar to that of PE1, the final amount of grafting for PE1, EPM and PP is different (Figure 5.3). The highest amount is obtained for PE1 (1.7 wt.%) and the lowest for PP (0.64 wt.%), whereas the MA graft content of EPM is close to that of PE1. Similar differences have been observed by other authors [24,25]. It has been proposed [26] that the dependence of the MA graft level on

the polyolefin composition is due to competition between grafting and β-scission or crosslinking. The latter seems to correlate with the fraction of non-PPP triads.

Table 5.5 – Dynamic viscosity (200 ºC, 7x10-3 Hz) along the extruder for polypropylene grafted with maleic anhydride.

Polyolefin	Experiment	Dynamic viscosity (Pa.s)					
		B	C	D	E	F	Extrudate
PP	12	$3.2x10^3$	$1.1x10^3$	$2.7x10^2$	$2.4x10^2$	$2.5x10^2$	$2.3x10^2$
	13	$1.8x10^4$	$1.7x10^4$	$6.0x10^2$	$5.0x10^1$	$2.7x10^1$	$2.7x10^1$
	14	$2.1x10^1$	$1.9x10^1$	$1.9x10^1$	$1.4x10^1$	$1.3x10^1$	$1.4x10^1$

Tables 5.4 and 5.5 show the gel content for PE1, PE2 and EPM and the dynamic viscosity of PP, respectively. In the case of PE1 (with 5 phr MA and 1 phr DHBP at 200 ºC - experiment 1), the rheological measurements showed (Figure 5.5) a very strong increase of viscosity (from 450 to $1.5x10^5$ Pa.s at $7x10^{-3}$ Hz) and elasticity (from 450 to $1.5x10^5$ Pa at $7x10^{-3}$ Hz) at location B, indicating severe crosslinking. Beyond location B the materials response did not change significantly, although elasticity seems to decrease slightly downstream. Therefore, crosslinking occurs initially as a side reaction, followed by some degradation. However, measurements of the gel content showed that crosslinking continues along the screw until location E, as seen in Figure 5.6. The decrease in gel content observed beyond E, is not associated with the peroxide, since it is fully decomposed. Both the decrease in storage modulus and gel content indicates network degradation, probably due shearing apart the PE1 gels.

The final gel content for PE1 grafted with MA is quite different from that obtained when PE1 is processed with peroxide only (for more details, see Part I [22]). In the latter case, a higher and constant gel content was obtained. The presence of tertiary C-atoms in grafted PE, which are weak links in polyolefin chains, may explain the lower gel contents for MA grafted PE1.

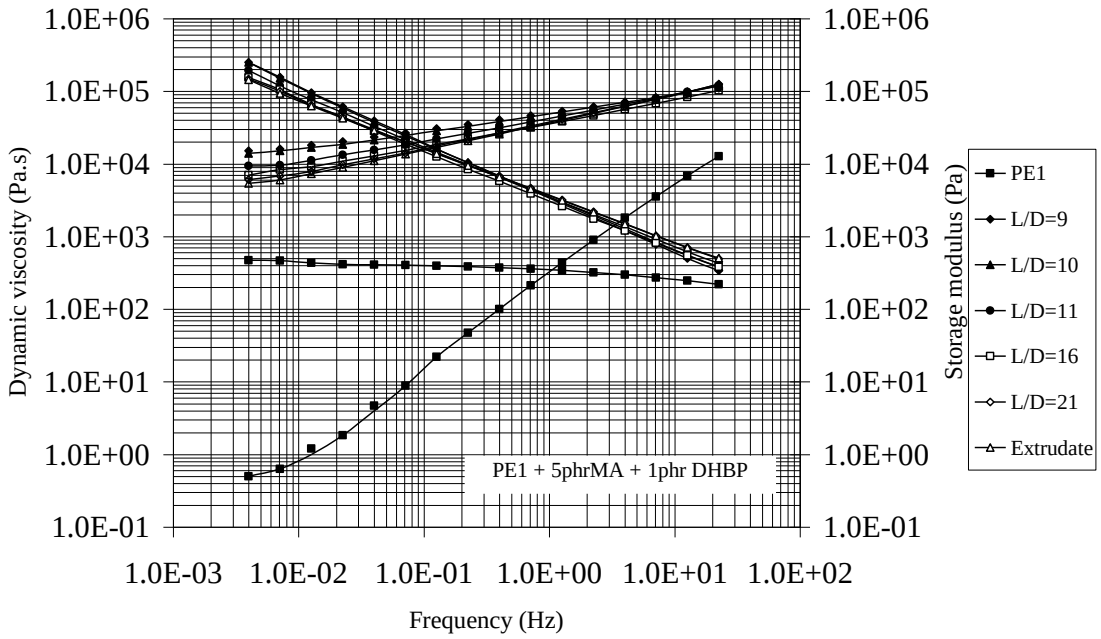

Figure 5.5 - Rheological behaviour of graft PE1 along the extruder (dynamic viscosity and storage modulus).

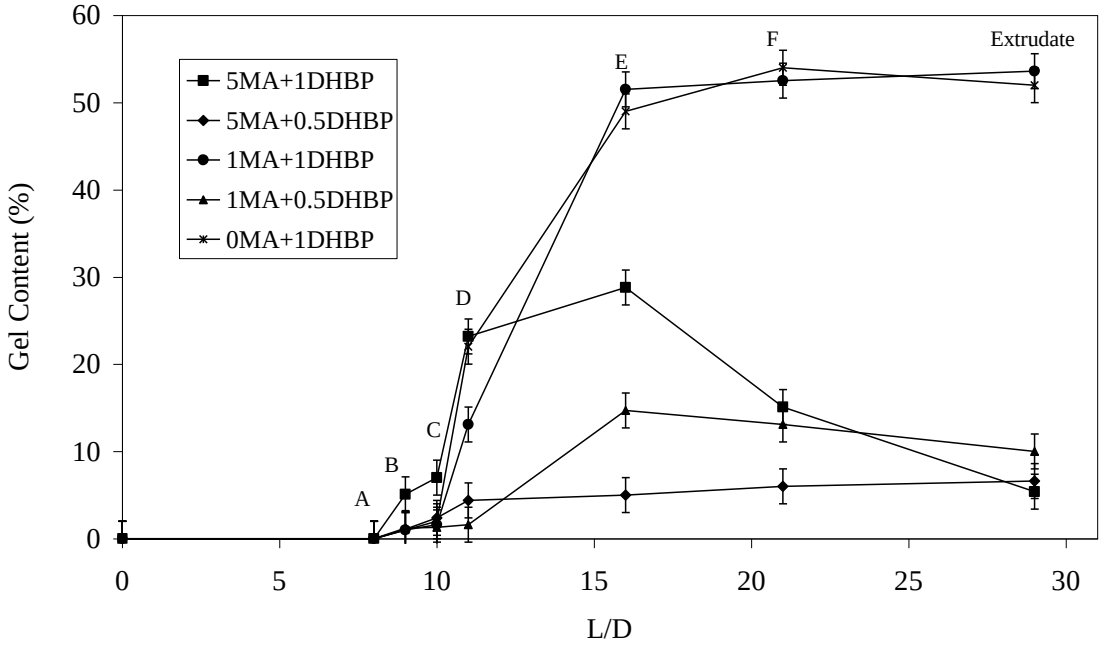

Figure 5.6 – Gel content of MA grafted PE1 along the extruder using different recipes.

When PE2 with a lower molecular weight was grafted, using the same grafting recipe and processing conditions as for PE1, a higher MA graft content was obtained (1.9 wt.%) - Figure 5.3 - and gel formation was not observed (Table 5.4). Since PE1 and PE2 have the same structure, the significant difference in the grafting content should be related to the low molecular weight (lower viscosity) of PE2. In fact, according to Rosales *et al.* [14], high-viscosity materials yield lower degree of functionalization.

From the gel content (Table 5.4) one can observe that for EPM crosslinking is significantly small.

Table 5.5 demonstrates a dramatic decrease of the dynamic viscosity along the extruder for PP modified with 5 phr MA and 1 phr peroxide at 200 ºC. This global behaviour has been reported by many authors for samples taken from the extrudate and is attributed to β-scission of tertiary PP radicals. However, a close look at Table 5.5 will show that the dynamic viscosity continues to decrease beyond sampling position D, although the peroxide is fully decomposed and the MA content has reached a plateau. Thermo-oxidative PP degradation, known to occur when processing PP as such [27,28], may explain this behaviour. The decrease of the dynamic viscosity for MA grafted PP is smaller in comparison with that of PP processed with peroxide (experiments 12 and 14 in Tables 5.1 and 5.5). This has been previously observed for samples taken from the extrudate and was related with the grafted MA onto PP [29], has simply be attributed to competition between MA grafting onto PP and β-scission. This explanation seems rather superficial, since β-scission does not result in loss of free radical species. A more detailed mechanistic explanation is put forward in Figure 5.7. Hydrogen abstraction from PP will occur mainly from tertiary C-atoms and, subsequently, MA will add to the tertiary radical. Heinen *et al.* [30] have shown that two PP-g-MA structures with a ~ 50/50 ratio are eventually formed. The first one is formed via H-transfer of the PP-g-MA radical, resulting in a single succinic anhydride unit attached on the PP chain and a new tertiary PP radical, which may undergo β-scission. The second graft structure is formed from the first graft structure via H-abstraction by a tertiary PP radical followed by β-scission, yielding a terminal, unsaturated itaconic-anhydride-like structure and a primary PP radical. The latter is not susceptible to β-scission and, thus, will terminate,

probably via combination. As a result of the formation of the terminal grafted MA PP, tertiary PP radicals are converted and thus degradation is suppressed.

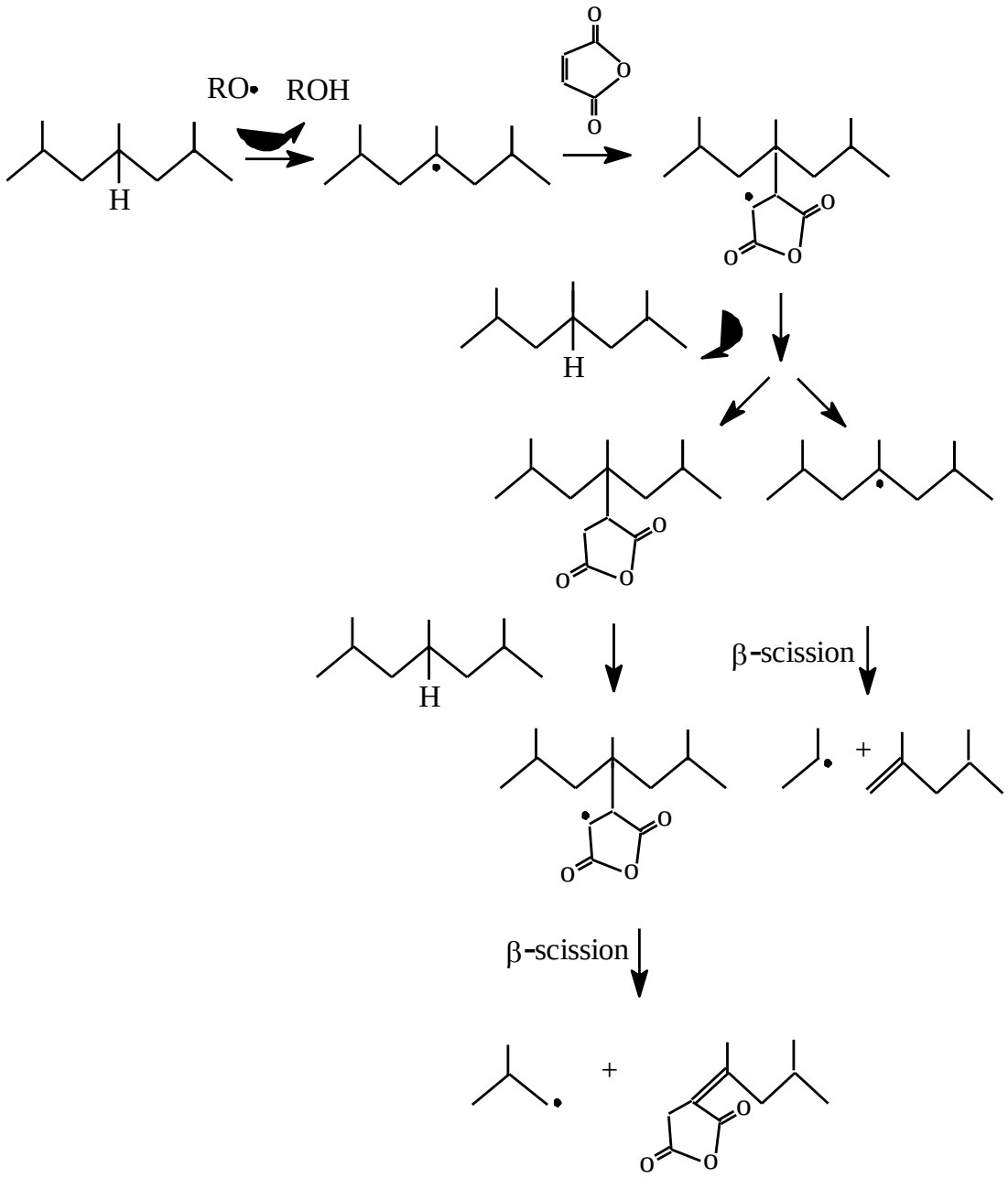

Figure 5.7 – Mechanism of free radical grafting of MA onto PP.

5.3.4 - Effect of recipe and peroxide type on grafting profile

As shown in Table 5.1, PE1 was processed using various grafting recipes (experiments 1 to 6, 8 and 9). The results are presented in Tables 5.2, 5.4 and in Figure 5.8. As expected, there is a significant decrease of the amount of grafted MA along the extruder axis when the MA feed is reduced from 5 to 1 phr (DHBP = 1 phr). However, and within the experimental error, the profiles become similar when the peroxide content is decreased from 1 to 0.5 phr (MA = 5 phr).

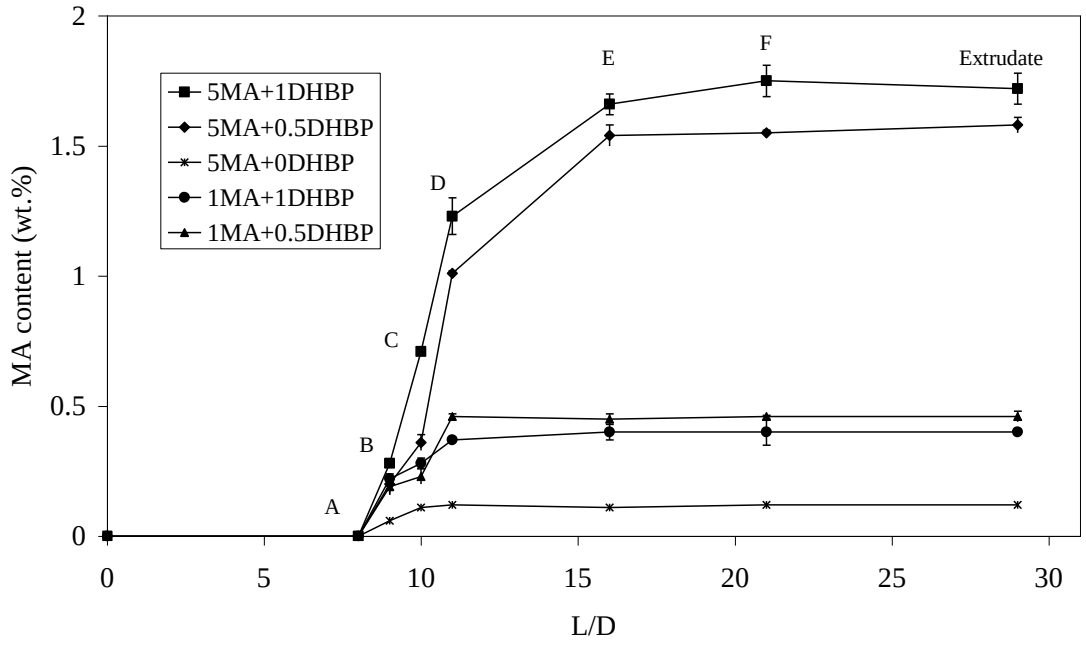

Figure 5.8 – MA graft content of PE1 along the extruder using different grafting recipes.

Some authors [24,31,32] reported a maximum level of grafted MA when using 2 phr MA, but the results of these studies are difficult to compare directly with our data, since different reactors, set temperatures, mixing conditions and/or peroxides were used. The effect of thermal grafting (no peroxide) was also investigated and as one can see the level of grafted MA is rather low (~ 0.1 wt.%) (Table 5.2, Figure 5.8) and no effect on dynamic viscosity was detected. In this case, grafting is probably due to thermal-oxidative formation of free radicals.

Gel content of PE1 (Figure 5.6) increases dramatically when 1 phr MA plus 1 phr DHBP is used. The values are much lower when 0.5 phr peroxide is used either with 1 or with 5 phr MA. The latter has even a lower gel content than the former. This is probably related to the higher graft content obtained when using 5phr MA, as discussed above.

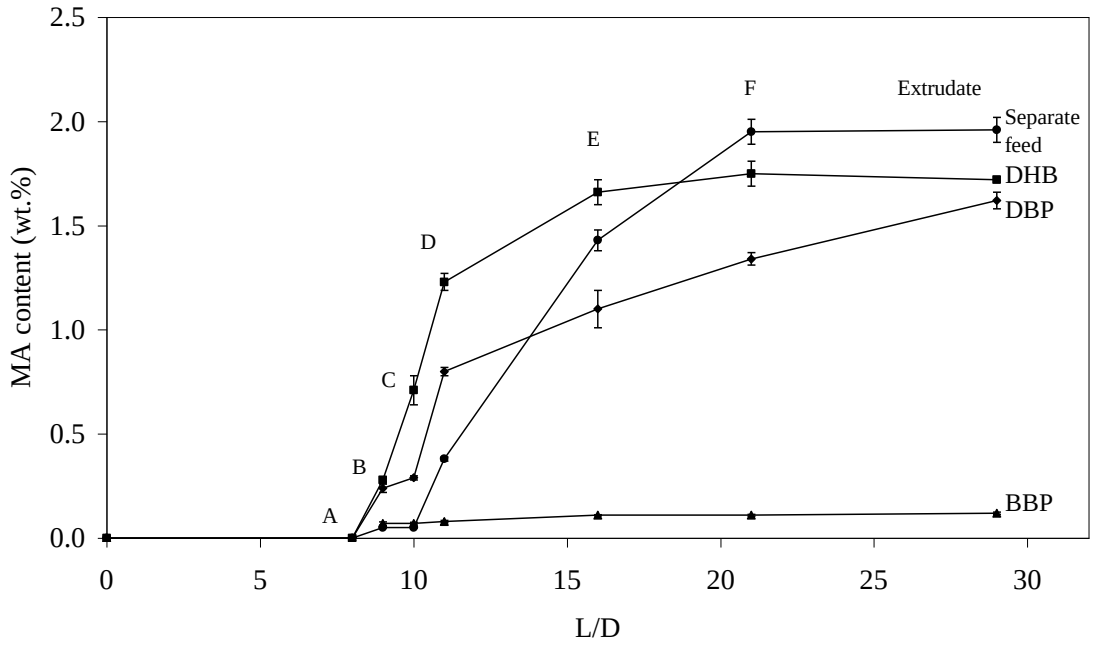

Figure 5.9 – MA graft content of PE1 along the extruder using different peroxides and separate feed with 5phr MA and 1 phr DHBP at 200 ºC.

The results of grafting MA onto PE1 using different peroxides (DHBP, BBP and DBP) are shown in Table 5.2 (experiments 1, 8 and 9) and in Figure 5.9. Despite using the same number of moles of peroxide in the three experiments, the grafting profiles are clearly different. Figures 5.4, 5.10 and 5.11 plot the experimental MA graft content and the calculated peroxide decomposition as a function of the average residence time. Since BBP decomposes quickly, a very low amount of MA is grafted onto PE1 (Figure 5.10). Probably, BBP decomposes before itself, or MA is completely dissolved in PE1. Thus, the amount of grafted MA is strongly reduced. On the other hand, DBP decomposes slower, the calculated peroxide decomposition is only complete at the end of the extruder, and as a result the grafting reaction can continue along the whole extruder. This is in accordance with the experimental results, which show that the MA

grafting level has a lower value in the first part of the screw (location C), but it steadily increases along the extruder without reaching a plateau (Figure 5.11).

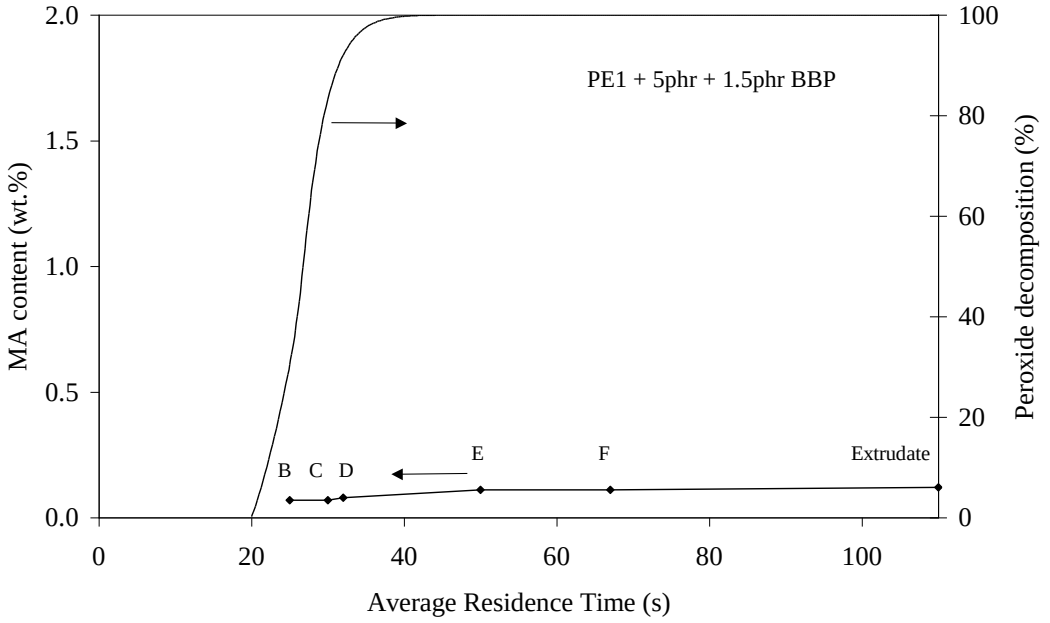

Figure 5.10 – MA graft content for PE1 and calculated peroxide decomposition, with 5 phr and 1.5 phr BBP at 200 ºC, as a function of average residence time.

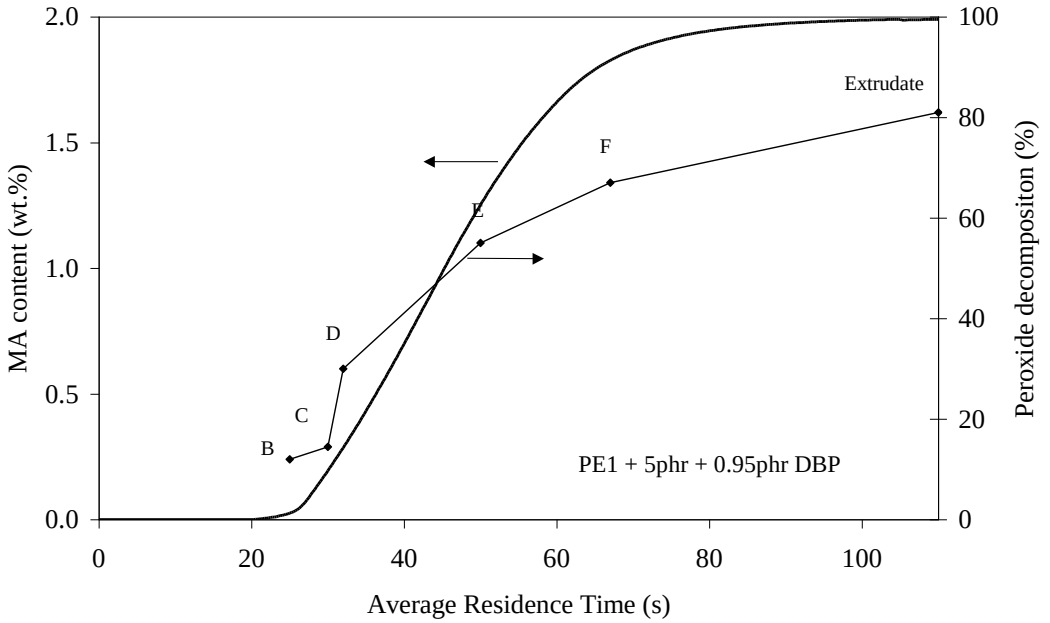

Figure 5.11 – MA graft content for PE1 and calculated peroxide decomposition, with 5 phr and 0.95 phr DBP at 200 ºC, as a function of average residence time.

DHBP behaves in between BBP and DBP. The calculated decomposition is complete at location E and, consequently, grafting continues until the MA graft content reaches a plateau when all peroxide is decomposed.

A correlation between the experimental MA graft content and the calculated peroxide decomposition is shown in Figure 5.12. Both for DHBP and DBP a convex correlation is observed indicating that grafting efficiency, defined as the degree of grafting normalized to the peroxide decomposition, decreases during the grafting process.

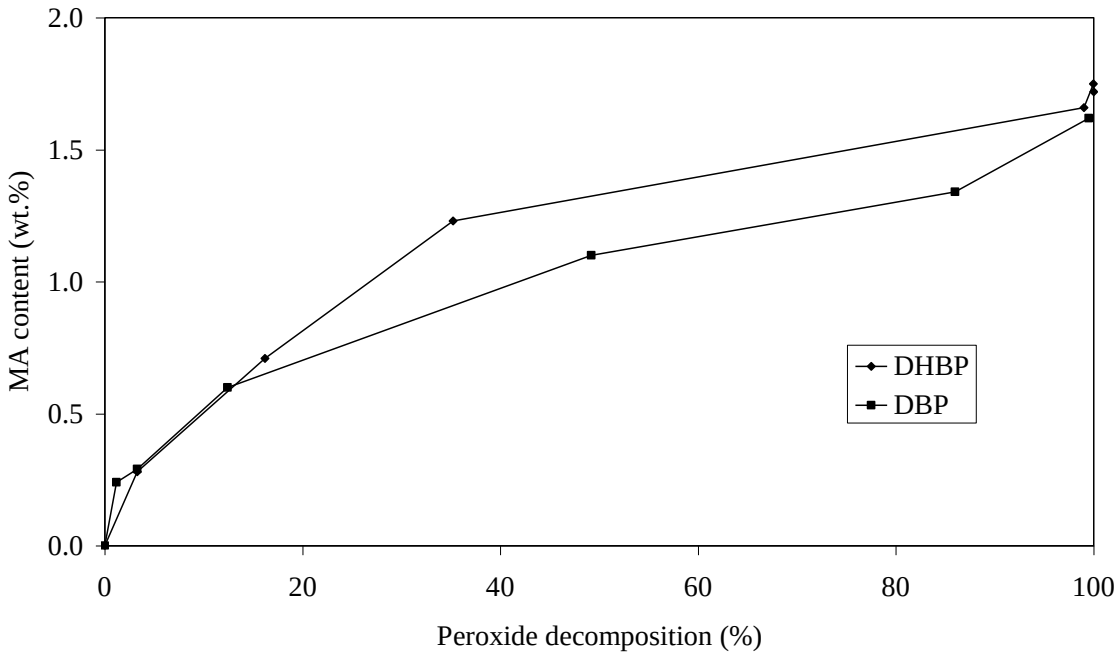

Figure 5.12 – Correlation between MA graft content for PE1 and calculated peroxide decomposition (DHBP and DBP).

5.3.5 - Separate feed of peroxide

The effect of incorporating the peroxide after MA has dissolved in the molten polymer was investigated for PE1 and PP (experiments 7 and 13, respectively). As demonstrated in Figure 5.9 (for PE1), up to location C - where the peroxide was added - only thermal grafting is possible, consequently the MA graft contents are very small. At location D, which is one L/D downstream, an increase of the MA content can already be observed. The final amount of grafted MA is higher than in the case of simultaneous

MA/peroxide feed. This shows that simultaneous feed dispersion and/or dissolution of MA into the polymer melt is, at least, one of the limiting factors of the grafting yield. The gel content of PE1 was similar to the highest gel content obtained when the components are pre-mixed. The difference is that for simultaneous feed there seem to be no time for degradation of the network. For PP the grafting MA evolution along the extruder is similar as for PE1, but the final MA content is not significantly different of simultaneous feed (Table 5.2). However, dynamic viscosity values after location D are lower compared to the values obtained when the components are pre-mixed (Table 5.5).

5.4 - CONCLUSIONS

Grafting of MA onto polyolefins with different ethene/propene ratios was studied along an extruder axis using a series of sampling devices. The MA graft content follows the same profile along the axis when the same conditions (recipe, peroxide and processing conditions) were used, regardless of the choice of polyolefin and MA and peroxide concentrations. However, the final MA graft content depends on the polyolefins composition: PE>EPM>>PP. As expected, in the case of PE crosslinking occurs besides grafting, but at sufficient screw length the PE network is degraded again. As in Part I, where changes in rheological behaviour could be related to the peroxide decomposition, a good correlation could be established between experimental grafting and calculated peroxide decomposition profiles.

It was generally concluded that the degree of branching/crosslinking and/or degradation, as well as the MA graft content, depends essentially on the ethene/propene ratio of the polyolefin. Chemical reactions occur along the extruder until the peroxide is fully converted.

5.5 - REFERENCES

[1] – Reactive Extrusion, M. Xanthos (Ed.), Hanser Publishers, New York, 1992.

[2] –Reactive Modifiers for Polymers, S. Al-Malaika (Ed.), Blackie Academic & Professional, London, 1997.

[3] – D. H. Roberts, R. C. Constable, and S. Thiruvengada, *Polym. Eng. Sci.*, 3**7**, 1421 (1997).

[4] – W. Gabara and S. Porejko, *J. Polym. Sci.: Part A: Polym. Chem*, **5**, 1539 (1967).

[5] – T. Bray, S. Damiris, A. Grace, G. Moad, M. O'Shea, E. Rizzardo and G. V. Diepen, *Macromol. Symp.*, **129**, 109 (1998).

[6] – B. J. Kim and J. L. White, *Intern. Polym. Processing X*, 213 (1995).

[7] – H. Chiu and W. Chiu, *J. Appl. Polym. Sci*., **68**, 977 (1998).

[8] – R. M. Ho, A. C. Su, C. H. Wu and S. I. Chen, *Polymer*, **34**, 3264 (1993).

[9] – C. H. Wu and A. C. Su, *Polym. Eng. Sci.*, **31**, 1629 (1991).

[10] – C. Wu, C. Chen, E.Woo and J. Kuo, *J. Polym. Sci.: Part A: Polym. Chem.*, **31**, 3405 (1993).

[11] – N. G. Gaylord, M. Mehta and R. Mehta, *J. Appl. Polym. Sci*., **33**, 2549 (1987).

[12] – A. J. Oostenbrink and R. J. Gaymans, *Polymer*, **33**, 3086 (1992).

[13] – A. K. Ray, A. Jha and A. K. Bhowmick, *J. Elast. Plast.*, **29**, 201 (1997).

[14] – C. Rosales, R. Perera, M. Ichazo, J. Gonzalez, H. Rojas, A. Sánchez and A. Barrios, *J. Appl. Polym. Sci*., **70**, 161 (1998).

[15] – B. De Roover, M. Aclavons, V. Carlier, J. Devaux, R. Legras and A. Momtaz, *J. Polym. Sci.: Part A: Polym. Chem.*, **33**, 829 (1995).

[16] – W. Michaeli and A. Grefenstein, *Polym. Eng. Sci.*, 3**5**, 1485 (1995).

[17] – L. P. B. M. Janssen, *Polym. Eng. Sci.*, 3**8**, 2010 (1998).

[18] – B. Kim and J. L. White, *Polym. Eng. Sci.*, 3**7**, 576 (1997).

[19] – P. E. Gloor, Y. Tang, A: E. Kostanska and A. E. Hamielec, *Polymer*, 3**4**, 1012 (1994).

[20] - A.V. Machado, J. A. Covas and M. van Duin, *J. Appl. Polym. Sci*., **71**, 135 (1999).

[21] – A. V. Machado, J. A. Covas and M. van Duin, *J. Polym. Sci.: Part A: Polym. Chem.*, **31**, 1311 (1999).

[22] – A. V. Machado, J. A. Covas and M. van Duin, submitted to J. Appl. Polym. Sci..

[23] - O. S. Carneiro, G. Caldeira, and J. A. Covas, Proc. *Mat. Proc. Tech.*, **92-93**, 309 (1999).

[24] – A. H. Hogt, Proc. Compalloy'90, New Orleans, USA, 1990.

[25] – M. Avela, N. Lanzetta and G.Maglio, Polymer Blends (Eds M. Kryszewski, A. Galeski and E. Martuscelli), vol.2, Plenum, New York, 1984.

[26] – A. V. Machado, M. van Duin and J. A. Covas, submitted to Polymer.

[27] – A. C. Kolbert, J: G. Didier and L. Xu, Macromolecules, 8598 (1996).

[28] – M. G. Lachtermacher and A. Rudin, J. Appl. Polym. Sci., 58, 2077 (1995).

[29] – B. Wong and W. E. Baker, *Polyme*r, **38**, 2781 (1997).

[30] – W. Heinen, C. H. Rosenmöller, C. B. Wenzel, H. J. M. de Groot, J. Lugtenburg and M. van Duin, *Macromolecules*, **29**, 1151 (1996).

[31] – S. Porejko, W. Gabara and J. Kuleska, *J. Polym. Sci.: Part A-1*, **5**, 1563 (1967).

[32] – N. Gaylord, R. Mehta, D. R. Mohan and V. Kumar, *J. Appl. Polym. Sci*., **44**, 1941 (1992).

Part III

Compatibilization of Polymer Blends

6.1 - INTRODUCTION

Polyamides (PAs) are extensively used in engineering applications due to their relatively high toughness and excellent chemical and abrasion resistance. However, toughness deteriorates significantly at low temperatures, thus preventing usage in specific applications. Blending PA with a small amount of a functional rubber has been shown to improve toughness. In fact, it has found widespread commercial application and has probably become one of the most studied examples of "in-situ" compatibilization of polymer blends. Maleic anhydride (MA) modified styrene/ethylene/butylene/styrene block copolymers (SEBS-g-MA) [1,2], acrylonitrile/butadiene/styrene terpolymers (ABS) in combination with MA containing compatibilizers [1-3], emulsion-made core-shell rubbers (e.g, acrylic or butadiene-based rubber core and poly(methyl methacrylate) shell) [4] and MA modified ethylene/propylene elastomers (EPM-g-MA) [1,2,5-9] have been successfully used for impact modification of PAs.

It was demonstrated that the MA grafted onto the rubber undergoes chemical reactions during melt blending with PA, the rubber's anhydride groups reacting with the polyamide's amine end groups to produce PA grafts on the rubber via imide linkages [1,5-8]. While non-compatibilized blends of PA-6/EPM exhibit a morphology with large dispersed particles without adhesion to the PA matrix, functionalized rubbers induce a very fine and stable dispersion of the rubber phase and act as an "interfacial agent" promoting adhesion between the matrix and the dispersed phase [1,5-7]. As for the effects of MA and of rubber concentration on the impact behaviour of PA/rubbers blends, it is by now well-established that the brittle-ductile transition temperature shifts to lower values with increasing rubber concentration and decreasing particle size, and that the interfacial adhesion has no influence on that temperature [1,6].

The above studies focussed on the extrudates produced upon melt blending. However, it is well known that the geometry of the mixing equipment and the operating conditions have a strong effect on the mixing intensity and quality. Consequently, the chemical conversion, the morphology and the rheology of the blends will be affected. It

should be realized that the processing of such reactive PA blends is of high complexity, since chemistry, morphology and rheology continuously and mutually interact. Finally, the morphology and the interphase determine the physical/mechanical properties of the blends [1,8-11].

Therefore, it is important to investigate how chemistry, rheology and morphology interact during the preparation of the blend. Surprisingly, there is little previous work on this area. Sundararaj *et al*. [12] published the first study of morphology changes along the length of a plasticating "clamshell" type twin-screw extruder. They concluded that the major morphology changes occurred in the first kneading section; samples 20 mm further down the extruder exhibited a significant morphology evolution. However, sample collecting was relatively slow (the reported sampling times varied between 40 and 60 s), thus allowing for a significant relaxation of both matrix and dispersed polymer to occur after cessation of the shear. Later, the authors [13] showed that a high amount of interfacial area is generated very rapidly during melt mixing. This is important in the case of reactive blends, since it favors a high degree of interfacial reaction. Experimental observations related to recent efforts to speed up the material sampling procedure in order to produce more reliable samples [14-16] have confirmed the rapid development of morphology at the melting zone. As far as the evolution of chemical conversion along the extruder is concerned, Majumdar *et al.* [3], again using a "clamshell" type extruder, recently reported that the degree of chemical conversion of some PA based blends reaches a plateau in the initial regions of the screw and that the extent of the reaction varies with screw speed. A correlation between the extent of the reaction and the particle size of the dispersed phase could be established.

The present work aims at studying the evolution of the chemical reaction of PA-6/EPM/EPM-g-MA blends in a twin-screw extruder and how this correlates with the development and stability of the morphology along the screw length. For this purpose, small amounts of material were collected quickly at relevant locations from inside an extruder working under steady state conditions using a recently developed sampling device [16], and quenched for subsequent characterization. The effect of changes of the blend composition was also studied.

6.2 - EXPERIMENTAL PROCEDURE

6.2.1 - Materials

Commercial PA-6 (Akulon® K123) and EPM (Keltan® 740) produced by DSM, the Netherlands, were used. EPM-g-MA (Exxelor VA 1801, 1803, 1820 and 1810, containing 0.49, 0.47, 0.31 and 0.22 wt.% of MA, respectively, as determined by FT-IR) were kindly provided by Exxon, Spain. The amount of PA-6 was kept constant in all blends (80 wt.%), whereas the concentration of EPM and EPM-g-MA was varied as shown in Table 6.1.

Table 6.1 – Composition of the PA-6/EPM/EPM-g-MA blends

Blend	EPM (wt.%)	EPM-g-MA		MA content of the rubber phase (wt.%)	MA content of the blend (wt.%)
		(wt.%)	MA content (wt.%)		
80/20/0	20	0	0	0	0
80/15/5	15	5	0.49	0.13	0.025
80/10/10	10	10	0.49	0.25	0.049
80/5/15	5	15	0.49	0.37	0.074
80/0/20a	0	20	0.49	0.49	0.098
80/0/20b	0	20	0.31	0.31	0.062
80/11.5/8.5	11.5	8.5	0.47	0.20	0.040
80/8/12	8	12	0.22	0.13	0.026

6.2.2 - Preparation of the blends

The blends were prepared in a laboratory modular Leistritz LSM 30.34 intermeshing co-rotating twin-screw extruder coupled to the relevant downstream accessories. Blends were compounded with the screws rotating at 200 rpm, with a flow rate of 6 kg/h and set temperatures of 220 - 230 ºC in the barrel and 220 ºC at the die. Both the configuration of the screws and the axial location of the sampling devices (see [16] for

a more complete description of these tools) are depicted in Figure 6.1. The material was collected at zones where the melt was being subjected to more intensive mixing and significant changes in morphology and/or chemistry would be anticipated, i.e. at staggering kneading blocks and at left-handed screw elements. Immediately after collection the samples were quenched in liquid nitrogen in order to prevent further reaction or coalescence.

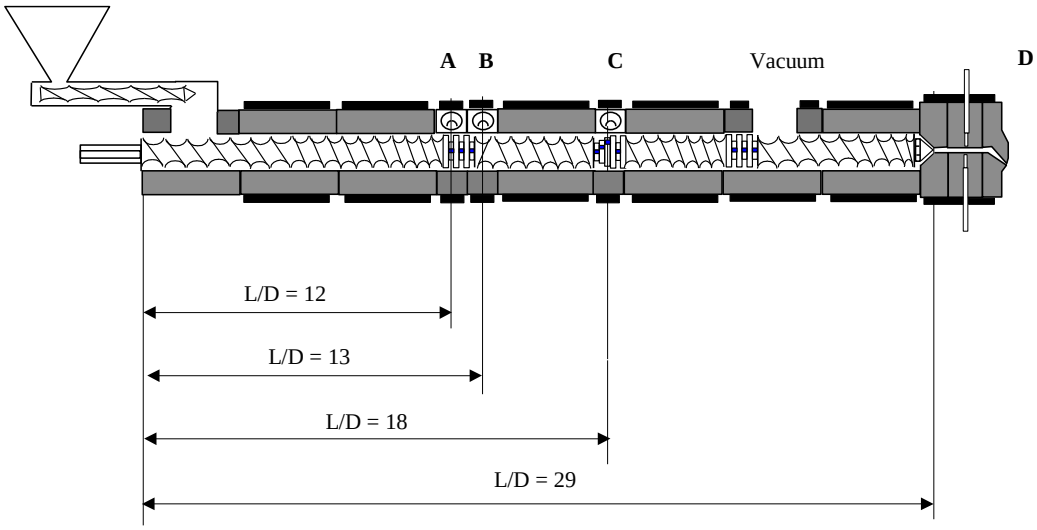

Figure 6.1 - Screw configuration and sampling locations.

6.2.3 - Characterization of Materials

The details of the chemical characterization of the PA blends are discussed elsewhere [10]. The samples were initially milled and dried overnight. Then, part of the samples was stirred in formic acid at room temperature during 24 hours in order to extract all free PA-6. The nitrogen content of the centrifuged residues was determined with a LECO FP-428 Nitrogen Analyser. The remaining of the samples was hydrolysed with hydrochloric acid for 6 hours and subsequently filtered, washed with water and dried for one hour at 180 ºC, in order to convert dicarboxylic acid back to anhydride. Thin films were prepared by compression-moulding and characterized by FT-IR (Perkin Elmer 1720 spectrometer). The anhydride carbonyl peak at 1785 cm^{-1} (see Figure

6.2a), together with an IR calibration formula obtained with a set of references, allowed the quantitative determination of the MA content in the hydrochloric acid residues.

After fracture of the samples in liquid nitrogen, etching with boiling xylene to remove the rubber from the surface and gold plating, the morphology of the blends was studied using a Jeol JSM 6310F Scanning Electron Microscope. Samples were trimmed (in 0.1 x 0.2 mm bits) at room temperature and stained with a 50/50 osmium tetroxide/formaldehyde mixture. Cryo-coupes of about 70 nm thickness were cut at – 100 ºC and then analysed with a Philips EM420 Transmission Electron Microscope at 120 kV. The morphology was characterized in terms of the size and the size distribution of the dispersed phase. A Leica Quantimet 550 image analysis system was used to quantify the equivalent circle diameters, which were computed from individual particle areas, whereas the distribution width was estimated from the variance. At least 300 particles for each micrograph were observed for this purpose.

The thermal characterization of the blends was carried out in a power compensated Perkin Elmer DSC7. Circa 6-10 mg of each sample was scanned in the range 25-220 ºC at 10 ºC/min.

6.3 - RESULTS AND DISCUSSION

The sampling locations A to D are specified in Figure 6.1. They were chosen in order to follow the reactive blending process in real time. While A and C correspond to modules of kneading blocks in the screw, B is adjacent to a left-handed screw section. In all cases, high pressure and shear are developed, providing conditions for chemical reaction and/or droplet break-up. The collection of samples from conveying zones was avoided, since one anticipates that coalescence of the disperse phase will take place. Location D corresponds to the die exit (i.e. the extrudate).

The actual occurrence of a reaction between PA-6 and the MA modified rubber under the processing conditions selected was initially investigated. Figure 6.2 shows the FT-IR spectra of the 80/0/20a (w/w/w) blend at location A after hydrolysis with hydrochloric acid removing all aminocaproic acid units but not the one attached to

EPM-g-MA (Figure 6.2a) and of the initial EPM-g-MA (Figure 6.2b). A comparison of these two spectra evidences the strong reduction of the peak intensity at 1785 cm^{-1} upon blending, which implies that almost all anhydride groups have reacted. Moreover, the observation of a new peak at 1720 cm^{-1} due to an imide group confirms the reaction between the MA modified rubber and the PA-6 in the blend, yielding a PA-EPM graft copolymer [1].

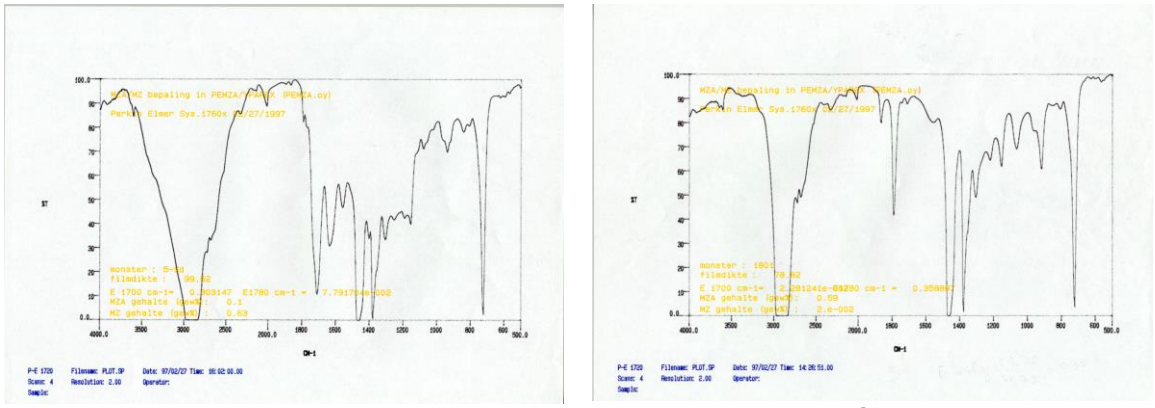

a) b)

Figure 6.2 – Infra-red spectra of: a) PA-6/EPM-g-MA (80/0/20a w/w/w) blend after hydrolysis with hydrochloric acid and b) EPM-g-MA before blending.

Table 6.2 shows the residual MA content of EPM-g-MA for the various blends along the extruder, as determined by FT-IR. The MA content of the 80/0/20a blend, i.e. containing the largest amount of MA, decreased significantly from its original value in location A (0.49→0.07) and remains unchanged thereafter. As for the other blends with less MA the ratio between the initial and the residual MA content is similar (0,13→0,02 for blend 80/15/5; 0,25→0,03 for blend 80/10/10; 0,37→0,06 for blend 80/5/15), and the value at location A is already very small, it was considered sufficient to present data only for locations A and D.

The results indicate that for all blend compositions the MA content decreases drastically in the first part of the extruder up to the first kneading zone (location A), i.e., upon melting of the material, as will be seen later. Since almost all MA has reacted, an additional decrease further on the extruder is not possible. This conclusion is in line with that of Scott [17], who monitored this reaction in a batch mixer and reported a

very fast reaction. The residual MA groups are probably located inside the rubber particles and not at the interface. This residual MA content along the extruder seems to be largely independent of the original MA content.

Table 6.2 – Chemical conversion of PA-6/EPM/EPM-g-MA blends as a function of the screw length.

Blend	Sampling location	Residual MA content of EPM-g-MA (wt.%)	Reacted MA (%)	N (%)	PA-6 grafted on 20 g of EPM+EPM-g-MA (g)	$\overline{M}_n$ of grafted PA-6 (g/mol)
80/15/5	A	0.02	85	0.14	0.22	1000
	D	0	100	0.23	0.38	1400
80/10/10	A	0.03	88	0.50	0.84	1900
	D	0.01	96	0.48	0.81	1700
80/5/15	A	0.06	84	0.39	0.65	1000
	D	0.04	89	0.48	0.81	1200
80/0/20a	A	0.07	86	0.45	0.75	900
	B	0.07	86	-	-	-
	C	0.08	84	0.51	0.86	1000
	D	0.07	86	0.48	0.81	1000
80/0/20b	A	0.07	68	-	-	-
	D	0.04	82	-	-	-
80/11.5/8.5	A	0.03	85	-	-	-
	D	0.02	90	-	-	-
80/8/12	A	0.05	75	-	-	-
	D	0.03	84	-	-	-

Both the amount of PA grafted during blending and the molecular weight of these grafts were computed from the nitrogen content of the residues, obtained after extraction of all free PA-6 from the blends and from the residual MA content, respectively (Table 6.2). Within the experimental error, the PA graft content is independent of the sampling location, which is in agreement with the FT-IR observation that most MA is converted in location A. As the original MA content of the blends increases, the amount of PA grafted at the interface increases until it reaches a constant level of 0.8 g PA / 20 g EPM+EPM-g-MA. Parallelly, the molecular weight of

the grafted PA increases with increasing blend MA content. In summary, the number of chains grafted increases, and reaches a plateau, so their length decreases. Similar observations were reported by Duin *et al.* [10] and are related to the degradation of the PA chains grafted onto the modified rubber. When there is an excess of MA the degraded grafted PA chains will form new grafts, due to the reaction of amine groups formed from the amide bonds broken with MA groups of the rubber.

Since it has already been shown [10] that the degradation of PA can occur due to the effect of water formed as a product of the imide reaction during blending of PA and MA containing polymers, this was not pursued in this work. Degradation of PA can occur especially when the amount of MA is equal to or larger than the amount of PA end groups. Duin *et al*.[10] showed that for a SMA/PA-6 blend the molecular weight of the PA was about 0.05 of that of the original PA, i.e. 20 amide bonds of each PA chain were broken. This is not just thermal degradation, but a process which occurs in the presence of anhydrides only. Now, the reaction between anhydride and amide towards imide can not be a direct one, since a molecule of water is missing in the reaction equation. This molecule of water may come from the water molecule released upon reaction of amine with anhydride to imide. Although the actual mechanism has not been proven, it is thought that there is a reaction cycle: first anhydride plus amine gives imide and water, then amide plus water gives amine etc. This is not surprising, since the solubility of water in PA-6 is very high and the equilibrium acid + amine $\leftrightarrow$ amide + water is shifted to the left at higher temperatures. Finally, although the extruder is vented at the end, there will be sufficient pressure at other parts of the extruder to prevent water from devolatilizing.

Figures 6.3 to 6.5 show the evolution of the morphology of blends 80/20/0, 80/15/5 and 80/0/20a along the extruder, as observed by SEM after extraction of the rubber and by TEM for blend 80/0/20a, which has the highest MA content and exhibits a finer morphology. Figures 6.3a and 6.4a clearly show the presence of a solid PA pellet at location A surrounded by molten polyamide and rubber, which has the lowest T_g (-30 ºC). At location B (Figures 6.3b and 6.4b), which is 4 cm downstream (see Figure 6.1), the solid pellets are no longer present, only dispersed domains a few microns in size can be observed. These domains correspond to the rubber phase which was, as referred

previously, extracted with hot xylene. Therefore, one can postulate that initially the rubber becomes the continuous phase, surrounding the solid PA-6 pellets. Upon melting of the PA-6 phase inversion will take place i.e., rubber will constitute the dispersed phase. The observed occlusions in the rubber particles (Figure 6.5) support this hypothesis. Clear evidence of this process is difficult to obtain, as changes in processing conditions did not alter significantly the rate of evolution of the morphology. If a high amount of interfacial area was already generated very rapidly upon melting, the phase inversion process may produce a further increase and, consequently, contribute to higher rates of conversion at this stage.

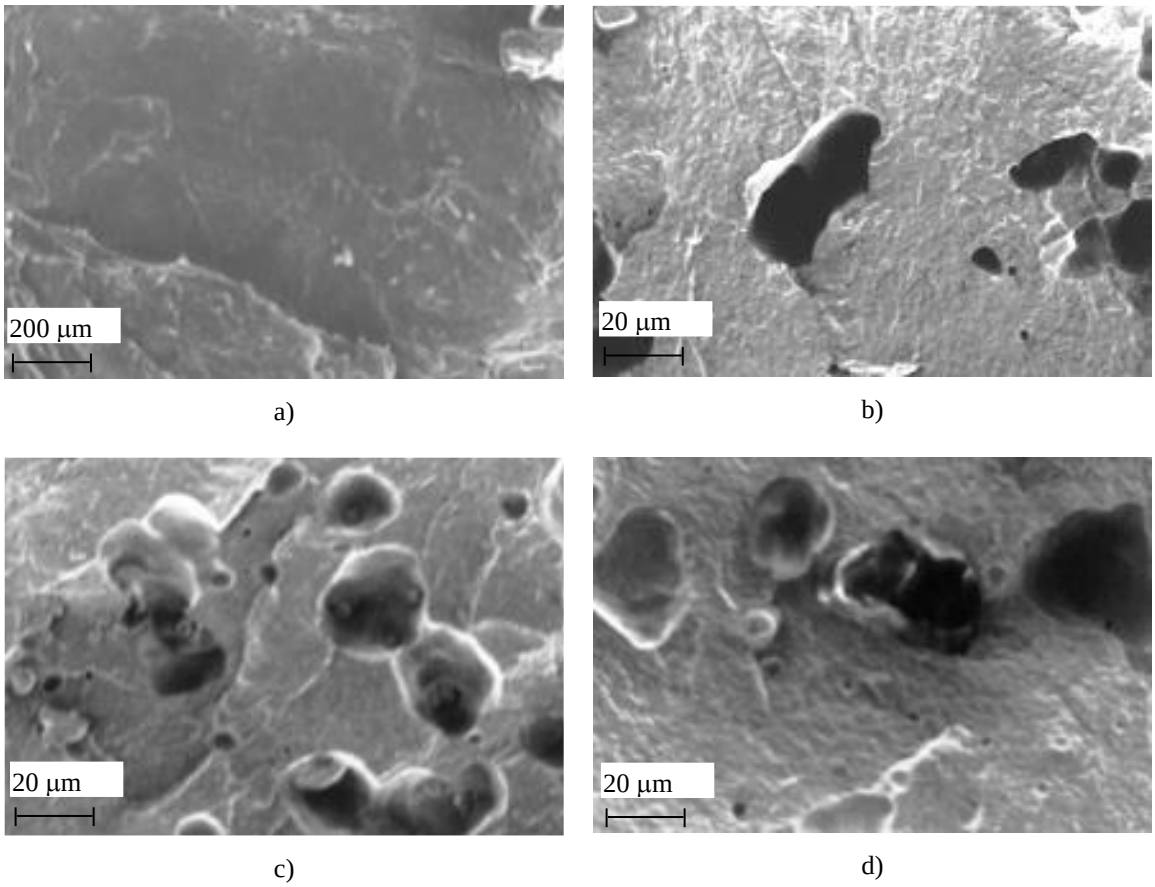

Figure 6.3 - SEM micrographs of uncompatibilized PA-6/EPM (80/20 w/w) blend collected along the extruder at locations A to D (a, b, c and d, respectively).

The dimensional characterization of the dispersed rubber particles is presented in Table 6.3. Data for location A was not obtained, since PA is still partially unmolten and each specific blend was not yet produced. The non-reactive PA/EPM blend (Figure 6.3) exhibits a rather large average particle size and no visible interfacial adhesion.

Although the particle size decreases along the extruder, the most significant changes in morphology occur during and immediately after melting. This type of behaviour was previously observed by Sundararaj et al. [12], who also suggested that a high amount of interfacial area is generated very rapidly [13], thus favouring a high degree of interfacial reaction in the case of reactive blends. For the 80/5/15 blend (Table 6.3 and Figure 6.4) the average rubber particle size is essentially constant (about 2.5 μm), but the particle size distribution significantly narrows. The same type of evolution was observed with the 80/0/20a blend. The material that had already melted at location A shows an irregular morphology with both spherical particles and ribbons or threads (Figure 6.5a), whereas towards the die (Figures 6.5b to 6.5d, respectively) fine regular spherical particles can be noticed.

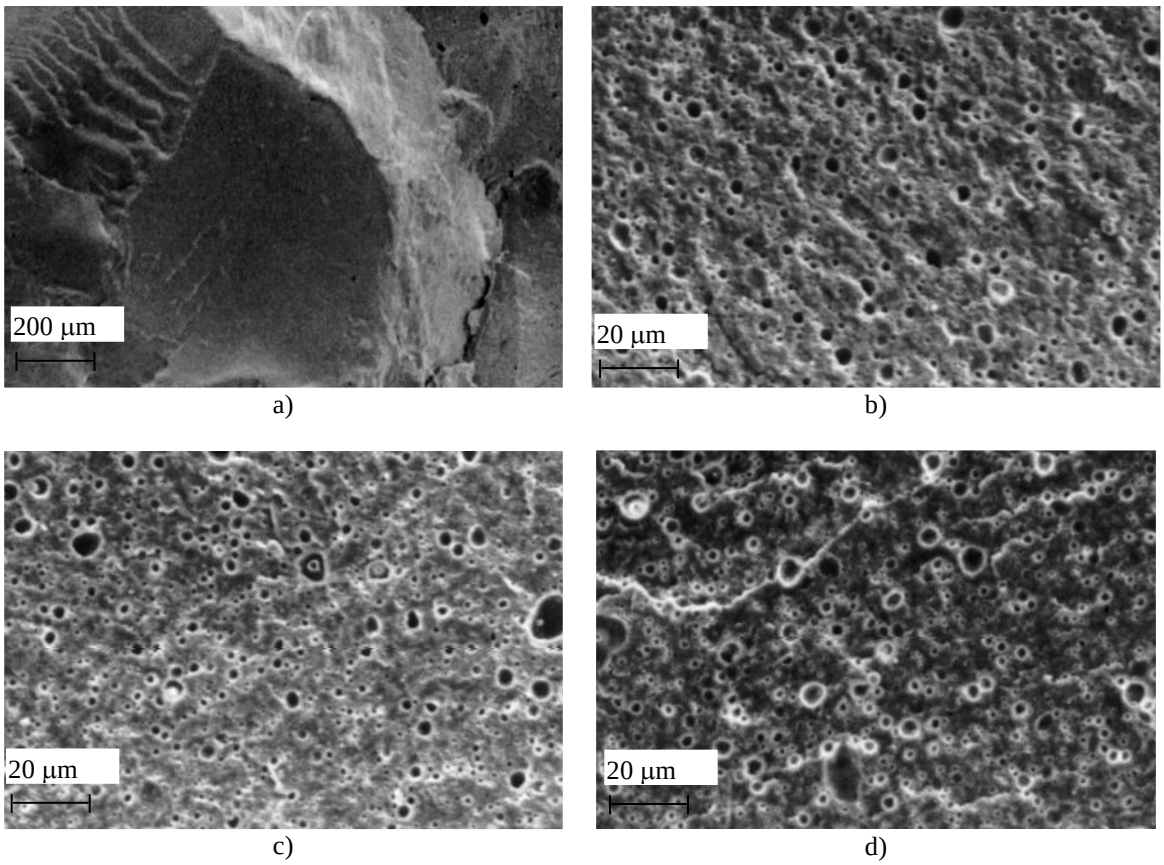

Figure 6.4 - SEM micrographs of PA-6/EPM/EPM-g-MA (80/15/5 w/w/w) collected along the extruder at locations A to D (a, b, c and d, respectively).

When the EPM-g-MA content of the blends is increased from 0 to 5 wt.% there is a strong decrease in particle size (distribution) due to “in-situ” compatibilization. A

further increase in EPM-g-MA content from 5 to 15 wt.% does not affect the particle size (2.7→2.4→2.3 μm), but does result in a narrower distribution (6.5→1.2→0.7 μm^2). However, a step change occurs when only EPM-g-MA is used and no non-functionalized EPM is added to the blend (80/0/20a). The particle size decreases to about 0.3 μm and the distribution further narrows. This step change is probably due to the fact that all rubber chains are now converted into graft copolymers and for enthalpic reasons are driven to the interface. A strong increase in interfacial area, and thus a strong reduction in particle size, is needed to allow this.

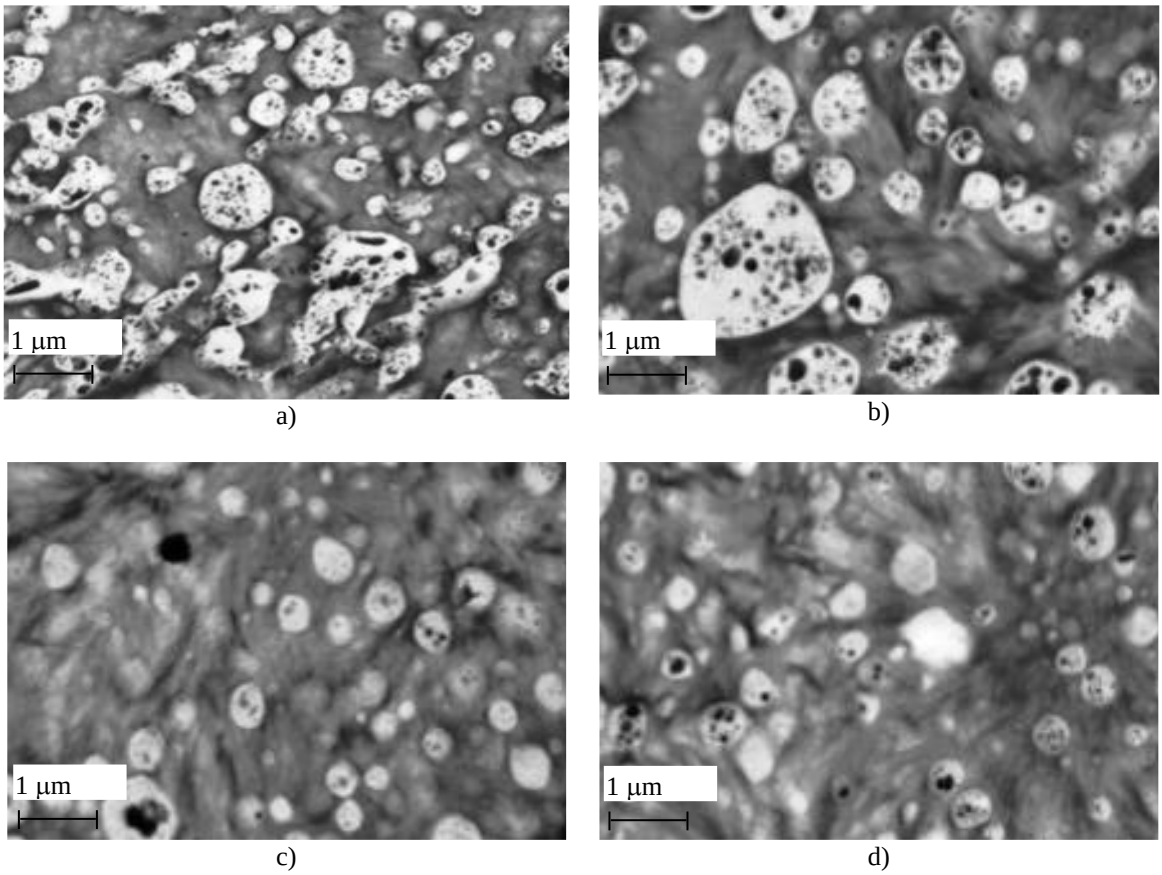

Figure 6.5 - TEM micrographs of PA-6/EPM/EPM-g-MA (80/0/20a w/w/w) collected along the extruder at locations A to D (a, b, c and d, respectively).

The above results indicate the existence of a correlation between melting of the blend components, the conversion of the grafting reaction and the evolution of the morphology of the reactive blend. Major changes on morphology development are associated with high rates of chemical conversion. As seen above, the major

morphology development occurs in the first part of the extruder, where a high amount of interfacial area is generated. On the other hand, it is well known that the reaction between anhydride and aliphatic amine is one of the fastest [18]. Thus, interfacial area and reactivity are intrinsically associated for these systems. Since the intensive mechanical mixing after melting created by the staggered kneading blocks will not induce significant changes in morphology and, therefore, in chemical conversion (see Tables 6.2 and 6.3), the graft copolymers formed upstream at the interface seem to provide sufficient steric stabilization against coalescence of the dispersed phase particles further down the extruder. Conversely, non-reactive blends are more sensitive to the intensity of mixing and to the thermal history.

Table 6.3 - Dispersed rubber particle size of PA-6/EPM/EPM-g-MA blends as determined with electron microscopy.

Blend	Sampling location	Particle Size		
		Average (μm)	Range (μm)	Variance (μm^2)
80/20/0	B	15.8	2.4-49.8	151.3
	C	10.3	2.4-35.7	106.1
	D	9.0	2.0-31.0	92.2
80/15/5	B	2.8	1.5-35.6	8.1
	C	2.7	1.5-24.1	7.5
	D	2.6	1.5-22.5	3.8
80/10/10	B	2.4	1.5-10.2	1.4
	C	2.4	1.5-8.7	1.2
	D	2.3	1.5-8.6	1.1
80/5/15	B	2.3	1.5-4.7	0.7
	C	2.3	1.5-4.8	0.7
	D	2.2	1.5-5.2	0.7
80/0/20a	B	0.4	0.1-1.3	0.06
	C	0.3	0.1-0.7	0.03
	D	0.3	0.1-0.7	0.02
80/11.5/8.5	B	2.5	1.5-10.3	2.0
	C	2.4	1.5-7.2	1.4
	D	2.2	1.5-6.8	0.8

The data also demonstrates that most of the chemical reaction occurs at the surface of the PA-6 pellets during the melting stage. The reaction between EPM-g-MA and PA proceeds already at the interface of the molten EPM phase and the solid PA particles.

The thermal properties (melting temperature and degree of crystallinity) of all the blends along the extruder, as determined by differential calorimetry, do not differ significantly from those of an extruded PA-6 reference (T_m=223 ºC; ΔH_m= 56.5 J/g). This is probably due to the high percentage of PA-6 in the blend, in combination with the low amount of copolymer formed at the interface (Table 6.2: less than 1.1 wt.% of grafted PA relatively to PA present).

6.4 - CONCLUSIONS

This work focussed on the evolution of the grafting reaction and of the morphology development of PA-6/EPM/EPM-g-MA blends in a co-rotating twin-screw extruder.

A correlation between morphology and chemical conversion could be established. Most of the chemical conversion and morphology changes occurred during melting. Since the intensive mechanical mixing induced further on in the extruder did not produce significant changes in morphology, it was postulated that the graft copolymers initially formed at the interface provide steric stabilization and avoid coalescence or break-up of the rubber particles.

6.5 - REFERENCES

[1] – S. Datta and D. Lohse, *Polymeric Compatibilizers*, Hanser Publishers, New York, 1996.

[2] – L. A. Utracki, *Encyclopaedic Dictionary of Commercial Polymer Blends*, ChemTec Publishing, Toronto, 1994.

[3] – B. Majumdar, D. R. Paul, and A. J. Oshinski, *Polymer*, **38**, 1787 (1997).

[4] – M. Lu, H. Keskkula, and D. R. Paul, *J. Appl. Polym. Sci*., **59**, 1467 (1996).

[5] – M. T. Hahn, R. W. Hertzberg, and J. A. Manson, *J. Polym. Sci.*, **18**, 3551 (1983).

[6] – D. Chen, and J. P. Kennedy, *Polymer Bulletin*, **17**, 71 (1987).

[7] – J. W. Kim, and S. C. Kim, *Polym. Adv. Tech.*, **2**, 177 (1991).

[8] – A. Crespy, C. Caze, D. Coupe, P. Dupont, and J. P. Cavrot, *Polym. Eng. Sci.*, **32**, 273 (1992).

[9] – Y. Seo, S. S. Hawang, K. U. Kim, J. Lee, and S. Hong, *Polymer*, **34**, 1667 (1993).

[10] – M. van Duin, M. Aussems, and R. J. M. Borggreve, *J. Polym. Sci.: Part A: Polym. Chem.*, **36**, 179 (1998).

[11] – H. Cartier, G. H. Hu, Proc. Polyblends 97, Boucherville, Canada, 1997.

[12] – U. Sundararaj, C W. Macosko, R. J. Rolando and H. T. Chan, *Polym. Eng. Sci.*, **32**, 1814 (1992).

[13] – U. Sundararaj, C W. Macosko, A. Nakayama and T. Inoue, *Polym. Eng. Sci.*, **35**, 100 (1995).

[14] – T. Sakai, *Adv. Polym. Tech.*, **14**, 277 (1995).

[15] - M. Stephan, O. Franzheim, T. Rische, P. Heidemeyer, U. Burkhardt, and A. Kiani, *Adv. Polym. Tech.*, **16**, 1 (1997).

[16] – A. V. Machado, J. A. Covas, and M. van Duin, accepted for publication in *J. Appl. Polym. Sci.* (1997).

[17] – C. E. Scott, and C. W. Macosko, *Intern. Polym. Processing X*, **1**, 36 (1995).

[18] – M. Retzsch, *Prog. Polym. Sci*., **13**, 277 (1988).

7.1 - INTRODUCTION

Polyamides are very attractive polymers for various engineering applications, but they have some drawbacks, such as moisture uptake and low temperature toughness. In order to improve the performance, polyamides (PAs) have been blended with various rubbers [1-5], such as acrylonitrile-butadiene-styrene (ABS), ethylene propylene (EPM), styrene-butadiene-styrene (SBS) and styrene-ethylene-butadiene-styrene SEBS for increased (low temperature) toughness, and with polypropylene (PP) [3-6] and polyethylene (PE) [1,7-12] in order to improve water uptake and reduce material costs. These blends are usually compatibilized via reactive blending in the presence of maleic anhydride (MA) containing polymers. The MA groups of the compatibilizer react with the amine groups of the polyamide to form copolymers. It is now well accepted that these graft copolymers formed at the interface: i) lower the interfacial tension, improve the interfacial adhesion and prevent coalescence, thus, ii) decrease the domain size of the dispersed phase and stabilize the blend morphology and, consequently, iii) determine the mechanical properties of the final blend [1-12]. Up to now most in-situ compatibilization studies have used black-box approaches, where blend composition, extruder lay-out and processing conditions are correlated with the morphology and mechanical properties of the extruded blends. In a limited number of studies it was attempted to gain more insight into reactive blending by drawing screws or taking samples from the melt, followed by off-line analysis [6, 13-15]. For example, it was shown [6] that the morphology development of a PP-g-MA/PA-6 blend was very rapid and took place during melting. However, most of these studies suffer from the fact that sampling is too slow and the results may not be representative. Recently, we developed a device that allows taking representative samples of the material being processed within a few seconds [16].

A series of such sampling devices was used to study the chemical conversion and the morphological evolution of reactive blends of PA-6 and EPM (PA-6/EPM and PA-6/EPM/EPM-g-MA) along a co-rotating intermeshing twin-screw extruder [17]. It was shown that the MA content of the modified rubber decreases strongly upon melting of

the PA pellets and melt flow through the first set of staggering kneading blocks, i.e. the grafting reaction is very fast. Simultaneously, the morphology changed dramatically in this zone of the extruder, from mm to (sub)μm level. Further downstream the chemical conversion and the morphology hardly changed anymore.

It would be interesting to study the effect of several variables on the chemical reaction and the morphology evolution along the extruder, in order to obtain more detailed information about the physico-chemical processes occurring during blending, such as the eventual development of occlusions of PA-6 on the dispersed rubber particles. In the present study several routes were followed in order to reach these goals. MA-containing materials with higher softening or melting temperatures than EPM (T_g = -45 ºC) were used: PE-g-MA (T_m = 132 ºC), PP-g-MA (T_m = 165 ºC) and SMI (T_g = 190 ºC). PA-6/EPM-g-MA blends with varying composition were prepared changing the ratio of anhydride/amine groups. The feeding sequence of the blend components and the processing conditions (screw speed and temperature profile) were also varied.

7.2 - EXPERIMENTAL

7.2.1 – Materials

PA-6 (Akulon® K123 with M_n = 13.000 g/mol, NH_2 = 55 meq/g and COOH = 60 meq/g), PE-g-MA (HDPE, 0.93 wt.% MA) and SMA imidised with aniline (SMI:1.4 wt. % MA) were obtained from DSM, the Netherlands. EPM-g-MA (Exxelor VA 1801: 0.49 wt.% MA) and PP-g-MA (Epolene E-43 and G-3003, with 2.5 and 0.3 wt.% MA, respectively) were kindly supplied by Exxon, Spain and Eastman Kodak, USA, respectively.

The composition of the various blends studied in this work is shown in Table 7.1. Taking blend 1 as the basis of comparison, in the case of blends 2 to 5 EPM-g-MA was replaced by PE-g-MA, two different PP-g-MA and SMI, respectively. In blends 6 to 8 the PA/EPM blend ratio was changed, i.e. the ratio of reactive groups (amine and MA) was varied from 2.2 to 0.06 mol NH_2/mol MA. In blend 9 EPM with hydrolysed MA

groups (24 hours in boiling water) was used. Blends 10 to 13 have the same PA/EPM-g-MA composition, but were prepared using different processing conditions.

Table 7.1 – Composition and processing conditions of blends of PA-6 and MA-containing polymers (set temperature = 230ºC; throughput = 6 kg/h; screw rotation = 200 rpm).

Blend	PA-6 (wt%)	MA-containing polymer (wt.%)	Extruder lay-out (Figure 7.1)	Comments
1	80	EPM-g-MA (20)	a	
2	80	PE-g-MA (20)	a	0.93 wt.% MA
3	80	PP-g-MA1 (20)	a	2.5 wt.% MA
4	80	PP-g-MA2 (20)	a	0.3 wt.% MA
5	80	SMI (20)	a	1.4 wt.% MA
6	50	EPM-g-MA (50)	a	
7	20	EPM-g-MA (80)	a	
8	10	EPM-g-MA (90)	a	
9	80	EPM-g-MA (20)	a	hydrolysed MA groups
10	80	EPM-g-MA (20)	b	side feed of EPM-g-MA
11	80	EPM-g-MA (20)	c	
12	80	EPM-g-MA (20)	c	Low set temperature profile in the first part of the extruder
13	80	EPM-g-MA (20)	c	screw rotation = 120 rpm throughput = 4 kg/h low set temperature in the first part of the extruder

7.2.2 - Blend preparation

All experiments were carried out in a laboratory modular Leistritz LSM 30.34 intermeshing co-rotating twin-screw extruder. As illustrated in Figure 7.1, two screw configurations were used in this study (Figures 7.1a and 7.1b, respectively). In order to collect small amounts of sample from the extruder during blending, sampling devices

were inserted at specific locations along the barrel (for details see reference [17]), identified in the Figures by capital letters.

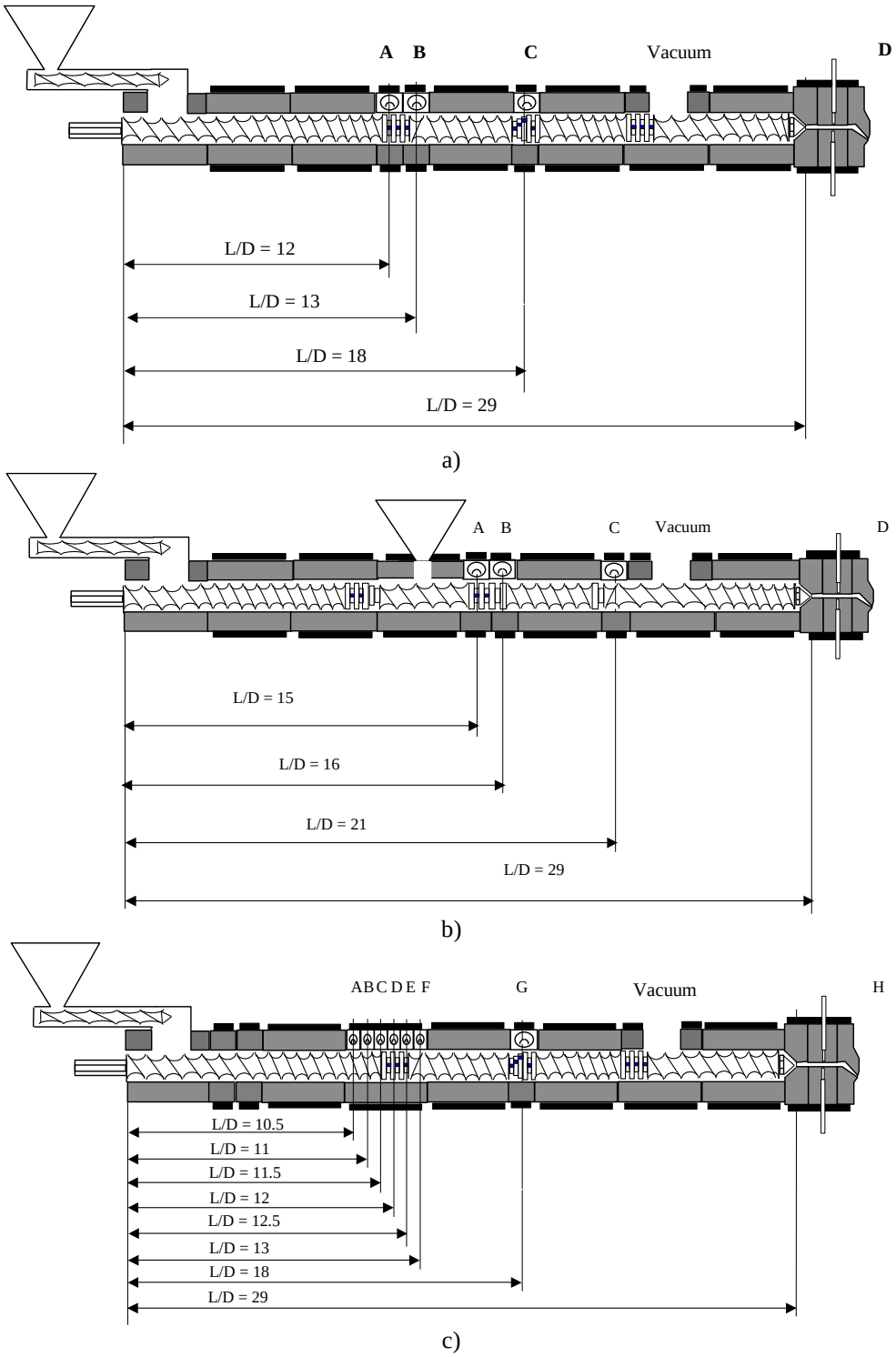

Figure 7.1 – Screw configurations and sampling locations used in this study: a) blends 1-9, b) blend 10 and c) blends 11-13.

.

These were generally zones where high pressure was developed, since not only the main changes in morphology/chemistry will take place here, but also because polymer melt can more easily be removed from the barrel. Circa 2 g of sample were collected within 2 to 3 seconds. In order to avoid further reaction and/or morphological changes such as coalescence of the dispersed phase, all samples were quenched in liquid nitrogen for subsequent characterization.

Blends 1 to 9 were compounded under identical processing conditions (Table 7.1) using the screw configuration shown in Figure 7.1a. This includes three mixing zones comprising staggered kneading blocks, in order to produce significant dispersive mixing downstream. The first kneading block is followed by a reverse element, thus inducing complete melting, while the final mixing section contributes to an effective venting.

In the case of blend 10, the two polymers were fed separately. PA-6 was starve fed as usual and, after melting, EPM-g-MA was added downstream. The screw configuration, as well as the feeding and sampling locations, are indicated in Figure 7.1b. The screw set-up for this experiment includes a first kneading section with neutral staggering disks and a left-ended element in order to ensure complete PA melting, a conveying zone for rubber feeding, as well as second kneading section with neutral staggering elements to promote chemical reaction and development of morphology. A third mixing section before vacuum ensures further mixing. Blends 11 to 13 were prepared using the extruder layout depicted in Figure 7.1c. The screw configuration is the same as in Figure 7.1a but the barrel set up provides the opportunity for collecting more samples along the screw. Devolatilization before pumping the melt through the die was common to all experiments.

7.2.3 - Materials Characterization

Since a good agreement between FT-IR and nitrogen content data was obtained in a previous study [17], i.e. between the residual MA content and amount of graft PA, in this study only FT-IR data was used for chemical characterization. The samples collected along the extruder were analysed following the methodology previously

developed [4] and illustrated in Figure 7.2. Milled samples were hydrolysed with refluxing 6N hydrochloric acid during 6 hours. Thin films of the residues were prepared by compression-moulding and analysed by FT-IR (Perkin Elmer 1720 spectrometer). The residual MA content was quantified using the anhydride carbonyl absorption at 1785 cm^{-1} after IR calibration with a set of references. The MA conversion (in %) is defined as $[(MA_{original} - MA_{residual})/ MA_{original}]x100$.

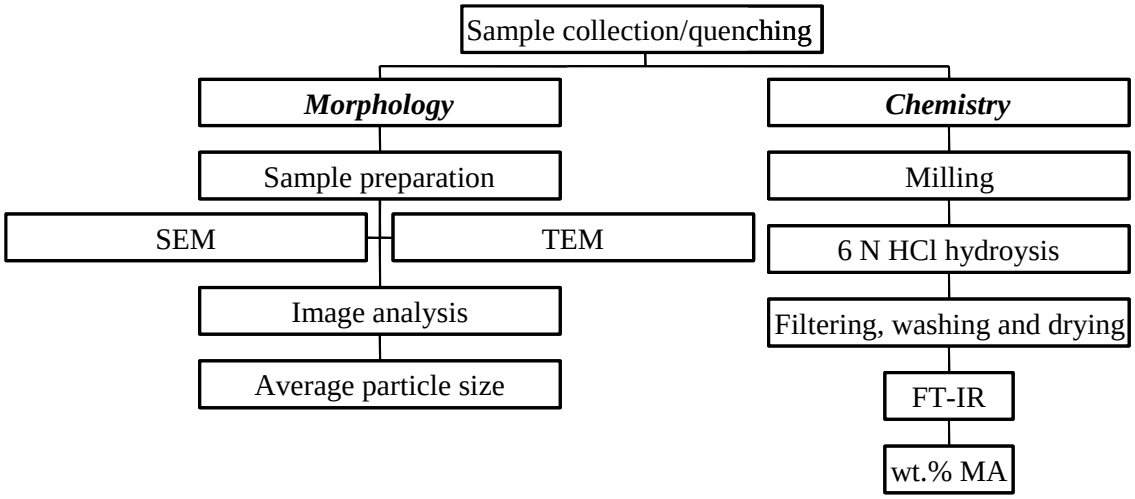

Figure 7.2 – Characterization of collected PA-6 blend samples.

The morphology of the blends was analysed by electron microscopy using a Philips CM200 Transmission Electron Microscope (TEM). For this purpose, very thin coupes (70 nm) were cut at – 100 ºC from samples previously stained with a 50/50 osmium tetroxide/formaldehyde mixture. Some samples were characterized after extraction of the rubber with boiling xylene using a Jeol JSM 6310F Scanning Electron Microscope (SEM). The average size and the size distribution of the dispersed phase were determined from TEM and SEM micrographs using an automatic method of image analysis (Leica Quantimet 550) assuming an equivalent circle diameter for each particle (see reference [17] for more details). The results were obtained after studying typically 200 particles.

7.3 - RESULTS AND DISCUSSION

7.3.1 - Change of MA-containing polymers

The residual MA contents of the MA-containing polymers of the PA-6 blends sampled along the extruder, as determined by FT-IR, are given in Table 7.2. As shown in a previous study [17], the MA content of the EPM-g-MA in a PA-6/EPM-g-MA (80/20, w/w) blend (blend 1) decreased strongly from 0.7 to less than 0.1 wt.% at sampling position A, i.e., upon melting. When other MA-containing polymers with a higher softening/melting temperature, PE-g-MA, PP-g-MA and SMI (blends 2 to 5), were used as the minor blend phase instead of EPM-g-MA, the results were significantly different. As shown in Figure 7.3, the residual MA contents were relatively high at location A, they decreased up to location C and then remained fairly constant. The results show that when the softening/melting temperature of the MA-containing polymer increases (EPM-g-MA→PE-g-MA→PP-g-MA(1 and 2)→SMI) melting and subsequent blend dispersion is delayed, resulting in a slower MA conversion. In the case of PE-g-MA and PP-g-MA2, the physico-chemical processes are still fast enough to result in more or less full MA conversion. For PP-g-MA1, the original MA content is probably too high to reach complete MA conversion even at the die. Nevertheless, the absolute MA conversion of PP-g-MA1 is relatively large (2.5→1.4 wt.% MA), again indicating that "in-situ" compatibilization is a very fast process. Finally, for the MA-containing polymer with the highest softening point, i.e., SMI, the reactive blending process is slowed down considerably, as witnessed by the small absolute and relative MA conversions (1.4→1.1 wt.% MA and 20 %, respectively).

Table 7.2 – Chemical conversion, particle size and particle size distribution of blends of PA-6 with MA-containing polymers as a function of screw length.

Blend	Sampling location	Residual MA content of MA-containing polymer (wt%)	Reacted MA (%)	Particle Size		
				Average (μm)	Range (μm)	Variance (μm^2)
1	A	0.07	86	0.48	0.16-1.38	0.06
	B	0.07	86	0.35	0.15-0.74	0.03
	C	0.08	84	0.33	0.16-0.75	0.02

Blend	Sampling location	Residual MA content of MA-containing polymer (wt%)	Reacted MA (%)	Particle Size		
				Average (μm)	Range (μm)	Variance (μm^2)
	D	0.07	86	-	-	-
2	A	0.30	68	-	-	-
	B	0.21	77	-	-	-
	C	0.16	82	-	-	-
	D	0.13	85	0.22	0.13-0.54	0.02
3	A	1.89	25	0.46	0.17-3.92	0.36
	B	1.58	37	0.42	0.15-2.91	0.22
	C	1.52	40	0.44	0.15-2.51	0.22
	D	1.48	42	0.44	0.15-2.90	0.26
4	A	0.08	72	-	-	-
	B	0.07	77	-	-	-
	C	0.04	87	-	-	-
	D	0.04	87	-	-	-
5	A	1.34	5	-	-	-
	B	1.20	14	-	-	-
	C	1.13	20	-	-	-
	D	-	-	0.20	0.10-0.51	0.02
6	A	0.10	80	-	-	-
	B	0.07	86	-	-	-
	C	0.05	90	-	-	-
	D	-	-	-	-	-
7	A	0.10	80	-	-	-
	B	0.05	90	-	-	-
	C	0.04	92	-	-	-
	D	-	-	-	-	-
8	A	0.09	82	0.063	0.012-0.19	0.001
	B	0.07	86	0.069	0.012-0.19	0.001
	C	0.05	90	0.064	0.012-0.18	0.001
	D	0.03	94	0.060	0.012-0.15	0.001
9	A	0.07	86	-	-	-

Blend	Sampling location	Residual MA content of MA-containing polymer (wt%)	Reacted MA (%)	Particle Size		
				Average (μm)	Range (μm)	Variance (μm^2)
	B	0.08	84	-	-	-
	C	0.06	88	-	-	-
	D	-	-	-	-	-
10	A	0.13	73	0.34	0.17-0.68	0.014
	B	0.07	86	0.31	0.15-0.56	0.010
	C	0.06	88	0.27	0.15-0.44	0.006
	D	-	-	-	-	-
11	A	0.49	0	-	-	-
	B	0.49	0	-	-	-
	C	0.13	68	-	-	-
	D	0.11	73	0.42	0.14-0.83	0.06
	E	0.07	83	-	-	-
	F	0.08	80	-	-	-
	G	-	-	-	-	-
	H	-	-	0.31	0.15-0.71	0.02
12	A	0.49	0	-	-	-
	B	0.49	0	-	-	-
	C	0.25	49	-	-	-
	D	0.07	76	0.44	0.14-2.32	0.08
	E	0.03	86	-	-	-
	F	-	-	-	-	-
	G	-	-	-	-	-
	H	-	-	0.30	0.14-0.81	0.02
13	A	0.49	0	-	-	-
	B	0.35	29	-	-	-
	C	0.09	82	0.45	0.15-1.45	0.05
	D	0.01	98	0.30	0.14-0.62	0.02
	E	-	-	0.31	0.14-0.54	0.02
	F	-	-	-	-	-
	G	-	-	-	-	-
	H	-	-	-	-	-

The evolution of the morphology was determined for a selected number of blends. Table 7.2 presents the evolution along the extruder of the particle size and particle size distribution, in terms of the average size, range of sizes and variance. Although the MA conversion of the PA-6/PP-g-MA1 blend (blend 3) was clearly far from complete, the dispersion of this blend is more or less accomplished at location A (see also Figure 7.4), where the average particle size is approximately 0.5 μm. Only a decrease of the particle size distribution is observed thereafter, as observed with blend 1. This is consistent with the high absolute MA conversion (Table 7.2). The subsequent increase of the MA conversion beyond location A hardly affects the morphology of the PA-6/PP-g-MA blend. Hence, the differences in particle size of the PA-6 blends with the varying MA-containing polymers (blends 2 to 5) collected at the die are probably not due to differences in the conversion of the reactive blending process, but they are most likely related to differences in viscosity and interfacial tension.

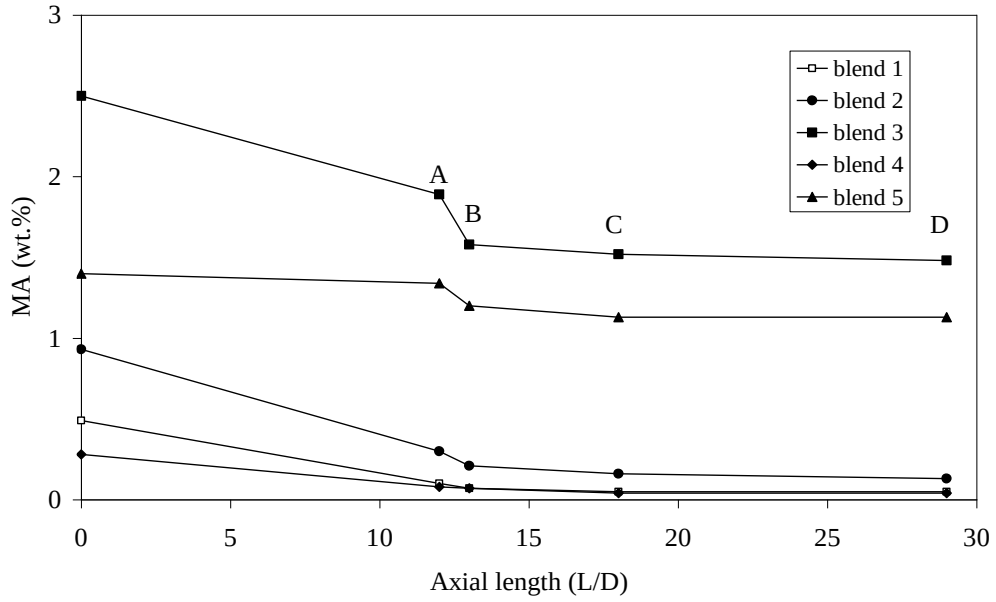

Figure 7.3 – MA conversion of blends 1-5 along the screw for various MA containing polymers (80/20, w/w).

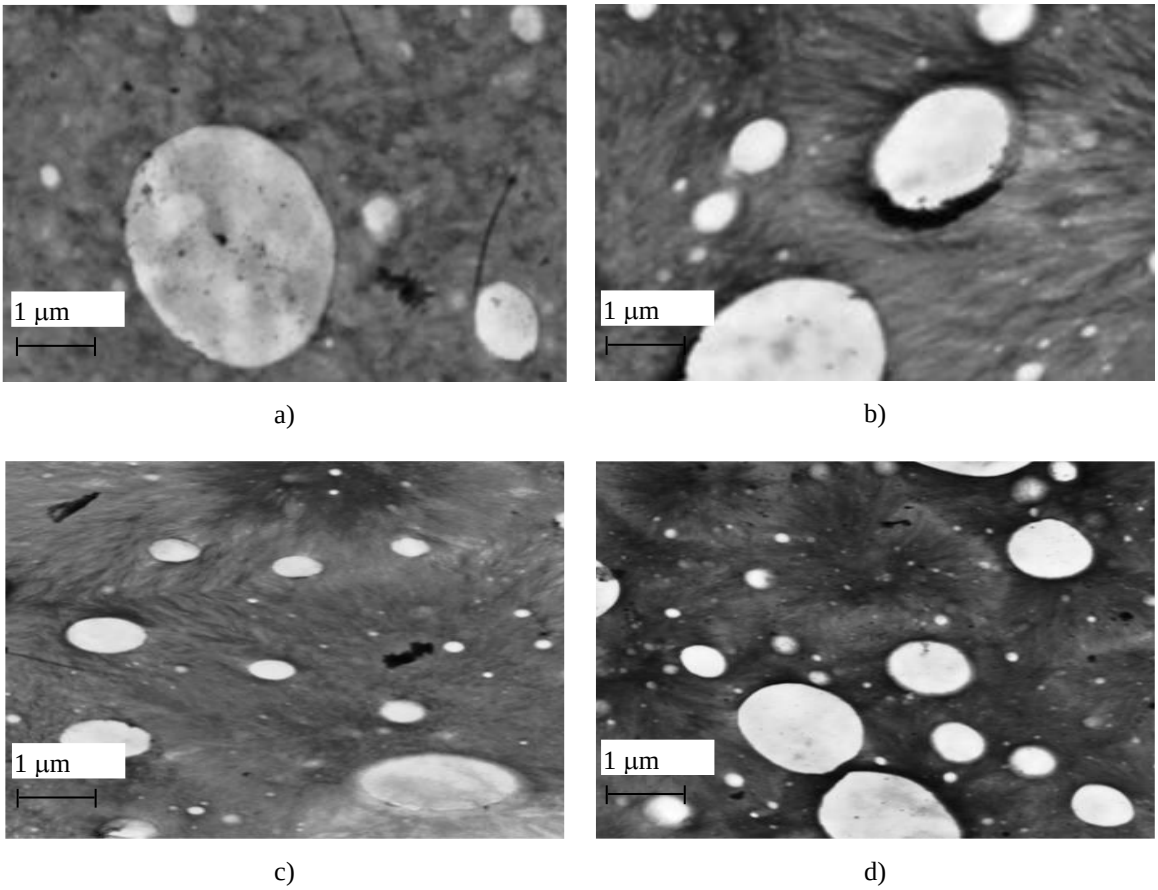

Figure 7.4 – TEM micrographs of blend 4 [PA-6/PP-g-MA (80/20; w/w)] collected along the screw at locations A, B, C and D (a, b, c and d, respectively).

7.3.2 – Change of PA-6/EPM-g-MA blend composition

The composition of the PA-6/EPM-g-MA blends was varied in order to have different ratios of reactive groups (MA and amine) and to study their effect on chemistry and blend morphology. The results presented in Table 7.2 and Figure 7.5 for blends 1 and blends 6 to 8 show a substantial decrease of the MA content at the first kneading zone (location A) from 0.5 to approximately 0.1 wt.% MA and only a slight decrease further downstream. In all cases, the "in-situ" compabilization reactions occur in the melting zone within a few seconds, regardless of the ratio of MA and amine groups in the blend. Nevertheless, the interfacial structure in these blends is distinct, because the average length of the PA grafts decreases as the composition of the PA-6/EPM-g-MA blends goes from 80/20 to 10/90. In the former, the original MA/amine molar ratio is

0.13 and PA chains are predominantly coupled to EPM-g-MA chains via the PA amine end groups. In the latter (10/90, w/w) the MA/amine ratio is 4.5 and still the MA conversion is more or less complete. Therefore, not only the PA amine end groups but also the PA chain amide groups must have reacted with EPM-g-MA. As a result, PA chain scission must have occurred, resulting in relatively short lengths of the PA grafts [14].

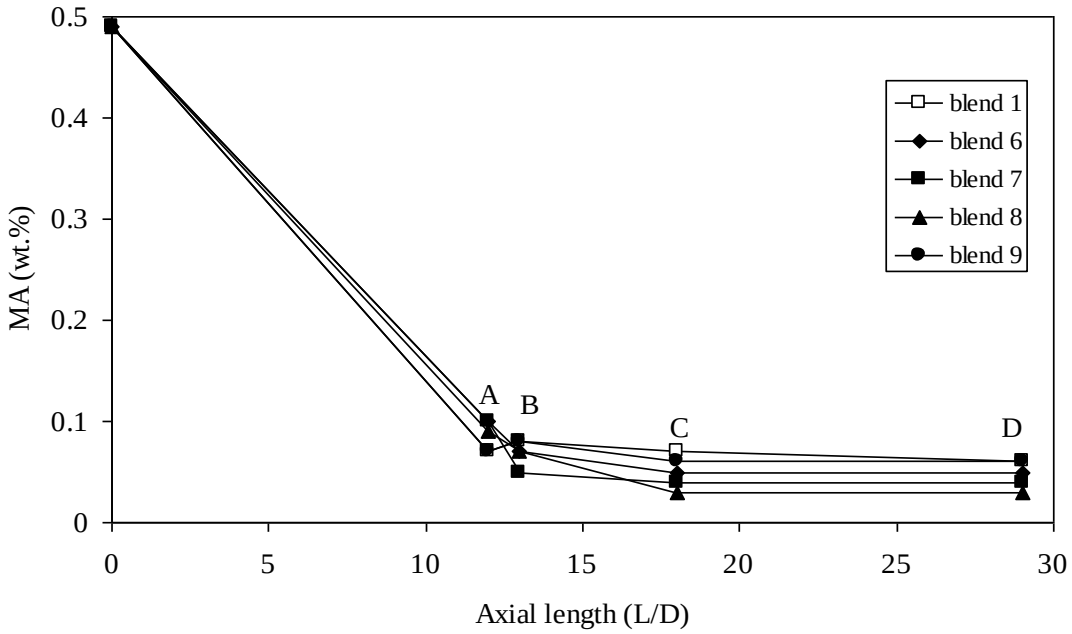

Figure 7.5 – MA conversion of blends 1, and 6-9 [PA-6/EPM-g-MA] along the screw for various compositions.

The morphology development of blends 6 and 7 along the extruder was not studied, because it must be similar to that of blend 1, with relative differences being directly explained by differences in blend composition. For instance, in the case of blend 8 the modified rubber is the matrix and PA-6 is the dispersed phase, as expected for a PA-6/EPM-g-MA volume ratio much smaller than unity. Not surprisingly, Table 7.2 shows that the average dispersed particle size and the particle size distribution are almost constant along the extruder.

Since it was not possible to slow down the “in-situ” compatibilization by varying the PA-6/EPM-g-MA blend composition, an attempt was made to decrease the reactivity of EPM-g-MA by using EPM-g-MA hydrolysed to its diacid form (blend 9). As shown in

Table 7.2, the residual MA content is rather low at location A, and then remains constant. These results are identical to those obtained for blend 1 with non-hydrolysed MA groups, indicating that the hydrolysis of EPM-g-MA does not influence the formation of PA-6/EPM-g-MA graft copolymer. Upon blending all diacid is converted into MA and directly into imide due to grafting of PA-6. Probably, the hydrolysed groups are easily converted back to anhydrides at these elevated temperatures.

7.3.3 - Separate feed of EPM-g-MA

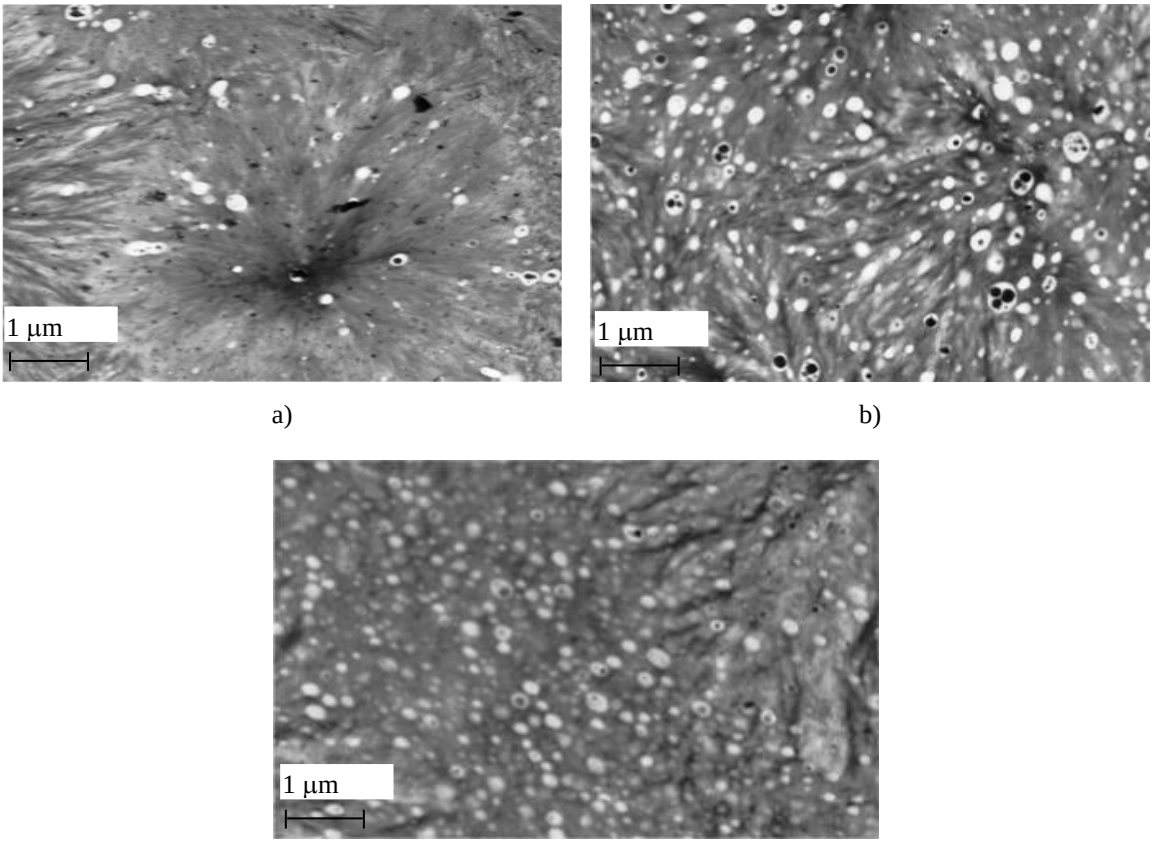

Figure 7.6 – TEM micrographs of blend 10 [PA-6/EPM-g-MA (80/20; w/w)] with EPM-g-MA side fed sampled along the screw at locations A, B and C (a, b and c, respectively).

The effect of side feed of EPM-g-MA was studied for a (80/20, w/w) composition (blend 10). Although fast chemical conversion is again observed, the residual MA content of EPM-g-MA at location A is significantly higher than that of the same blend prepared with premixed components (Table 7.2, blend 10 versus blend 1, i.e., 0.13

versus 0.07 wt.% MA). Here, the residual MA content decreases from location A to B and then remains constant. Differences in the morphological evolution can also be observed. As shown in Figure 7.6a, when using separate feed rubber phase dispersion is not yet complete at location A, where rubber particles with different sizes are visible. At location B the degree of dispersion improved and at location C a good dispersion is obtained (Figure 7.6b). Table 7.2 presents a progressive decrease in both the average particle size and the particle size distribution.

7.3.4 – Change of processing conditions

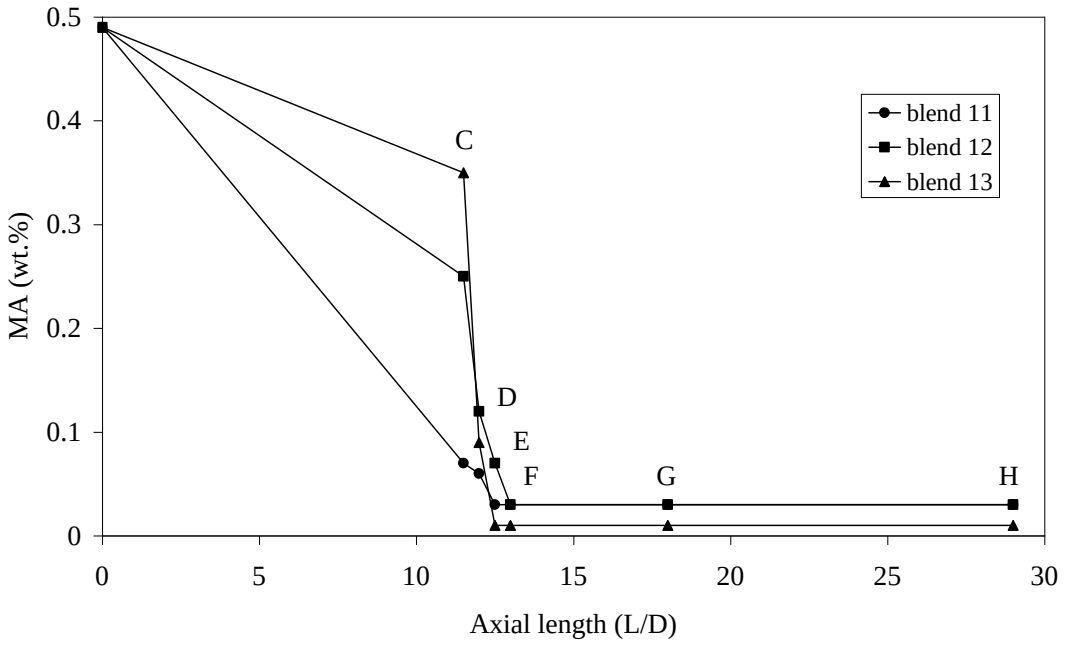

Figure 7.7 – MA conversion of blends 11,12 and 13 [PA-6/EPM-g-MA, (80/20; w/w)] along the screw.

Given the high rate of MA conversion observed above, a special barrel segment containing six collecting devices over 12 cm in the axis direction was designed and built. As shown in Figure 7.1c, these devices replaced the previous A and B devices, thus providing more sampling for chemical and morphological characterization. Blends 11 to 13 were processed using this arrangement. Blends 11 and 12, which were prepared using a different temperature profile up to L/D=13, clearly yielded different results (Table 7.2 and Figure 7.7). While blend 11 exhibit roughly the same chemical

evolution as blend 1, blend 12 (processed under a lower set temperature), presents a high residual MA content (0.25 wt.%) at location C. In fact, PA-6 pellets embedded in a continuous rubber phase (Figure 7.8a) can still be observed. Between locations C and D - which are only 2 centimeters apart in the axial direction - the material melts completely and the MA content decreases significantly (0.25 to 0.09 wt.%).

Since it is well known that screw speed has a strong effect on morphology development, an attempt at slowing down the "in-situ" compatibilization by decreasing the screw rotation was carried out (blend 13). Although at location C the MA content is higher than for blend 12 (0.35 versus 0.25 wt.%), no significant differences in morphology were observed (Table 7.2). Probably more information on morphology development would be obtained when using very low screw speeds, but this would also require changes in the throughput and would be unrealistic from an industrial point of view.

Blend 12 seemed appropriate for a more detailed morphology study. SEM micrographs of this blend at location C (Figure 7.8a) show that the rubber is molten and surrounds the PA-6 pellets. It is also possible to observe molten PA-6 threads dispersed in the rubber. These features are more clearly visible when PA-6 was removed with formic acid (Figure 7.8b). TEM analysis at location C shows a very heterogeneous morphology (Figure 7.8c). Clearly, the dispersion process at this stage of the process is very complex. Large rubber particles and unmolten PA-6 pellets (not visible in the micrographs, since they were lost during preparation of the TEM coupes) are present in close vicinity to a finely dispersed PA-6/EPM-g-MA mixture (rubber particle size: 0.25 - 1 μm). All sorts of morphologies with intermediate dimensions are observed: thin PA-6 regions drawn from the unmolten PA-6 pellets, EPM-g-MA sheets, thin elongated EPM-g-MA and PA-6 domains, EPM threads in the process of breaking up, etc. Upon using a higher magnification, a very unusual morphology at the PA-6/EPM-g-MA interface can be observed (Figure 7.8d). Stretched, wave-like rubber domains perpendicular to the PA-6 surface and thin spider-web-like filaments are visible. Although most of these morphological features have been observed before for blends produced in a batch kneader [18-19], our results were obtained in a commercial twin-screw extruder under industrially relevant processing conditions.

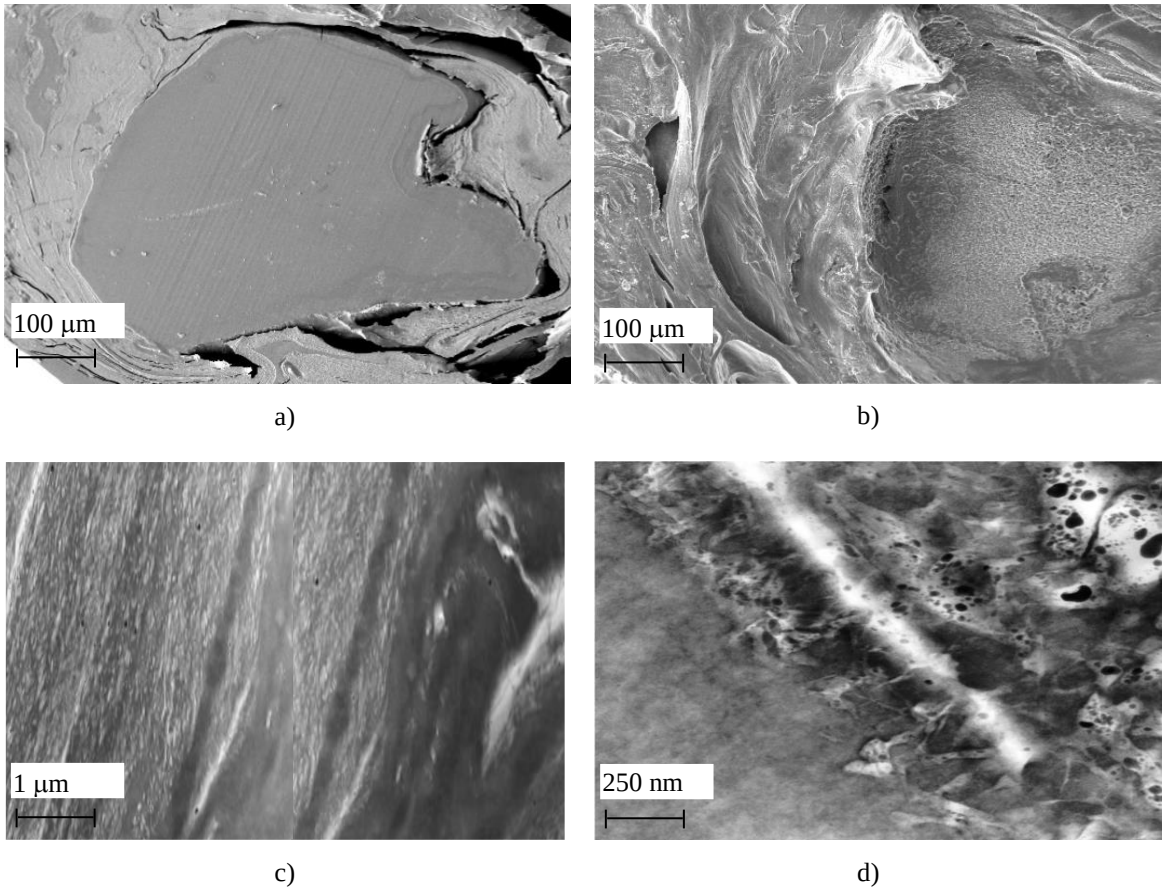

Figure 7.8 – Micrographs of blend 12 [PA-6/EPM-g-MA (80/20; w/w)] collected at location C: a) SEM of the sample, b) SEM of the sample after dissolution of PA-6, c) TEM panorama at the interface and d) TEM using higher magnification.

Finally, a remark relating to the phenomenon of phase inversion seems relevant. Generally, phase inversion has been shown to occur in A/B blends with A being the major blend component (with a higher softening point) and B the minor blend component (with a lower softening point) [18]. First, B will soften and form the matrix for the not yet molten A phase. After the melting of A phase inversion occurs, which yields a blend in which A is the matrix and B is the dispersed phase. However, during the experiment with the PA-6/EPM-g-MA (80/20, w/w) blend 12 (A/B), phase inversion was not observed. At location B - just upstream of the kneading zone - the EPM-g-MA crumbs are only partially stretched and glued to the PA pellets, coating partially the surface of the PA pellets. A dispersion of PA pellets in the EPM matrix is not observed, probably due to the low EPM content (20 wt.%) in combination with the highly viscous character of the EPM phase. A detailed inspection of the TEM

micrographs of the samples taken at position C (Figure 7.8c) indicates that nowhere in the first part of the kneading/melting zone is the EPM phase continuous. So, for obtaining the final morphology at position D, i.e., EPM particles dispersed in a continuous PA matrix, phase inversion does not occur.

7.3.5 – Occlusions

In the blends of PA-6 with EPM-g-MA as the minor phase (blends 1 and 10 to 13) PA occlusions were observed in the rubber particles (Figure 7.8d). As pointed out by a few authors [17-19], these occlusions may be formed upon melting of the PA-6 pellets. The PA-6 already bound at the interface is drawn into the rubber phase when the latter becomes the dispersed phase. The rubber particles themselves are then stabilized by the newly formed PA-6/ EPM graft copolymer.

The fraction of rubber particles with PA occlusions was taken as a measure of the degree of occlusion. The data shown in Table 7.3 seems to indicate that the degree of occlusion does not vary along the extruder axis. This means that, likewise to PA-6/EPM-g-MA graft copolymer formation and blend dispersion, the development of occlusions occurs in the melting zone, i.e. just before and/or in the first kneading zone, where interfacial area and high shearing are generated. The degree of occlusion of blends 1, 11 and 12 is quite similar, but that of blend 10 is much smaller. In fact, when EPM-g-MA is side fed after all PA-6 has been molten, most PA-6/EPM-g-MA graft copolymer is at the interface and there is no driving force for drawing these graft copolymer inside the rubber dispersion. This supports the assumption that occlusions are formed from PA-6/EPM-g-MA graft copolymers upon melting of PA-6 pellets.

In the blends with the other MA-containing polymers, no PA-6 occlusions were observed in the dispersed phase (Figures 7.4a to 7.4d). This may be attributed to the relatively high softening points of the other MA-containing polymers and/or its high viscoelastic behaviour.

Table 7.3 – PA-6 occlusions in dispersed EPM-g-MA particles of PA-6/EPM-g-MA blends as a function of the screw length.

Blend	Sampling Location	Fraction of rubber particles with PA-6 occlusions
1	A	0.74
	B	0.86
	C	0.88
	D	0.85
10	A	0.20
	B	0.22
	C	0.18
11	C	0.70
	H	0.78
12	C	0.90
	H	0.88
13	C	0.73
	H	0.84

7.4 - CONCLUSIONS

The use of sampling devices located along the barrel of a twin screw extruder allows a detailed study of chemical and morphological evolution during blending. It was shown that during melt blending of PA-6 and EPM-g-MA both processes (chemical conversion and morphology development) are very fast, occurring within a few seconds over a few centimeters. The evolution of morphology is associated with the chemical conversion. When the MA groups of EPM-g-MA are almost completely converted, the morphology of the blend is also fully developed. However, by varying the experimental set-up it was possible to get a better insight into the process and obtain more information about morphology development. Replacing EPM-g-MA by MA-containing polymers with higher softening temperatures and varying the processing conditions (particularly the temperature profile and the screw speed) affects the chemical conversion and therefore, the morphology evolution.

With the processing conditions used in this work (which are industrially relevant) and with the specific characteristics of the components used in the PA-6/EPM-g-MA blends, the final dispersion of rubber particles in the PA-6 matrix is obtained without the occurrence of phase inversion.

Finally, it was shown that PA-6 occlusions in the dispersed rubber phase are formed during melting and initial dispersion phase. The degree of occlusion is not affected by further processing.

7.5 - REFERENCES

[1] – S. Datta and D. Lohse, *Polymeric Compatibilizers*, Hanser Publishers, New York, 1996.

[2] – L.A. Utracki, Encyclopaedic Dictionary of Commercial Polymer Blends, ChemTec Publishing, Toronto, 1994.

[3] – S. Datta and D.J. Lohse, "Polymeric Compatibilizers, Uses and Benefits in Polymer Blends", Hanser Publishers, Munich, 1996.

[4] – M. van Duin, M. Aussems and R. J. M. Borggreve, *J. Polym. Sci.: Part A: Polym. Chem.*, **36**, 179 (1998).

[5] – V. J. Triacca, S. Ziaee, J. W. Barlow, H. Keskkula and D. R. Paul, *Polyer*, **32**, 1401 (1991).

[6] – H. Cartier and G.H. Hu, *J. Polym. Eng. Sci.*, **39**, 996 (1999).

[7] – F. P. Mantia, *Adv. Polym. Tech*., **12**, 47 (1993).

[8] – S. S. Dali, M. Xanthos and J. A. Biesenberger, *Polym. Eng. Sci.*, **43**, 1720 (1994).

[9] – J. D. Lee and S. M. Yang, *Polym. Eng. Sci.*, **35**, 1821 (1995).

[10] – F. Ide and A. Hasegawa, *J. Appl. Polym. Sci*., **18**, 963 (1974).

[11] – M. Seadan, D. Graebling and M. Lambla, *Polym. Networks Blends*, **3**, 115 (1993).

[12] – M. Lambla and M. Seadan, *Polym. Eng. Sci.*, **32**, 1587 (1992).

[13] – M. A. Huneault, M. F. Champagne and A. Luciani, *Polym. Eng. Sci*., **36**, 1694 (1996).

[14] – M. Stephan, O. Franzheim, T. Rische, P. Heidemeyer, U. Burkhardt and A. Kiani, *Adv. Polym. Tech.*, **16**, 1 (1997).

[15] – T. Sakai, *Adv. Polym. Tech.*, **14**, 277 (1995)

[16] – A. V. Machado, J. A. Covas and M. van Duin, *J. Appl. Polym. Sci.*,**71**, 136 (1999).

[17] – A. V. Machado, J. A. Covas and M. van Duin, *J. Polym. Sci.: Part A: Polym. Chem.*, **37**, 1311 (1999).

[18] – U. Sundararaj and C. W. Macosko, *Polym. Eng. Sci.*, **36**, 1769 (1996).

[19] – C. E. Scott and C. W. Macosko, *Polym. Bulletin*, **26**, 341 (1991).

8.1 - INTRODUCTION

Blending (immiscible) polymers has successfully been used as an alternative route for synthetic approaches to develop materials with an improved performance for specific applications [1-5]. In this type of blends, a two-phase material is typically obtained, where droplets of one polymer (dispersed phase) are embedded in a matrix of another polymer (continuous phase). Interfacial tension induces a spherical drop shape under static conditions, although other parameters, such as the rheological properties of each component, are also relevant. The characteristics of immiscible polymer blends are determined by the blend composition, the properties of the individual components and the morphology generated (i.e., which polymer is the matrix/dispersed phase and what is the size of the dispersed domains). The blend morphology is dictated by the interfacial interactions, the rheological properties of the components, and the kinetics of the relevant chemical and physical processes. Compatibilization of heterogeneous blends is generally used to control the interfacial properties and to stabilize the morphology against coalescence and thus affects the equilibrium degree of dispersion. It is generally accomplished by either adding a pre-synthesized block copolymer or via reactive processing [2-5]. In the latter case, the compatibilizer is generated "in-situ", during blending, via grafting or exchange reactions. These reactions must generate sufficient copolymer in order to optimise the morphology and thus the blend performance. Since the reactions occur across phase boundaries, high stresses must be applied to enlarge the interfacial area and ensure high reaction rates.

A considerable effort has been devoted to identify and understand the mechanisms that govern chemical conversion and/or morphology development during blending. Emulsions of low viscous liquids were initially studied both experimentally and theoretically, to simulate the two-phase morphology of blends. Several on- and off-line techniques such as microscopy, spectroscopy, molecular weight and rheology measurements have been used successfully for blend characterization [5]. If correlations between rheological behaviour and blend morphology could be established,

rheology could be used as a sensitive tool to monitor and control morphological changes.

The linear viscoelastic response of non-reactive blends under small amplitude oscillations has been used extensively to characterize the microscopic structure of the material provided the morphology is stable and no degradation occurs [6-15]. An increase in elasticity at low frequencies has been consistently reported and is usually attributed to the deformation of the dispersed particles and the recovery to their equilibrium shape due to interfacial tension [6-9]. This type of measurements is also very sensitive to the volume fraction and the copolymer nature. Palierne [16] developed a model accounting for this type of dynamic mechanical response of concentrated emulsions, where the deformation of the droplets and interfacial tension were considered. Large deformation flows can affect the blend morphology by deforming the dispersed phase. Also during blending coalescence and breakup also take place, depending on the composition and strain**.** Thus, the applied flow history will change the blend morphology (and consequently the rheological behaviour), i.e., the rheological properties measured are no longer characteristic of a specific morphology, but they reflect changes in morphology caused by flow [10]. Doi and Ohta [17] derived a constitutive equation for a blend of two immiscible Newtonian fluids with equal viscosity considering the latter phenomena. Later, Lee and Park [18] accounted for the effect of the viscosity ratio of the blend components.

Since the Palierne and the Doi-Ohta models predict quite different rheological characteristics, each has been used with relative success to describe the behaviour of, for example, immiscible blends of polyisoprene with polydimethylsiloxane with different viscosity ratios [7,11], polyethene with polystyrene, polyethyleneterephthalate with poly(ethene-co-vinylacetate), polypropylene with poly(ethene-co-vinylacetate) [13] and poly(methyl metacrylate) with acrylic impact modifiers [14]. Transient flow experiments, involving, for example, a step-up in the initial low shear rate followed by flow reversal, seem to be particularly suited to evaluate the potential of the above models and of their extensions to predict flow-induced changes in morphology [10,11].

Only a very small number of authors has used rheological measurements as a tool to monitor the chemical conversion in reactive blends (see, for example [20-22]). Generally, capillary pressure drop and oscillatory measurements have shown that interfacial adhesion – thus, blend viscosity - increases with increasing amounts of copolymer formed at the interface [20-22].

Most of the above studies examined the blend morphology and the rheological behaviour of samples previously prepared in extruders or batch mixers. Another approach has consisted in monitoring on-line the development of morphology (and corresponding rheology changes) of simple model blends under controlled flow conditions (see, for example [14,24]). The specific problem of the evolution of the characteristics of immiscible blends during their preparation under conditions relevant to the industrial practice has seldom been addressed [20]. This is associated with the practical difficulty in carrying out in-line measurements or in collecting representative samples for subsequent testing.

The objective of this work is to monitor the evolution of the rheological parameters of immiscible, reactive polymer blends during extrusion, and to correlate the rheological behaviour with the morphology evolution and chemical conversion along the extruder. Blends with varying compositions were prepared in a laboratorial intermeshing co-rotating twin-screw extruder and representative samples were collected along the screw axis for subsequent characterization using a sampling device recently developed [25]. Measurements under small amplitude oscillatory flow were carried out, in order to avoid unwanted morphology changes and/or material degradation (as checked by Scholz *et al* [24]).

Blends of polyamide-6 (PA-6), ethene-propene rubber (EPM) and EPM modified with maleic anhydride (MA) (EPM-g-MA) were selected for this purpose given their industrial relevance [1-5].

8.2 - EXPERIMENTAL

8.2.1 – Materials

Commercial polyamide-6 (PA-6 - Akulon® K123) and ethene-propene rubber (EPM - Keltan® 740) produced by DSM, the Netherlands, and ethene-propene rubber modified with maleic anhydride (EPM-g-MA - Exxelor VA 1801, containing 0.49 wt.% of MA, as determined by FT-IR) provided by Exxon, Spain, were selected for this work. Table 8.1 defines the composition of the various blends. The PA-6 content was kept constant in all blends, but the amount of modified rubber was varied in order to start with different amounts of maleic anhydride in each blend. PA-6 was dried for 16 hours at 110 ºC before extrusion.

Table 8.1 – Composition of the PA-6/EPM/EPM-g-MA blends.

Blend (w/w/w)	EPM-g-MA (wt.%)[a]	MA content of rubber phase (wt.%)[a]
80/20/0	0	0
80/15/5	5	0.13
80/10/10	10	0.25
80/5/15	15	0.37
80/0/20	20	0.49

a) MA content of EPM-g-MA is 0.49 wt.%; MA content of the rubber phase is the weight average of the combined EPM and EPM-g-MA rubber phase.

8.2.2 - Twin screw extrusion

The various blends of Table 8.1 were processed in a laboratory modular Leistritz LSM 30.34 intermeshing co-rotating twin-screw extruder under identical processing conditions. Figure 8.1 shows the extruder layout and the operating conditions selected. The screws have 3 mixing zones. The first comprises staggering kneading blocks offset 90º and a left element downstream. The second contains staggering blocks at 90º and –30º. Finally, the third mixing zone uses staggering blocks at –60º and 90º. The intensive

mixing and heat transfer generated in the first section will ensure complete material melting. Further mixing is induced upon flow through the subsequent mixing sections. Material samples were collected at the locations also indicated in Figure 8.1, through the use of sampling devices that are able to remove within 2-3 seconds *circa* 1 gram of material out of the extruder [25, 26]. They were immediately quenched in liquid nitrogen, in order to avoid further reaction or morphological changes.

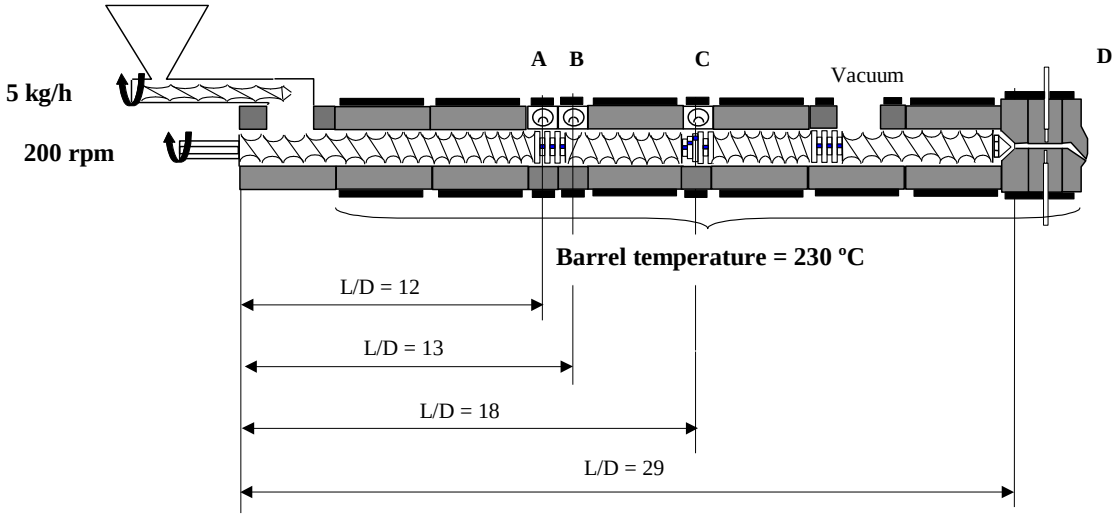

Figure 8.1 – Extruder layout and sampling locations.

8.2.3 - Materials Characterization

The details of the chemical and morphological characterization of the blends are given elsewhere [26]. Generally, after extracting all free PA-6 the nitrogen content of the residues was determined. Blends were also hydrolysed and the infra-red anhydride carbonyl peak at 1785 cm^{-1} allowed the quantitative determination of the MA content of the samples. The samples were either fractured in liquid nitrogen, etched with xylene to remove the rubber from the surface and observed with a Jeol JSM 6310F Scanning Electron Microscope, or cryo-cut and analysed with a Philips EM420 Transmission Electron Microscope. The average size and the particle size distribution of the dispersed phase were estimated from the equivalent particle area of individual particles, which was measured with a Leica Quantimet 550 Image Analysis System.

The average molecular weight and the molecular weight distribution of PA-6 were determined using gel permeation chromatography. Samples were dissolved in

1,1,1,3,3,3-hexafluoro-i-propanol and then the solutions were analysed in a Hewlett Packard 1090 M chromatograph with differential viscosimeter detector, at room temperature.

A few rheology experiments at high shear rates (50-30.000s^{-1}) were carried out using a Rosand RH7-2 twin-bore capillary rheometer. Viscosity measurements were performed at 230 ºC, using two 1 mm diameter dies (with L/D equal to 0.25 and 16) in order to carry out the Bagley correction for the end effects. The Rabinowitsch correction was performed to obtain the true shear rate. The material was pre-heated in the rheometer for 10 minutes, prior to each experiment.

Frequency sweeps (from $4x10^{-3}$ to 40 Hz) at 230 ºC were performed on a TA Instruments Weissenberg rheometer, using parallel-plate geometry (diameter = 40 mm) with a 2.00 mm gap. A linearity check confirmed that strains up to 0.01 would keep the material's response in the linear viscoelastic domain. Before any experiment, samples were vacuum dried at 80 ºC during 12 hours. The 1-2 g nut-shaped samples collected from the extruder were compression moulded for 10 minutes at 230 ºC under a pressure of 30 ton into discs 4 cm wide and 2 mm thick.

The possibility of three sources of error affecting the rheological data due to unwanted changes in morphology/chemistry during sample preparation or testing was initially considered. First, removing material from the extruder could affect the morphology due to flow through the sampling device and subsequent coalescence before cooling. In a separate study [25] the authors confronted this new technique with conventional screw pulling experiments. They showed that in the case of PA-6/EPM blending the samples collected with the devices exhibited smaller particles and narrower particle distributions, i.e., coalescence was avoided. Also, shear rates in the sampling device are negligible.

The limited melt flow during compression moulding increases the interfacial area and could therefore induce morphological and/or chemical conversion changes. However, as shown in Table 8.2 the morphology of non-reactive blend samples removed from the extruder remains unaffected regardless of the subsequent compression time.

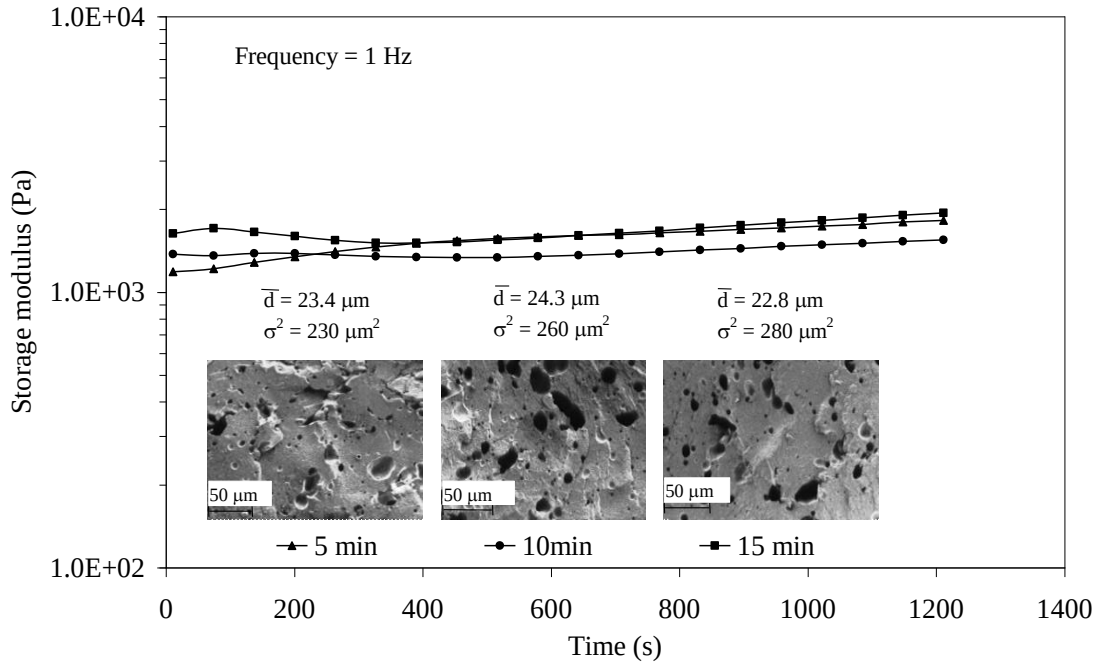

a)

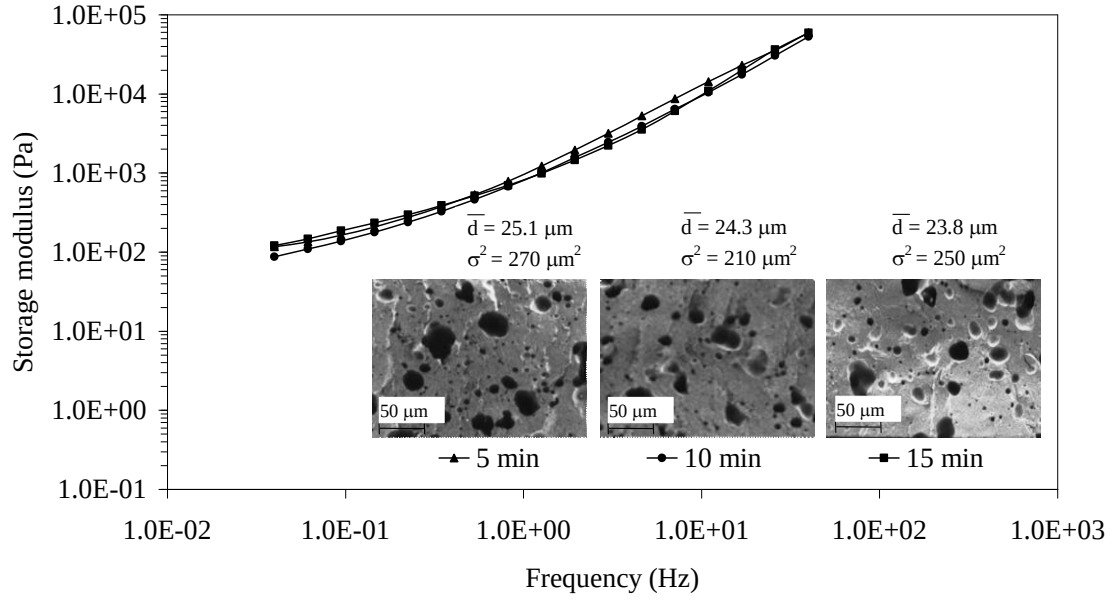

b)

Figure 8.2 – Storage modulus and SEM micrographs after rheological measurements of PA-6/EPM/EPM-g-MA (80/0/20, w/w/w) blend; a) as a function of time (ω = 1 Hz) and b) as a function of frequency.

Table 8.2 – Dispersed rubber particle size (distribution) of PA-6/EPM (80/20; w/w) blend for different compression times.

Compression time (min)	Particle Size	
	Average (μm)	Variance (μm^2)
0	22.6	189
5	23.0	201
10	23.2	188
15	22.8	194

Finally, although oscillatory measurements are commonly considered as a non-destructive technique for studying morphology/rheology correlations, the validity of this assumption was checked. Figure 8.2 (top) shows that no significant degradation and/or particle size change took place with continuing low frequency deformation. Within the experimental error, the final average particle diameters are coincident with those of the initial disks prepared with various compression moulding times (Table 8.2). Frequency sweeps (Figure 8.2, bottom) produced essentially the same conclusions.

Similar results were obtained with reactive blends.

8.3 - RESULTS AND DISCUSSION

Our previous studies on the chemical and morphological evolution of PA-6/EPM-g-MA blends along a co-rotating twin-screw extruder showed that a significant chemical conversion (0.50 to 0.05 wt.% MA) and a dramatic decrease in the particle size of the dispersed phase (mm to μm) occur immediately after melting, as a result of the increase in interfacial area promoted by flow through the staggered kneading blocks. Further downstream the evolution becomes rather small, since with respect to morphology only a decrease in particle size distribution is significant. Moreover, the amount of PA-6/EPM-g-MA graft copolymer formed at the interface increases with increasing EPM-g-MA content, until it reaches a plateau [26]. Therefore, significant variations in the rheological behaviour of the blends are also anticipated immediately after melting,

particularly for samples collected in ports A and B, located along the first mixing zone of the extruder (see Figure 8.1).

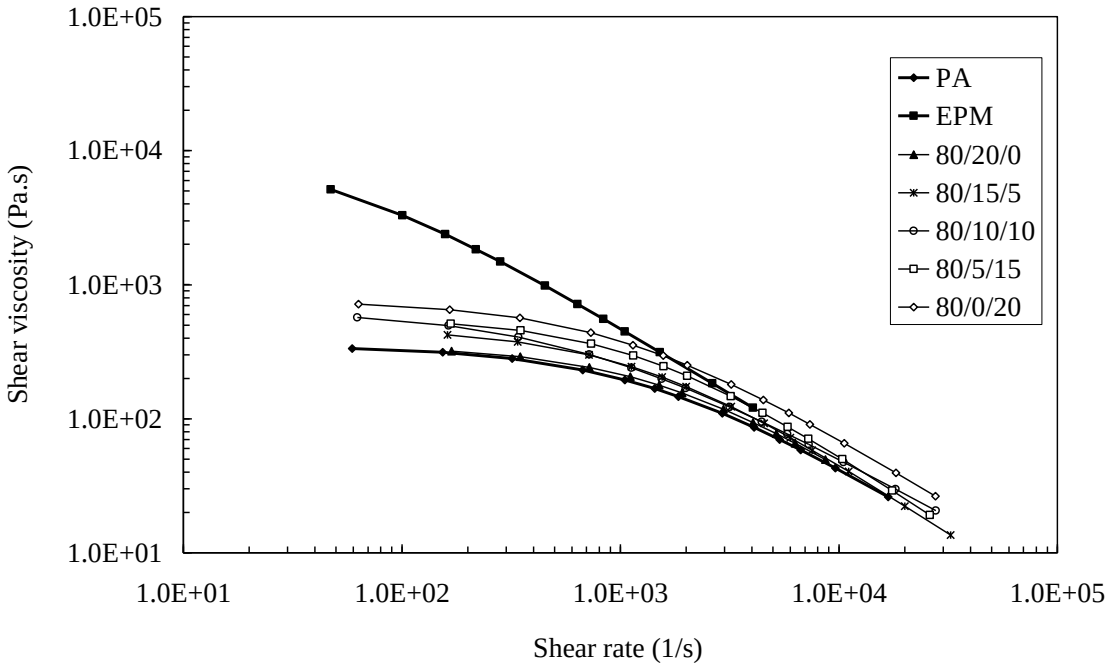

Figure 8.3 – Shear flow curves of the original polymers and their extruded blends.

Despite the probability that morphological changes could occur during steady shear flow, capillary rheometry was used to characterize both the individual polymers and the extruded blends under conditions relevant to subsequent processing. The steady pressure readings observed should correspond to a stabilized morphology, where breakup and coalescence of the dispersed phase are balanced. The flow curves are depicted in Figure 8.3. At high shear rates the viscosity of all materials is very similar. For the inert PA-6/EPM blend the viscosity curve is similar to that of the PA-6 reference. The increase in viscosity with increasing EPM-g-MA content could be due to an increased interfacial adhesion as a result of "in-situ" compatibilizer formation, although the flow conditions during measurement are also probably changing significantly the morphology of the dispersed phase. At the lower shear rate range the viscosity of the blends falls between those of the components. The blends are more viscous than the reference PA-6, but less viscous than the reference rubber. Moreover, the viscosity of the blends increases with increasing MA content in the rubber phase i.e., with the amount of copolymer formed at the interface. The shape of the curves

indicates that the rheology of the blends is mainly governed by the matrix, but the shift between the curves also suggests that other parameters also play a role.

The experimental data is plotted in Figure 8.4 in terms of apparent viscosity as a function of shear stress. The shape of the flow curves is anomalous, with the viscosity levelling off for stresses around 5-8x10^6 Pa. This type of behaviour was initially reported for printing inks [27] and has been attributed to particle migration towards the centre of the plate [28]. Earlier, Mooney and Wolstenholme [29] proposed a model for "supermolecular" flow, involving the movement and rotation of particles imbedded in the melt and causing a wall-slip like effect. In the present case, where the flow of a melt with a higher viscosity dispersed phase develops, it appears that above a critical stress (presumably related to volume level and average size of the dispersed phase) the rubber particles will start rotating and, eventually, rolling over each other, causing a slip-like effect. Therefore, the interpretation of the data observed with capillary flow of this type of immiscible reactive blends is complex and requires special precautions.

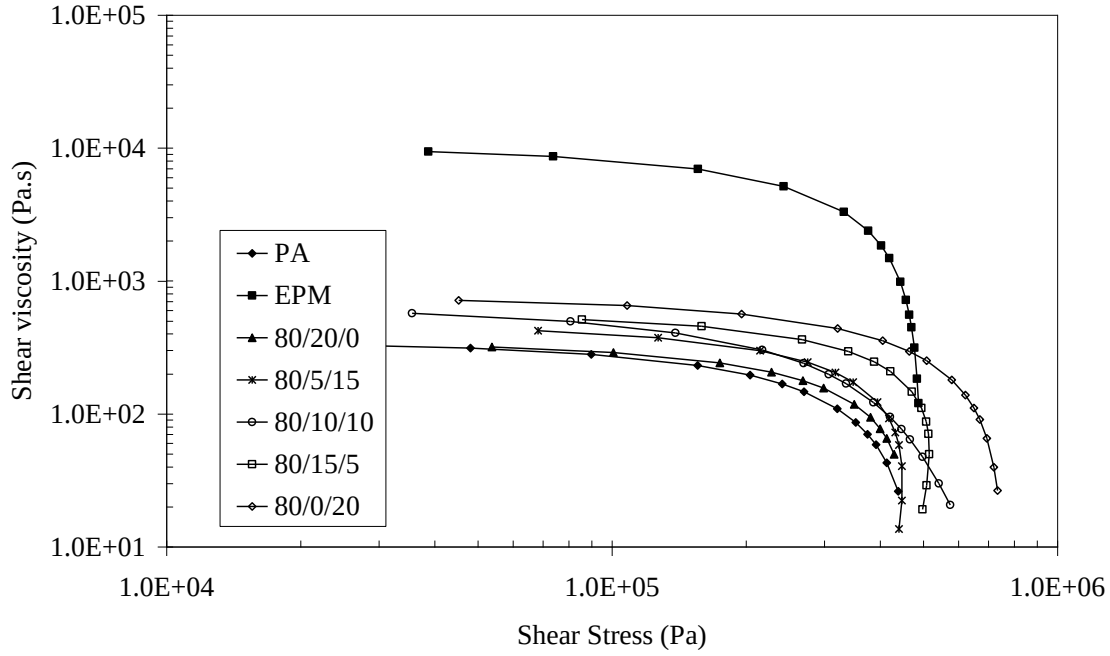

Figure 8.4 – Shear viscosity versus shear stress of the original polymers and their extruded blends.

Since oscillatory experiments preserve the morphology present before the rheological measurements, they will be used in the remaining of this work. The dynamic viscosity,

η', and storage modulus, G', of the original materials, PA-6, EPM and EPM-g-MA, and of the extruded blends of PA-6/EPM (80/20, w/w) and of PA-6/EPM-g-MA (80/20, w/w) are shown in Figure 8.5. The dynamic viscosities of both inert and reactive blends are always lower than those of the original components. The reactive blend is more viscous than the non-reactive blend, despite the lower viscosity of EPM-g-MA in relation to EPM, due to the formation of graft copolymer at the interface and to the fine rubber dispersion. The trends in the elastic behaviour of these materials as indicated by G' are similar to those for η'. The increase in elasticity of the blends at low frequencies, that has frequently been reported for other systems, is also observed here and can be associated with the deformation and recovery of the dispersed rubber particles due to interfacial tension [12-15], as mentioned previously. If this effect is discarded, the slopes of the η' and G' curves of the blends and of PA-6 are similar, confirming that the rheology of the blends is mainly dictated by the matrix. However, the relative magnitude of η' and G′ of these materials is difficult to account for, as one would expect that the viscosity of both blends would largely fall between the values of the original materials. The study of the evolution of the rheological behaviour of the various materials along the extruder could provide some insight on these phenomena.

Figure 8.6 shows the rheological evolution of the non-reactive PA-6/EPM (80/20, w/w) blend along the screw length. Locations A, B and C (L/D=12, 13 and 18 in Figure 8.1, respectively) correspond to screw zones where high pressure and shear were developed and location D is the extrudate. Both the dynamic viscosity and the storage modulus decrease along the extruder. In principle, this could be attributed either to changes in the dispersed phase particle size (distribution) [12-15], changes in interfacial structure or to flow induced orientation [2,10,13]. The blend morphology (average particle size) at the same locations is presented in Figure 8.7. The data for location A are not depicted, because of the coexistence of solid and softened material. The decrease in particle size along the extruder, immediately after melting in particular (i.e., between A and B, which are only one L/D apart), and of particle size distribution, as inferred from the breath of the standard deviation, further on along the screw seem to explain the rheological behaviour. Flow induced particle orientation was not observed.

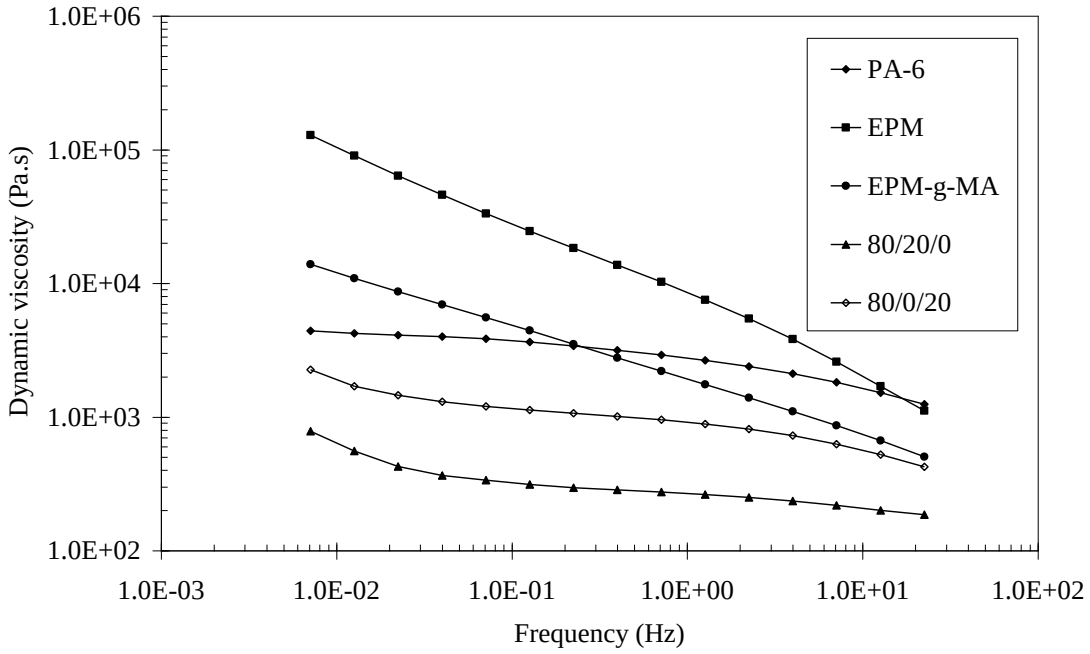

a)

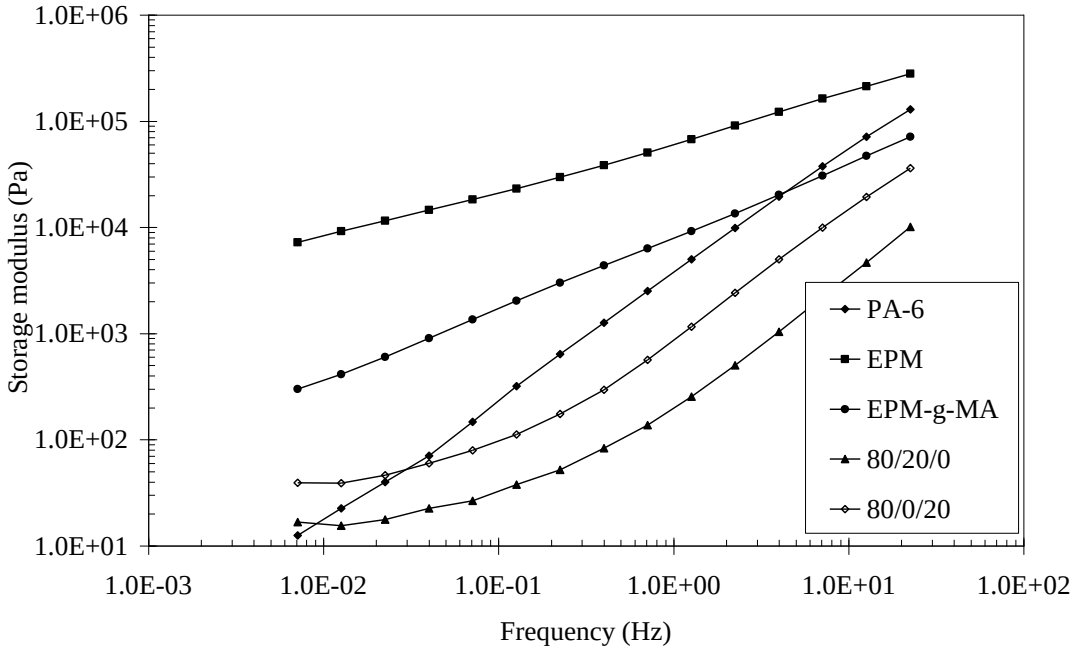

b)

Figure 8.5 – Rheological behaviour of the original polymers and their blends, a) dynamic viscosity and b) storage modulus.

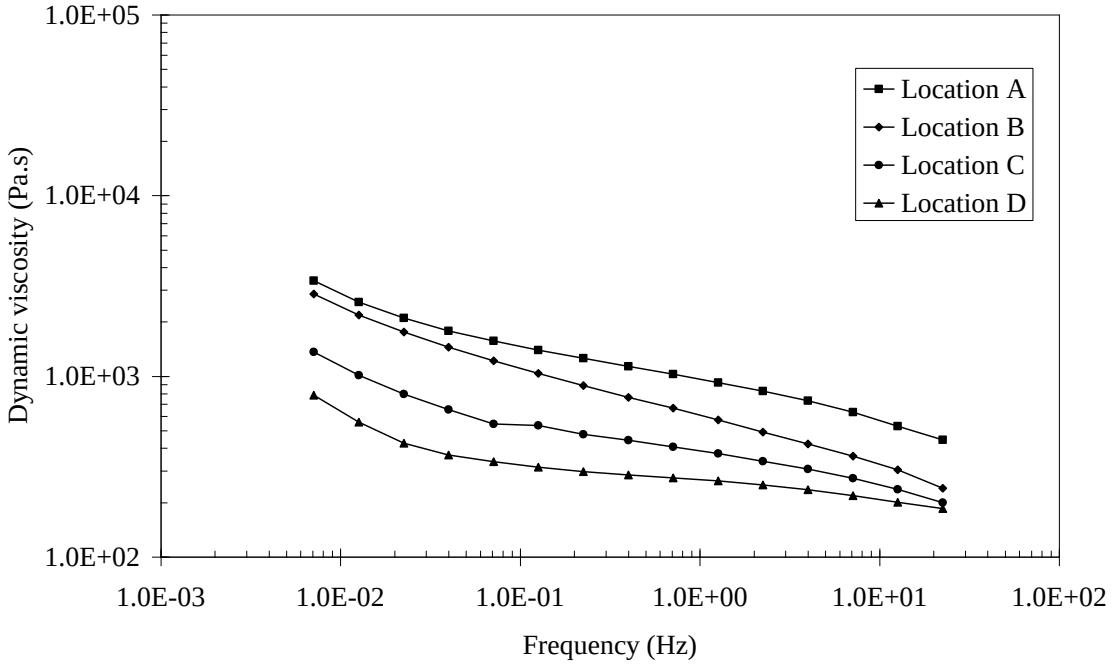

a)

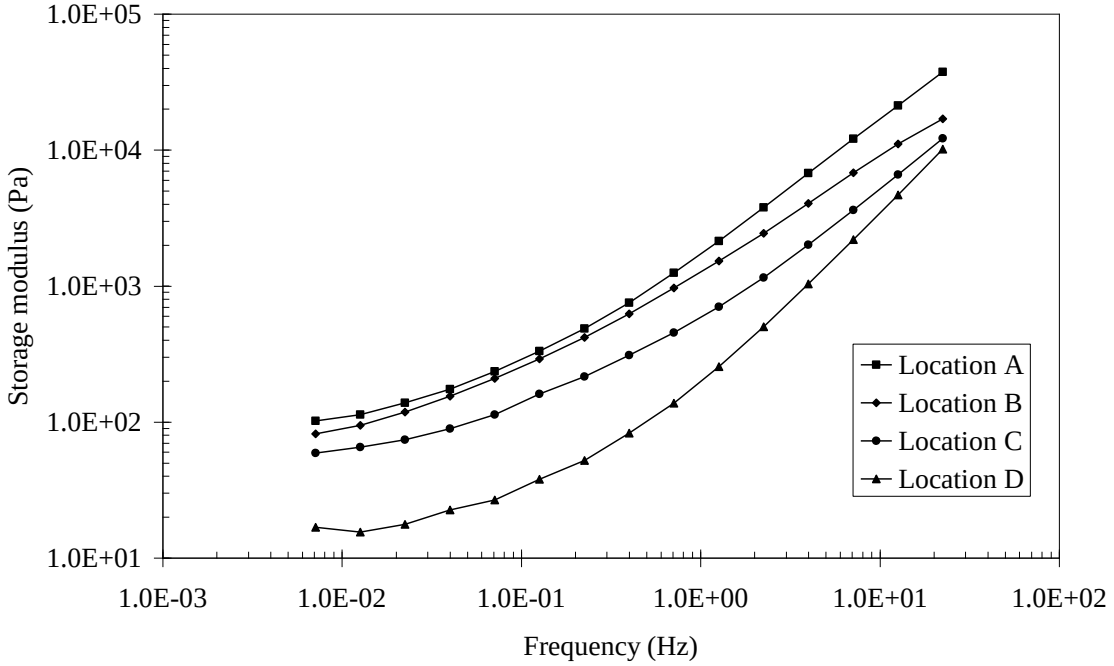

b)

Figure 8.6 – Rheological behaviour of PA-6/EPM/EPM-g-MA (80/20/0, w/w/w) blend along the extruder; a) dynamic viscosity and b) storage modulus.

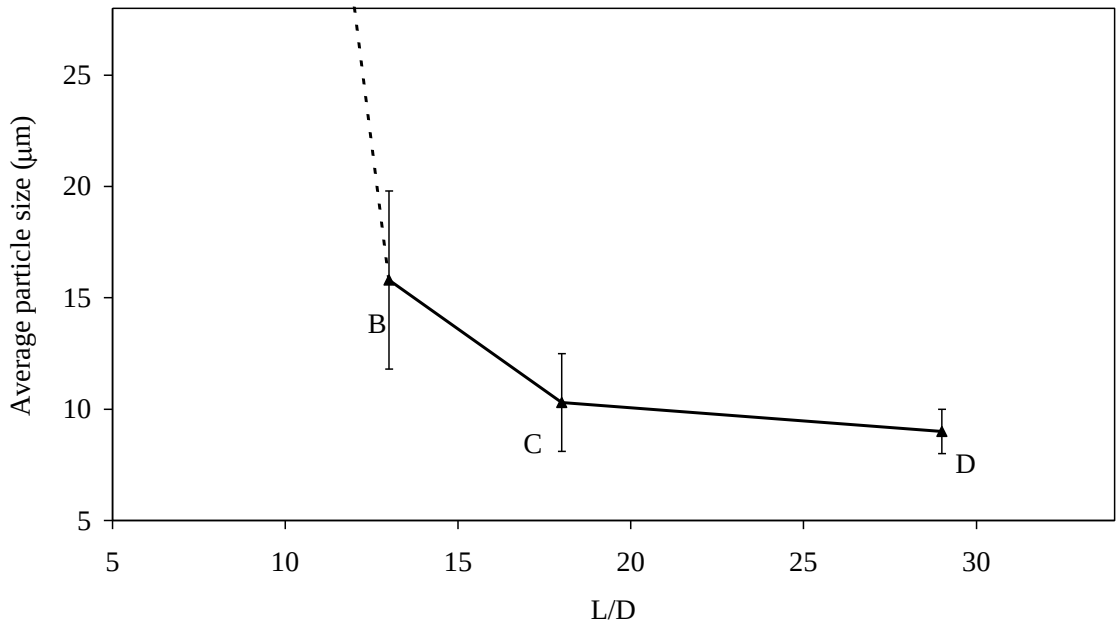

Figure 8.7 – Evolution of the dispersed phase particle size of PA-6/EPM/EPM-g-MA (80/20/0, w/w/w) blend along the extruder.

In the case of the reactive PA-6/EPM-g-MA (80/20, w/w) blend, differences between the individual η' and G' curves are clear at lower frequencies (Figure 8.8), where a progressive decrease of these parameters towards the die is observed. Differences between locations A and B are more pronounced than in the non-reactive counterpart. These results can be partially explained by the progressive decrease in particle size (distribution), as depicted in Figure 8.9. In our previous study, between locations A and B not only melting is completed, but also the average particle size decreases dramatically to sub-micrometer levels. TEM micrographs show a change from spherical and ribbon particles to a very regular morphology [26]. However, beyond location C no significant changes are detected.

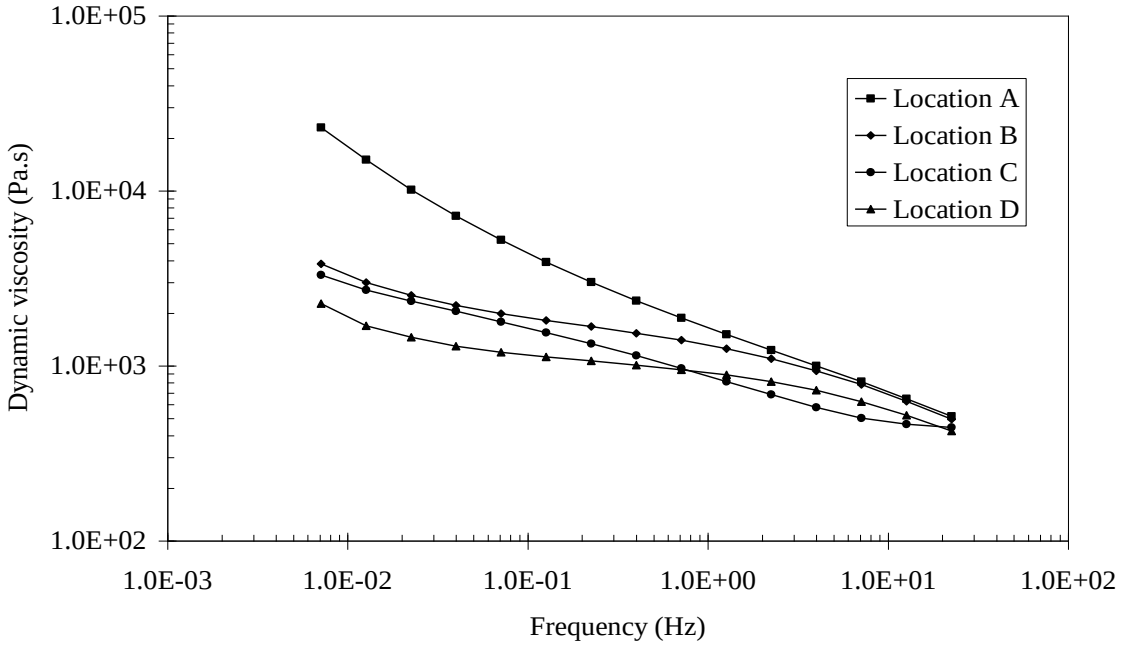

a)

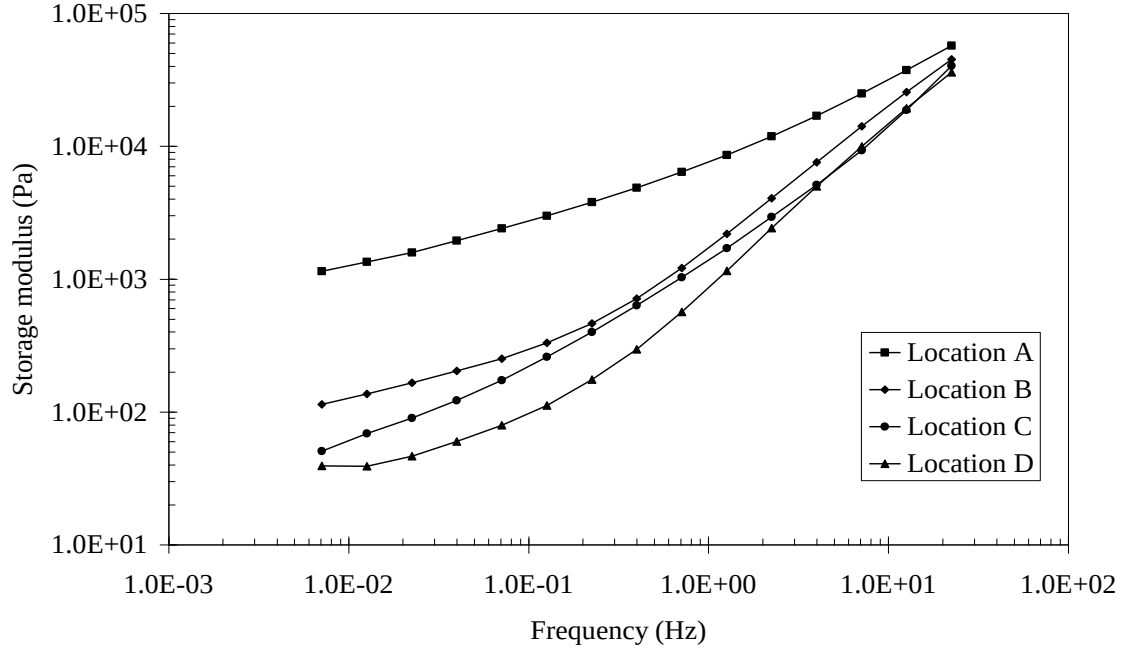

b

Figure 8.8 - Rheological behaviour of PA-6/EPM/EPM-g-MA (80/0/20, w/w/w) blend along the extruder; a) dynamic viscosity and b) storage modulus.

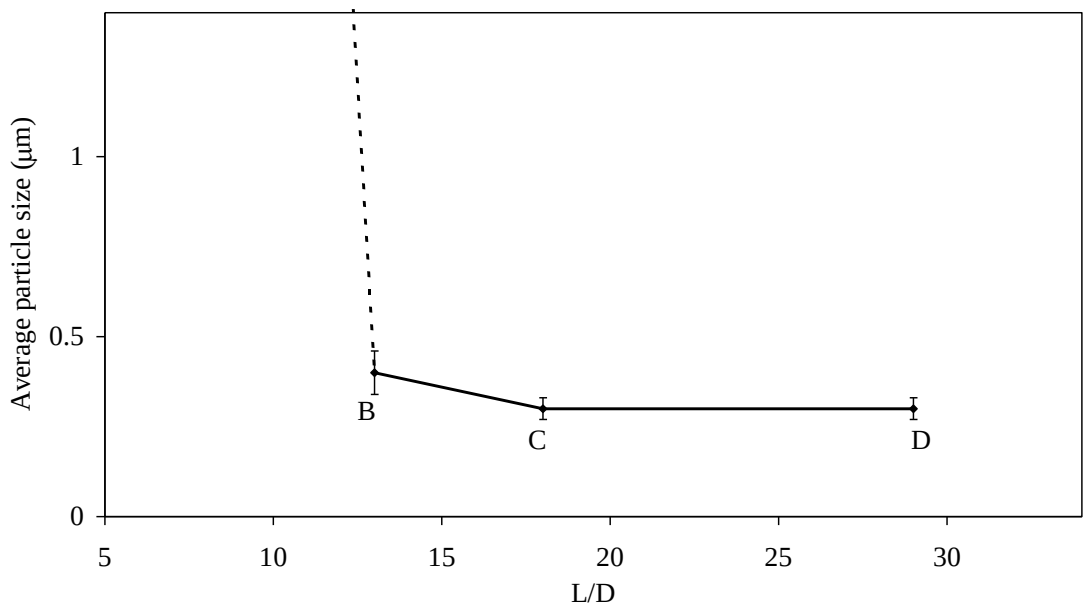

Figure 8.9 - Evolution of the dispersed particle size of PA-6/EPM/EPM-g-MA (80/0/20, w/w/w) blend along the extruder.

The progressive formation of PA-6/EPM-g-MA graft copolymer at the interface would result in an increasing viscosity and elasticity [30]. Figure 8.10 depicts the variation of the residual MA content of the blend along the screw (determined by FT-IR of hydrochloric acid residues [26]) and of the amount of PA grafted at the interface (computed from the nitrogen content of formic acid residues). The amount of MA decreases significantly from 0.49% to 0.07% in location B and remains constant thereafter. Complete conversion of all MA groups is difficult, since the residual unreacted MA groups are probably present in the interior of the dispersed rubber particles. The amount of PA grafted at the interface increases until it reaches a plateau level at location C of about 0.8g/20g EPM+EPM-g-MA. Brahimi *et al.* [31] showed that η' and G' are very sensitive to the nature and volume fraction of the copolymer present at the interface (in the case of copolymer-modified PE/PS blends). In short, if the conflicting effect between decrease in particle size and progressive presence of copolymer at the interface results in the decrease of η' and G' up to location C, further downstream this continuing decrease cannot be accounted for by the same morphology/chemical conversion effects.

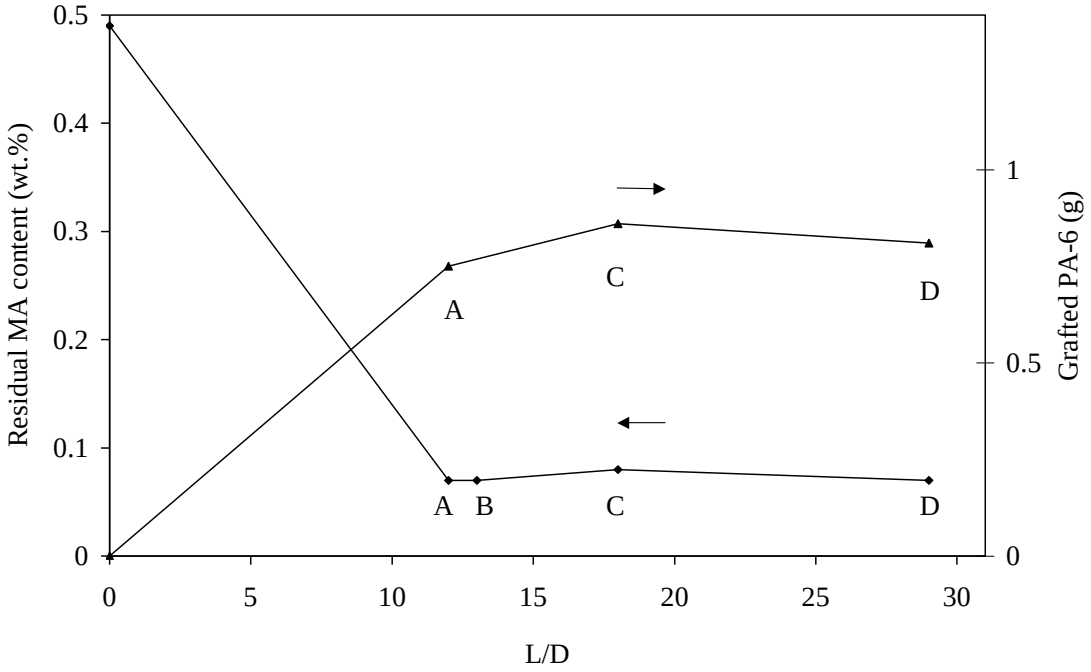

Figure 8.10 – Chemical evolution (MA content and amount of grafted PA-6 on the rubber phase) of PA-6/EPM/EPM-g-MA (80/0/20, w/w/w) blend along the extruder.

When PA-6 is processed as such under the same processing conditions used for the blends and its rheological behaviour along the screw is also monitored, the results presented in Figure 8.11 are obtained. Progressive degradation (probably due to chain scission) seems to take place. This is confirmed by gel permeation chromatography, where a shift to lower values of molecular weight is observed (the ratio Mw/Mn is 2.6 and 2.4 at locations A and D, respectively). In the case of the reactive PA-6/EPM-g-MA blend matrix degradation can be even more important, since the water formed during the reaction between the PA amine end groups and the EPM-g-MA anhydride groups can hydrolyse the amide groups of the polyamide chain increasing chain scission. In addition, the EPM-g-MA anhydride can also react with PA amide chain groups, resulting in direct degradation of the PA matrix [22].

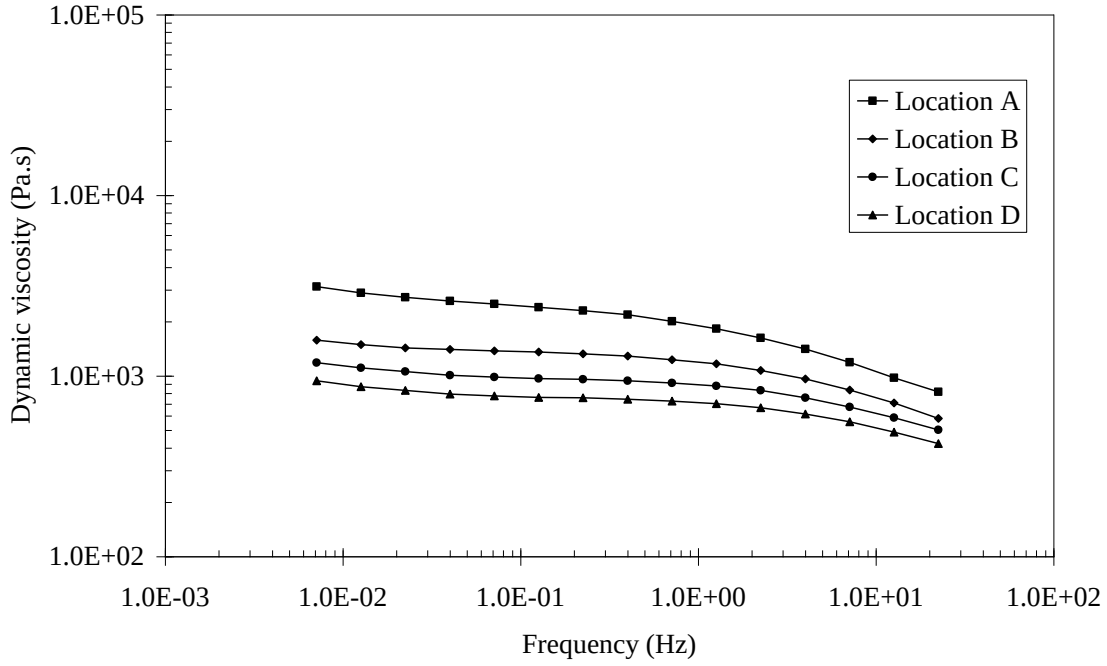

a)

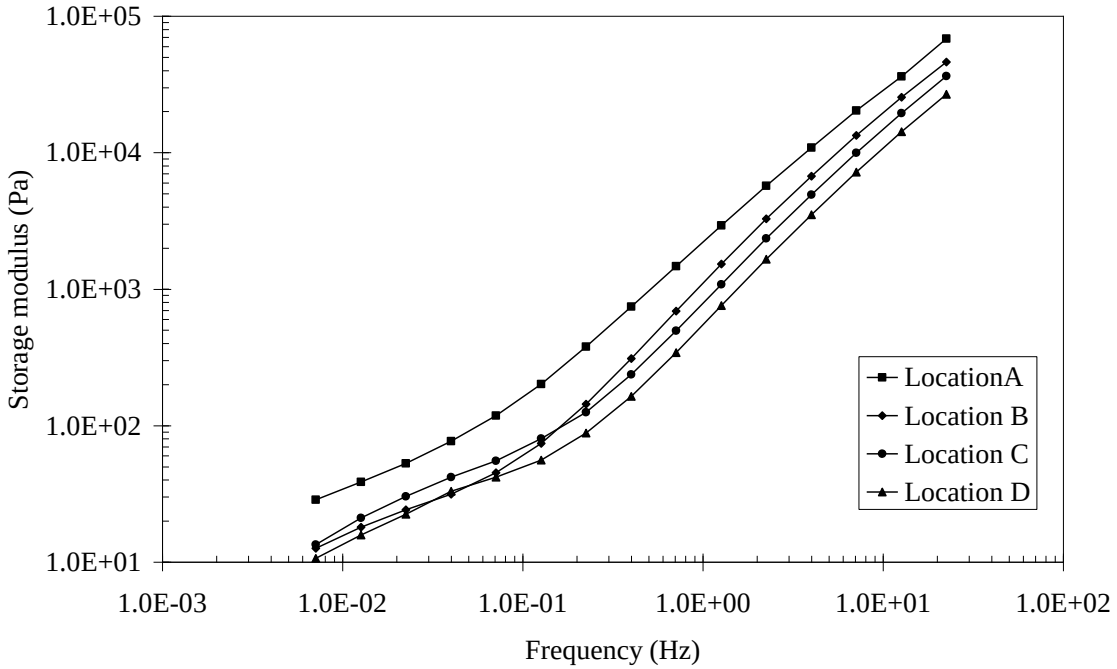

b)

Figure 8.11 - Rheological behaviour of PA-6 along the extruder; a) dynamic viscosity and b) storage modulus.

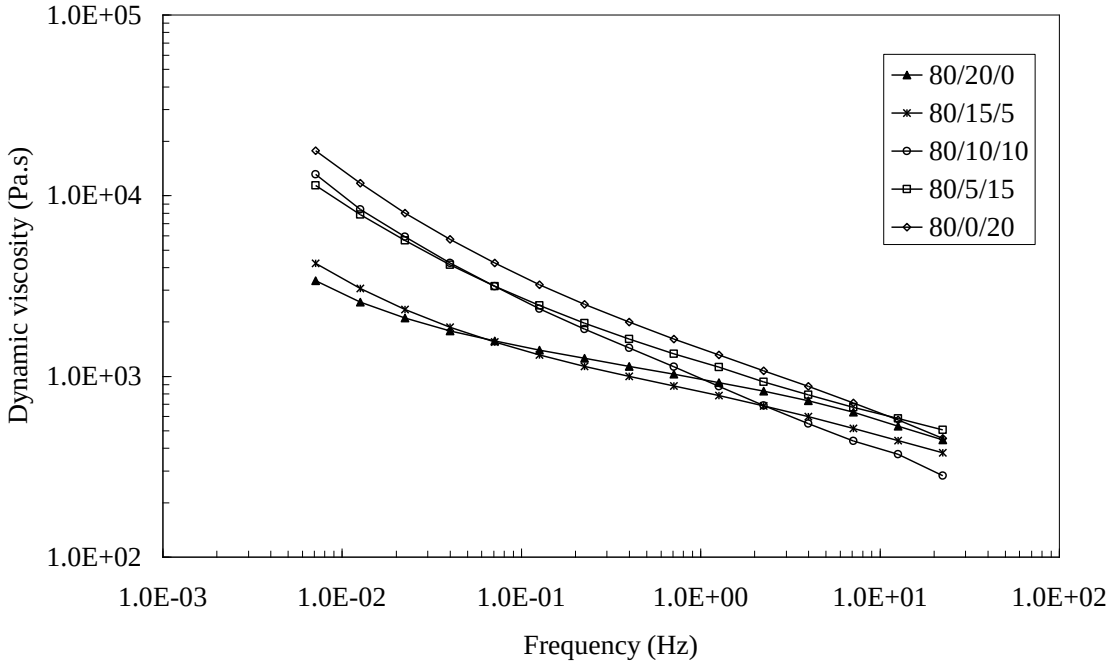

a)

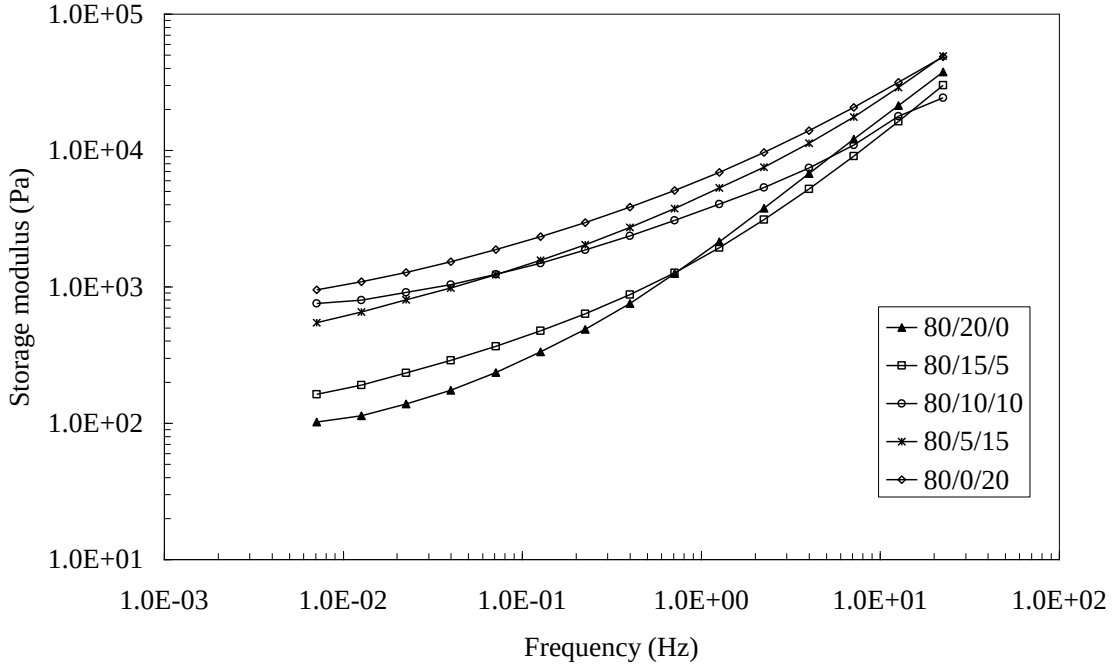

b)

Figure 8.12 - Rheological behaviour of blends with different compositions at location A; a) dynamic viscosity and b) storage modulus.

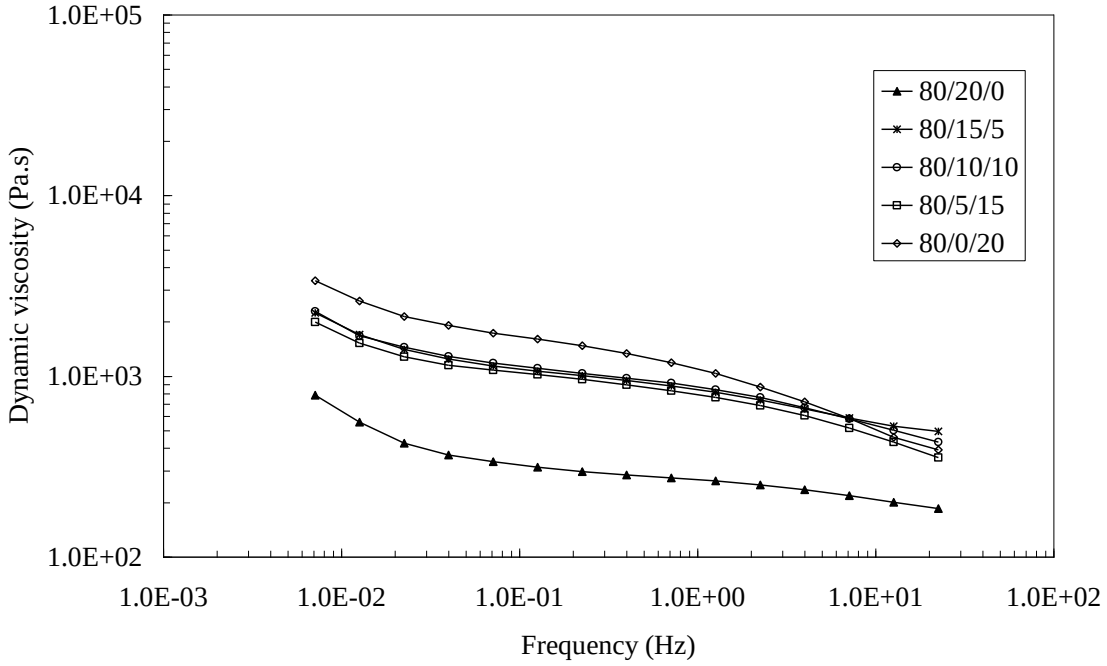

a)

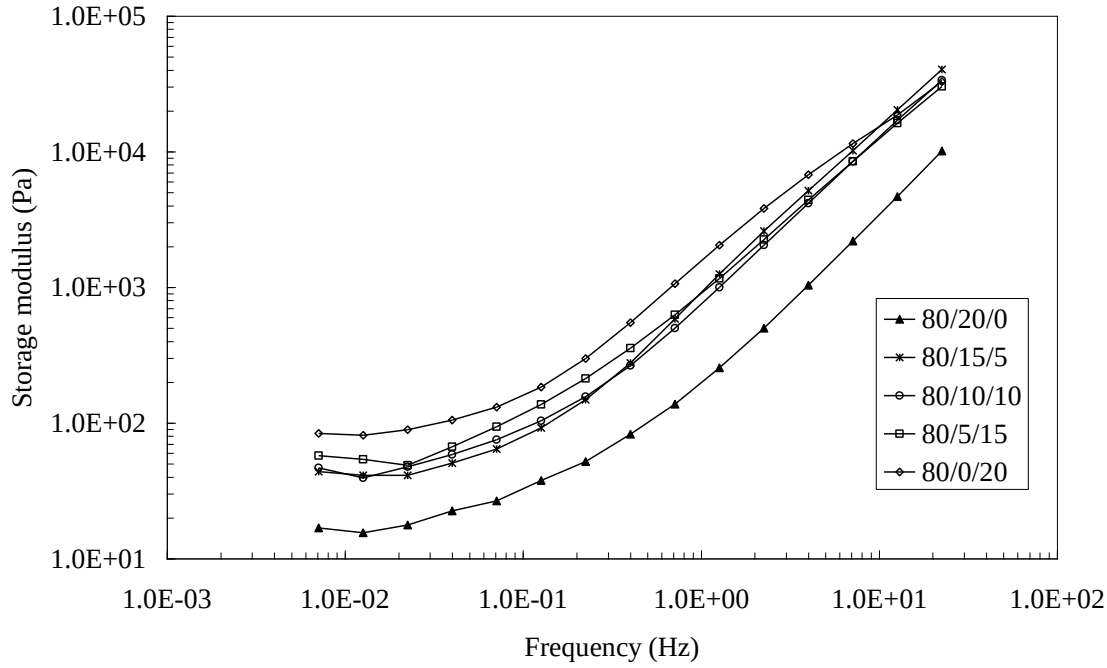

b)

Figure 8.13 - Rheological behaviour of blends with different compositions at location D; a) dynamic viscosity and b) storage modulus.

Consequently, matrix degradation seems to play a relevant part in the rheological behaviour of the blends studied in this work. If one uses again Figure 8.5 for a comparison of the relative viscosity and elasticity of the various materials, a shift of the curves corresponding to PA-6 to the lower values presented in Figure 8.11 should be considered. The rheological behaviour of the non-reactive blend would then follow closely that of PA-6, thus strengthening the previous observation that the behaviour of the blends studied in this work is governed by the matrix. Unfortunately, the morphology type (dispersed particles in a less viscous matrix), the presence of occlusions of PA-6 in the dispersed rubber particles and the matrix degradation jeopardize the applicability of the Palierne and/or Lee and Park models [16,18] for establishing the relationship between morphology and rheology.

The effect of the EPM-g-MA content on the rate of morphology and chemical conversion along the extruder is illustrated in Figures 8.12 (location A) and 8.13 (location D). As it could be anticipated from the above discussion, both the dynamic viscosity and the storage modulus increase with increasing volume fraction of the graft copolymer formed at the interface. This is in accordance with previous results [26] showing that the amount of PA-6 grafted at the interface increases with increasing MA content of the rubber phase. The anticipated lower viscosity and elasticity of the extrudate (location D) result, as discussed above, from the combined effects of morphology, chemical conversion and matrix degradation.

8.4 - CONCLUSIONS

This work showed that the linear viscoelastic behaviour of immiscible non-compatibilized and compatibilized polyamide-6/rubber blends along a twin-screw extruder is related to changes in morphology and/or formation of the “in-situ” compatibilizer. The dynamic viscosity and the storage modulus decrease substantially upon melting of the components, since this process is induced by a significant increase in interfacial area. However, the rheological data could not be analysed making use of available theoretical models (proposed, among others, by Palierne and Lee and Park), due to morphology type and matrix degradation. In fact, the phenomenon of matrix

degradation explains the relatively low viscosity levels of the blends, when compared with those of the original materials.

These results confirm that rheology can be a powerful method for probing the morphology development of immiscible polymer blends. The development of in- and on-line measurements should therefore be pursued, given their potential for real time monitoring and control of blend preparation under industrial conditions. This work is currently in progress [32].

8.4 - REFERENCES

[1] – D. Paul and S. Newman, *Polymer Blends*, Academic Press, New York, 1978.

[2] – L. A. Utracki, *Polymer Alloys and Blends*, Hanser Publishers, New York, 1990.

[3] – L. A. Utracki (Ed.), *Two-phase Polymer Systems*, Hanser Publishers, New York, 1991.

[4] – L. A. Utracki, *Encyclopaedic Dictionary of Commercial Polymer Blends*, ChemTec Publishing, Toronto, 1994.

[5] – S. Datta and D. Lohse, *Polymeric Compatibilizers*, Hanser Publishers, New York, 1996.

[6] – M. Bousmina and R. Muller, *Rheol Acta*, **35**, 369 (1996).

[7] – S. Kitade, A. Ichikawa, N. Imura, Y. Takahashi and I. Noda, *J. Rheol.*, **5**, 1039 (1997).

[8] – L. Nielsen, *Polymer Rheology*, Marcel Dekker, New York, 1977.

[9] – M. Xanthos, V. Tan and A. Ponnusamy, *Polym. Eng. Sci*, **37**, 1102 (1997).

[10] – C. Lacroix, M. Gramela and P. J. Carreau, *J. Rheol.*, **42**, 41 (1998).

[11] – I. Vinckier, P. Moldenaers and J. Mewis, *J. Rheol.*, **40**, 613 (1996).

[12] – M. Bousmina and R. Muller, *Rheol. Acta*, **35**, 369 (1996).

[13] – C. Lacroix, M. Aressy and P. J. Carreau, *Rheol. Acta*, **36**, 416 (1997).

[14] – N. Grizzuti and O. Bifulco, *Rheol. Acta*, **36**, 406 (1997).

[15] – A. Bouilloux, B. Ernest, A. Lobbrecht and R. Muller, *Polymer*, **38**, 4775 (1997).

[16] – J. F. Palierne, *Rheol. Acta*, **29**, 204 (1990).

[17] – M. Doi and T. Ohta, *J. Chem. Phys.*, **95**, 1242 (1991).

[18] – H. M. Lee and O. Park, *J. Rheol.*, **38**, 1405 (1994).

[19] – N. A. Memon and R. Muller, *J. Polym. Sci.: Part B: Polym. Physics*, **36**, 2623 (1998).

[20] – C. E. Scott and C. W. Macosko, *Polym. Eng. Sci*, **24**, 1938 (1995).

[21] – R. J. M. Borggreve and R. J. Gaymans, *Polymer*, **30**, 63 (1989).

[22] – M. van Duin, M. Aussems and R. J. M. Borggreve, *J. Polym. Sci.: Part A: Polym. Chem.*, **36**, 179 (1998).

[23] – H. Cartier and G. H. Hu, Proc. Polyblends 97, Boucherville, Canada, 1997.

[24] – P. Scholz, D. Froelich and R. Muller, *J. Rheol*., **33**, 481 (1989).

[25] - A. V. Machado, J. A. Covas and M. van Duin, *J. Appl. Polym. Sci*., **71**, 135 (1999).

[26] – A. V. Machado, J. A. Covas and M. van Duin, *J. Polym. Sci.: Part A: Polym. Chem.*, **31**, 1311 (1999).

[27] – T. Gregory and S. Mayers, *Surf. Coat. Int*, **76**, 82 (1993).

[28] – H. A. Barnes, *J. Non-Newton. Fluid Mech*, **56**, 221 (1995).

[29] – M. Mooney, *J. Appl. Phys.*, **25**, 1098 (1958).

[30] – Y. Germain, B. Ernst, O. Genelot and L. Dhamani, *J. Rheol*., **38**, 681 (1994).

[31] – B. Brahimi, A. Ait-Kadi, A. Ajji, R. Jerôme and R. Flat, *J. Rheol*., **35**, 1069 (1991).

[32] – J. A. Covas, J. M. Nobrega and J. M. Maia, *Polym. Testing*, **19**(2), 165 (2000).

Part IV

Conclusions

9.1 – CONCLUSIONS

In the last decades considerable efforts have been made for producing new polymer materials with an improved performance/costs balance. This can be achieved by attaching polar and/or reactive monomers on the polymer chains or by blending polymers, for example via reactive extrusion. The actual process occurring inside the extruder has remained largely unknown, which is due to the complexity of the complexity of the physico-chemical processes in the extruder and to difficulties in collecting representative samples from the extruder during processing. The methodology used in the present research to collect samples from extruders was initially validated with a non-reactive blend and with a reactive system. It was shown that screw-pulling experiments can result in experimental artefacts and, thus, induce erroneous conclusions on physical/chemical mechanisms developed. The methodology allowed a detailed study of the evolution of physico-chemical phenomena along a co-rotating twin-screw extruder, thus providing, a better understanding of the evolution of the reactive systems along the extruder.

When various polyolefins were processed in the presence of different concentrations of peroxide, considerable differences in viscosity were obtained depending on the structure of the polyolefin being used. Branching/crosslinking and/or degradation occur along the extruder until the peroxide is fully converted. The degree of branching/crosslinking and/or degradation depends essentially on the ethene/propene ratio. Braching/crosslinking occurs for polymers with high ethene content while degradation is the main reaction for polymers with high propene content.

During grafting of MA onto polyolefins with different ethene/propene ratios significant differences in MA grafting and rheological behaviour were obtained depending on the original polyolefin structure. The MA graft content was low for polyolefins with high propene content and became higher as the propene content decreased. A decrease of the propene content of the polyolefin results in a transition from degradation to branching/crosslinking. A detailed chemical mechanism was proposed to explain these results.

The MA graft content follows the same profile along the axis when the same peroxide type and set temperature are applied, independent of the choice of the polyolefin and the MA and peroxide concentrations. In a quantitative approach, combining the measured average temperature and residence time at each location with an algorithm that integrates numerically the peroxide decomposition for a given temperature and time, a good correlation between the experimental grafting profiles and calculated peroxide decomposition profiles could be established.

In the case of reactive blends (PA-6/EPM/EPM-g-MA), a correlation between morphology and chemical conversion could be established. Most of the chemical conversion and morphology changes occurred during melting of the components. Both processes are very fast, occurring within a few seconds over a few centimetres. When the MA groups of EPM-g-MA are almost completely converted, the morphology of the blend is also fully developed. Since the graft copolymers formed at the interface provide steric stabilization and prevent coalescence. Since both chemical conversion and morphology development are very fast, the insight into the processes was limited. However, by varying the experimental set-up it was possible to get a better understanding of the process and obtain more information about morphology development. Replacing EPM-g-MA by MA-containing polymers with higher softening temperatures and varying the processing conditions (particularly the temperature profile and the screw speed) slows the chemical conversion and, therefore, the morphology evolution. Using low temperatures and low screw speeds it became possible to observe and follow in real time the evolution of morphology development of a reactive blend. The dispersion process in the initial part of the extruder is very complex. Large rubber particles and unmolten PA-6 pellets are present in close vicinity to a finely dispersed PA-6/EPM-g-MA mixture (rubber particle size: 0.25 - 1 μm). All sorts of morphologies with intermediate dimensions are observed: thin PA-6 regions drawn from the unmolten PA-6 pellets, EPM-g-MA sheets, thin elongated EPM-g-MA and PA-6 domains, EPM threads in the process of breaking up, etc.

The methodology used, the new sampling device, seemed to be very efficient for the type of systems studied. It can be placed along the extruder in locations where significant changes either on chemistry or on morphology are expected, it is easy to

operate and the melt samples can be quickly removed from the extruder providing real time information about the phenomena. Since chemistry and/or morphology are not affected during sampling this device is considered an important tool for a better understanding reactive extrusion.

9.2 – FUTURE WORK

Given the results and conclusions of the present research, some future work can be recommended:

9.2.1 – Grafting monomers onto polyolefins

- To calculate the peroxide decomposition from the residence time distribution; allowing an accurate profile of calculated peroxide decomposition in order to make a correlation with the MA graft profile.
- To determine experimentally the residual peroxide concentration at each location of the extruder. This enable possible to relate experimental and calculated data of peroxide decomposition.
- To perform elongational rheometry of original and modified PE. This type of measurements can give more detail about the rheological changes along the extruder during grafting of MA.
- To optimise the grafting process in order to determine the processing conditions that maximize the MA graft content and minimize side reactions.
- To establish a mechanism of the grafting reaction along the extruder, qualitative and quantitative approach.
- To model the grafting reactions along the extruder.
- To study grafting of other vinyl monomers onto polyolefin in order to study the effect of monomer solubility on grafting reactions.

9.2.2 – Reactive blends

- To study the relationship between dynamic viscosity and interfacial tension to establish a correlation (model) between dynamic viscosity and interfacial tension.

- To investigate the influence of other type of reactive groups of the blend components on chemical and morphological evolution.

9.2.3 – Reactive Extrusion

Obviously other examples of reactive extrusion, such as chain extension, interchange reactions and dynamic vulcanisation can be studied by using the sampling devices.